International Ocean Discovery Program Expedition 383 Scientific Prospectus

Dynamics of the Pacific Antarctic Circumpolar Current (DYNAPACC)

Frank Lamy
Co-Chief Scientist
Alfred Wegener Institute
Helmholtz Zentrum für Polar
und Meeresforschung
Germany

Gisela Winckler
Co-Chief Scientist
Lamont-Doherty Earth Observatory
Columbia University
USA

Carlos A. Alvarez Zarikian
Expedition Project Manager/Staff Scientist
Integrated Ocean Drilling Program
Texas A&M University
USA

IODP
INTERNATIONAL OCEAN DISCOVERY PROGRAM

Publisher's notes

This publication was prepared by the *JOIDES Resolution* Science Operator (JRSO) at Texas A&M University (TAMU) as an account of work performed under the International Ocean Discovery Program (IODP). Funding for IODP is provided by the following international partners:

National Science Foundation (NSF), United States
Ministry of Education, Culture, Sports, Science and Technology (MEXT), Japan
European Consortium for Ocean Research Drilling (ECORD)
Ministry of Science and Technology (MOST), People's Republic of China
Korea Institute of Geoscience and Mineral Resources (KIGAM)
Australia-New Zealand IODP Consortium (ANZIC)
Ministry of Earth Sciences (MoES), India
Coordination for Improvement of Higher Education Personnel (CAPES), Brazil

Portions of this work may have been published in whole or in part in other IODP documents or publications.

This IODP *Scientific Prospectus* is based on precruise *JOIDES Resolution* Facility advisory panel discussions and scientific input from the designated Co-Chief Scientists on behalf of the drilling proponents. During the course of the cruise, actual site operations may indicate to the Co-Chief Scientists, the Staff Scientist/Expedition Project Manager, and the Operations Superintendent that it would be scientifically or operationally advantageous to amend the plan detailed in this prospectus. It should be understood that any proposed changes to the science deliverables outlined in the plan presented here are contingent upon the approval of the IODP JRSO Director.

Disclaimer

Any opinions, findings, and conclusions or recommendations expressed in this publication are those of the author(s) and do not necessarily reflect the views of the participating agencies, TAMU, or Texas A&M Research Foundation.

Copyright

Citation

Lamy, F., Winckler, G., and Alvarez Zarikian, C.A., 2018. *Expedition 383 Scientific Prospectus: Dynamics of the Pacific Antarctic Circumpolar Current (DYNAPACC)*. International Ocean Discovery Program. https://doi.org/10.14379/iodp.sp.383.2018

ISSN
World Wide Web: 2332-1385

Abstract

The Antarctic Circumpolar Current (ACC) is the world's strongest zonal current system that connects all three major ocean basins of the global ocean and therefore integrates and responds to global climate variability. Its flow is largely driven by strong westerly winds and constricted to its narrowest extent in the Drake Passage. Transport of fresh and cold surface and intermediate water masses through the Drake Passage (cold-water route) strongly affect the Atlantic Meridional Overturning Circulation (AMOC) together with the inflow of Indian Ocean water masses (warm-water route). Both oceanographic corridors are critical for the South Atlantic contribution to AMOC changes. In contrast to the Atlantic and Indian sectors of the ACC, and with the exception of drill cores from the Antarctic continental margin and off New Zealand, deep-sea drilling records of the Pacific sector of the ACC lack information on its Cenozoic paleoceanography. To advance our knowledge and understanding of Plio-Pleistocene atmosphere-ocean-cryosphere dynamics in the Pacific and their implications for regional and global climate and atmospheric CO_2, International Ocean Discovery Program Expedition 383 proposes the recovery of 180 to 500 m long high-resolution Plio-Pleistocene sediment sequences at (1) three primary sites located on a cross-frontal transect in the central South Pacific (CSP) between the modern Polar Front (Site CSP-3A) and the Subantarctic Zone (Sites CSP-1A and CSP-2B), (2) two sites (CHI-1C and CHI-4B) at the Chilean margin, and (3) one site from the pelagic eastern South Pacific (ESP; Site ESP-1A) close to the entrance to the Drake Passage. The planned sites represent a depth transect from ~1100 m at the Chilean margin (Site CHI-4B) to >5000 m in the Bellingshausen Sea (Site CSP-3A) that will allow investigation of Plio-Pleistocene changes in the vertical structure of the ACC—a key issue for understanding the role of the Southern Ocean in the global carbon cycle. All of the six primary and eight alternate sites were surveyed with seismic lines in 2009–2010 and most recently in 2016. The sites are located at latitudes and water depths where sediments will allow the application of a wide range of siliciclastic, carbonate, and opal-based proxies to address our objectives of reconstructing, with unprecedented stratigraphic detail, surface to deep ocean variations and their relation to atmosphere and cryosphere changes through stadial-to-interstadial, glacial-to-interglacial, and warmer-than-present time intervals.

Schedule for Expedition 383

Expedition 383 is based on International Ocean Discovery Program (IODP) drilling proposals 912-Full and 912-Add (**http://iodp.tamu.edu/scienceops/expeditions/dynamics_of_ pacific_ACC.html**). Following ranking by the IODP Scientific Advisory Structure, this scientific program was scheduled for the R/V *JOIDES Resolution*, operating under contract with the *JOIDES Resolution* Science Operator (JRSO) at Texas A&M University. At the time of publication of this *Scientific Prospectus*, Expedition 383 is scheduled to start in Punta Arenas, Chile, on 20 May 2019 and to end in Valparaiso, Chile, on 20 July 2019. The expedition has a total of 61 days available for the initial port call, transit, drilling, coring, and downhole measurements described in this report (Tables **T1**, **T2**; see **http://iodp.tamu.edu/scienceops** for the current ship schedule). Further details about the facilities aboard the *JOIDES Resolution* can be found at **http://iodp.tamu.edu/labs/ship.html**.

Introduction

Our knowledge of southern high-latitude paleoceanography comes mainly from conventional sediment coring and Deep Sea Drilling Project (DSDP)/Ocean Drilling Program (ODP) drilling in the Atlantic and Indian sectors of the Antarctic Circumpolar Current (ACC). A prominent example is the achievements of ODP Leg 177, which drilled sites arrayed along a north–south transect across the major ACC fronts documenting the Cenozoic history of the Atlantic sector of the Southern Ocean. These sites provided, for example, insights into changes in dust supply, marine productivity, and nutrient consumption (Martínez-García et al., 2009, 2011, 2014) opposite Southern Ocean productivity between the Antarctic Zone (AZ) and Subantarctic Zone (SAZ) on glacial–interglacial cycles (Jaccard et al., 2013) and between the ACC and the Antarctic margin on longer timescales (Cortese et al., 2004); sea surface temperature (SST) evolution since the Pliocene (Martínez-García et al., 2010); and Antarctic ice sheet (AIS) dynamics during the late Quaternary (Kanfoush et al., 2002; Teitler et al., 2010, 2015; Venz and Hodell, 2002; Hayes et al., 2014).

In contrast, the Pacific sector of the ACC is much less studied, with drilling records mostly from the Antarctic continental margin south of the ACC (e.g., Ross Sea, DSDP Leg 28; Antarctic Peninsula, ODP Leg 178) and the recovery of high-resolution proximal sediment records. Integrated Ocean Drilling Program Expedition 318 drilled Cenozoic sediments off Wilkes Land (eastern Indian Southern Ocean) and revealed significant vulnerability of the East Antarctic Ice Sheet (EAIS) to Pliocene warming (Cook et al., 2013; Expedition 318 Scientists, 2010). A substantial advance in constraining the history and stability of the West Antarctic Ice Sheet (WAIS) and Ross Ice Shelf (RIS) came from the Antarctic Geological Drilling (ANDRILL) project (e.g., Naish et al., 2009; Florindo et al., 2008; WAIS Divide Project Members, 2013), which documented that the WAIS/RIS underwent significant changes, with expanded cold and stable ice sheets between 13–11 Ma. The ice sheet became more dynamic in the late Miocene–early late Pliocene (10–2.5 Ma), with cyclic expansion of grounded ice sheets over the coring site after 2.5 Ma.

These on- and near-shore drilling programs have significantly advanced our understanding of AIS dynamics during the Cenozoic. However, to understand how these ice sheet changes are ultimately linked to climate, atmospheric CO_2 levels, and ocean circulation requires constraints of the ACC (i.e., the current system that connects Antarctica to the rest of the globe). In this context, our drilling in the Pacific ACC will be closely linked to the recently completed IODP expedition to the Ross Sea (Expedition 374) and the upcoming IODP expeditions to the Amundsen Sea and Scotia Sea (Expeditions 379 and 382, respectively). These expeditions target Antarctic near-shore records, which will likely be incomplete due to glacial erosion, and the potential for analyses of paleoceanographic proxies will be limited. Therefore, Expedition 383 pelagic sites will provide critical paleoceanographic baseline information, including rates of change for improving the understanding of reconstructed AIS changes and testing ice sheet models.

During Expedition 383, we will recover high-resolution Plio-Pleistocene sediment records at three primary (and three alternate) sites located on a cross-frontal transect in the central Pacific Southern Ocean. These sites in the central South Pacific (CSP) document the Plio-Quaternary ACC paleoenvironmental history at water

depths ranging from 5100 to 3600 m (Table **T1**). At the Chile margin, we propose two primary (and four alternate) sites, as well as one primary (plus one alternate) site from the pelagic eastern South Pacific (ESP), providing a depth transect (~1000–3900 m) across the major Southern Ocean water masses.

Background

The ACC is the world's largest current system and connects all three major basins of the global ocean (i.e., the Pacific, Atlantic, and Indian Oceans) (Figure **F1**) and therefore integrates and responds to climate signals throughout the globe (e.g., Talley, 2013). Through inducing pronounced upwelling and formation of new water masses, the ACC fundamentally affects the global meridional overturning circulation (MOC) (Marshall and Speer, 2012) and the stability of Antarctica's ice sheets.

The ACC has long been recognized as a key player in regulating atmospheric CO_2 variations and hence global climate based on the tight coupling between Southern Hemisphere temperatures and atmospheric CO_2 concentration (e.g., Parrenin et al., 2013). Through its steep density surfaces, the ACC provides a direct hydrographic link between the large deep-ocean reservoir of dissolved inorganic carbon (DIC) and the surface ocean, along which deep-water masses may ascend to the surface (e.g., Kuhlbrodt et al., 2007; Marshall and Speer, 2012). The ACC therefore acts as a window through which ocean and atmosphere interact and as a key player in regulating atmospheric CO_2 variations and hence global climate.

Biological utilization of nutrients in the Southern Ocean is particularly important in relation to changes in atmospheric CO_2 concentration because it regulates the preformed nutrient inventory for most of the deep ocean and therefore the global average efficiency of the biological pump (e.g., Sigman and Boyle, 2000; Sigman et al., 2010). Nutrient utilization is inefficient in the Southern Ocean today, in part because phytoplankton growth is limited by the scarcity of bioavailable iron (e.g., de Baar et al., 1995). Martin (1990) proposed that dust-borne iron fertilization of Southern Ocean phytoplankton caused the ice age reduction in atmospheric CO_2. However, the role of iron in explaining variation in opal export to the Southern Ocean sediments is complex. Chase et al. (2015) found a significant correlation between annual average net primary production and modeled dust deposition but not between dust deposition and opal burial. On glacial–interglacial timescales, proxy records from the Subantarctic support a positive relationship between dust flux and opal production (e.g., Chase et al., 2003; Bradtmiller et al., 2009; Lamy et al., 2014; Kumar et al., 1995; Anderson et al., 2014). By contrast, the opposite is true south of the Antarctic Polar Front (APF) (e.g., Chase et al., 2003; Jaccard et al., 2013), indicating that factors other than dust regulate the production and export of opal in the Southern Ocean and by association the strength and efficiency of the biological pump, as well. Leading candidates for these "other factors" include changes in water mass structure in the Southern Ocean locations of the fronts encircling Antarctica, which are related to the flow of the ACC, and the spatial and temporal variability of wind-driven upwelling that supplies nutrients and CO_2 to surface waters and glacial–interglacial changes in sea ice extent.

Oceanographic setting

Expedition 383 will drill sites located in the ACC current system in the central and eastern South Pacific, as well as at the southern Chile margin close to the Drake Passage. The flow of the ACC is largely driven by strong westerly winds (SWW) and is constricted to its narrowest extent in the Drake Passage. This so-called "cold-water route" transport through the Drake Passage is one important pathway for the return of fresh and cold waters from the Pacific to the Atlantic, which strongly affects the strength of the Atlantic Meridional Overturning Circulation (AMOC), in concert with the "warm-water route" inflow of warm and salty Indian Ocean water masses through the Agulhas Current system (Beal et al., 2011; Gordon, 1986). The Drake Passage is ~800 km wide and is located between Cape Horn and the western Antarctic Peninsula (Figure **F1**). Numerous hydrographic surveys across the Drake Passage since the 1970s have contributed to the understanding of seasonal and interannual variability in ACC transport through the Drake Passage and the mechanisms forcing physical and biological changes in the Southern Ocean (Meredith et al., 2011). However, even with hydrographic time series reaching back 20 y (Koenig et al., 2014) in this relatively well-constrained region of the ACC and more sophisticated model simulations (Meijers, 2014), important issues such as the role of zonal winds in forcing ACC transport remain controversial. The total ACC flow transported through the Drake Passage is estimated to be between ~130 and 150 Sv (Koenig et al., 2014; Meredith et al., 2011; Renault et al., 2011). The three major ACC oceanographic fronts (Orsi et al., 1995, 1999), the Subantarctic Front (SAF), the Polar Front (PF), and the Southern ACC Front (SACCF), can be identified from north to south in the Drake Passage. The modern winter sea ice (WSI) margin presently does not extend significantly north into the Drake Passage. Oceanographic studies robustly show that more than half of the total Drake Passage transport occurs at and north of the SAF (i.e., in the SAZ), followed by the Polar Frontal Zone (between SAF and PF). The relative contribution of Drake Passage transport south of the PF is generally less than 20%.

Along the southernmost Chile margin, the southward flowing Cape Horn Current (CHC), a northern branch of the ACC that continues toward the Drake Passage, provides a major fraction of the present-day northern Drake Passage transport (Well et al., 2003). Satellite-tracked surface drifters reveal that after crossing the East Pacific Rise (EPR), Subantarctic surface water of the ACC is transported northeastward across the Southeast Pacific toward the Chilean coast at ~45°S/75°W (Chaigneau and Pizarro, 2005). Here, presently only a minor part of the ACC is deflected northward into the Humboldt Current System (HCS), whereas the major fraction is deviated southward toward the Drake Passage. The CHC thus transports a significant amount of northern ACC water toward the Drake Passage in a narrow, ~100–150 km wide belt off the coast (Chaigneau and Pizarro, 2005) (Figure **F2**).

In the central Pacific, our sites cover a cross-frontal transect from the modern PF across the SAF. These ACC fronts form the core of the ACC and are partly constrained by the bathymetry of the Eastern Pacific Rise (EPR) in this area. Resulting from topographic forcing, frontal positions in the ACC close to large bathymetric features remain relatively stable at a seasonal and interannual timescale, whereas over abyssal plains their location appears to be fairly unstable (Sokolov and Rintoul, 2009). The SAF at our sites at the western and eastern flank of the EPR is thus partly constrained by topography and the location of major fracture zones (e.g., Eltanin Fracture Zone). The PF close to our southern site, located in the Southeast Pacific basin at the northern edge of the Amundsen Sea plain, is not strongly affected by topographic constraints. The oceanographic conditions in the South Pacific are influenced by the Southern Annular Mode (SAM) and the Amundsen Low but also by tropical variability and the El Niño-Southern Oscillation (ENSO)

(Thompson et al., 2011; Turner et al., 2009; Yuan, 2004). Interannual and decadal SST and sea ice changes are amplified in the Pacific sector, including, for example, a distinct increase in sea ice north of the Ross Sea embayment and a strong sea ice decrease in the Bellingshausen-Amundsen Sea, as documented by observational time series (1979–2011) (Maksym et al., 2012; Stammerjohn et al., 2012).

Deep water that upwells south of the PF feeds both Antarctic Bottom Water (AABW) close to Antarctica and Antarctic Intermediate and mode water formation north of the APF (e.g., Sloyan and Rintoul, 2001; Talley, 2013). The Southeast Pacific is known as the major Antarctic Intermediate Water (AAIW) formation area, where fresh, cold, high-oxygen and low-nutrient waters are formed. Originally, it was thought that AAIW originates from the subduction of Antarctic surface waters below the SAF (e.g., Deacon, 1937). Later is was suggested that the formation of AAIW is directly linked to the formation of Subantarctic Mode Water (SAMW) (McCartney, 1977), which has similar properties in the Southeast Pacific. More recent studies basically confirm the location of the major AAIW formation area in the Southeast Pacific related to deep mixed layer development leading to SAMW formation and finally to AAIW. The Southern Ocean's major water mass, Circumpolar Deep Water (CDW), is divided into an upper and lower branch. Lower CDW (LCDW) is identified by a salinity maximum that is inherited from North Atlantic Deep Water (NADW) (Reid and Lynn, 1971; Orsi et al., 1995). Upper CDW (UCDW) is typically identified as an oxygen minimum layer derived from oxygen-depleted, nutrient-rich Indian Deep Water (IDW) and North Pacific Deep Water (NPDW) (Callahan, 1972). LCDW and UCDW are transported into the North Pacific, where they are transformed into NPDW, and return to the Southern Ocean in the East Pacific along the South American continent at 1500–3500 m water depth (Kawabe and Fujio, 2010). North of the SAF, UCDW is centered at approximately 1500 m water depth and LCDW covers depths deeper than 2000 m. Below LCDW, northward spreading dense AABW, which is formed in the Weddell Sea, in the Ross Sea, and along the Adélie Coast, covers the abyss around Antarctica. In the South Pacific, the expansion of Ross Sea Bottom Water (RSBW), the coldest and saltiest variety of AABW, is restricted by bottom topography to areas south of the Pacific-Antarctic Ridge (Orsi et al., 1995).

Geological setting

The drill sites in the CSP are all located on oceanic crust. Proposed Site CSP-1A is located ~160 nmi west of the crest of the EPR, north of Eltanin Fracture Zone. The basement age (Figure **F3**; Eagles, 2006) at this location is about 10 Ma (late Miocene). Proposed Site CSP-2B and proposed alternate Sites CSP-4A and CSP-6A are located at a similar distance to the fracture zone but ~210 nmi east of the EPR crest on slightly older crust with a middle Miocene basement age of ~15 Ma (Figure **F3**). Proposed Southeast Pacific basin Site CSP-3A and proposed alternate Site CSP-5A also lie on middle Miocene age (~15 Ma) oceanic crust.

The sites at the Chilean continental margin are all located on continental crust. Tectonically, the southern Chile margin is characterized by a complex geodynamic setting with oblique convergence between plates, transcurrent motion, and tectonic rotation on land (Polonia et al., 2007). The geodynamic setting of the southernmost Chilean margin is driven by relative movements between three main plates: Antarctica, Scotia, and South America. This complex setting results in a strong segmentation of the southern Chile margin that is clearly visible in bathymetric data and the available multichannel seismic data (Polonia et al., 2007). The two major fore-arc basins at ~53°S–54.5°S and 55°S–56.5°S are characterized by sediment infill as thick as ~3 km (Figure **F4**). We plan to drill one site from the southern fore-arc basin (proposed Site CHI-1C). Seismic Line IT97-171 (Figure **F4**) documents ~3 km of remarkably undeformed sediments in this basin (Polonia et al., 2007). This southern basin most likely formed after the ridge consumption (144–10 Ma) when accretion resumed and contributed to construct the outer high that provided the barrier for the accumulation of continent-derived sediments.

North of ~53°S, subduction in the Chile Trench is more orthogonal and results in a steep slope incised by canyons that run perpendicular to the trench axis. Here, the transition between the undeformed Antarctic abyssal plain and the lower slope is very abrupt and results in a steep slope incised by canyons that run perpendicular to the trench axis. Recent sediment cover is minor at the lower slope, but a relatively small-scale sediment depocenter has been localized at the upper continental slope. This sediment drift (proposed Site CHI-4B and proposed alternate Sites CHI-5A, CHI-7A, and CHI-8A) contains a sediment sequence as thick ~700 m that most likely does not extend beyond the early Pleistocene due to high sedimentation rates.

Seismic studies/site survey data

Since the comprehensive USNS *Eltanin* expeditions in the 1960s to the Drake Passage and Pacific Southern Ocean, there has been scarce conventional sediment coring in the pelagic Pacific Southern Ocean, despite the region's significance in the global climate. In 2009–2010, R/V *Polarstern* Expedition PS75 retrieved sediment cores and seismic presite survey data across the ACC fronts in the South Pacific (Gersonde, 2011). A more recent expedition in spring 2016 (Expedition PS97; Lamy, 2016) focused on the Drake Passage area, recovering high-resolution sediment cores extending over one complete glacial–interglacial cycle, and provided key geophysical and geological surveys for potential IODP drilling locations at the Chilean continental slope and at a deep-sea location about 50 nmi west of the Chile Trench. Selected locations from these two cruises to the central (Expedition PS75) and eastern (Expedition PS97) South Pacific present the base for the present proposal for IODP drilling. Moreover, site selection at the Chile margin benefited from seismic studies by Polonia et al. (2007) based on geophysical surveys during the sixteenth expedition of the R/V *OGS Explora* in 1995. The supporting site survey data for Expedition 383 are archived at the IODP Site Survey Data Bank (**https://ssdb.iodp.org/SSDBquery/SSDBquery.php**; select "383" for proposal number).

Scientific objectives

The overall goal of Expedition 383 is to improve our knowledge of Plio-Pleistocene atmosphere-ocean dynamics of the ACC in the Pacific and their implications for regional and global climate and atmospheric CO_2 based on sediment records with the highest possible resolution. The planned sites (Table **T1**; Figure **F5**) are located at latitudes and water depths where sediments will allow the application of a wide range of siliciclastic, carbonate, and opal-based proxies for reconstructing surface to deep ocean variations and their relation to atmosphere and cryosphere changes with unprecedented stratigraphic detail.

The drilling strategy will allow us to test two major scientific hypotheses.

1. *Hypothesis H1: ACC dynamics and Drake Passage throughflow conditioned the global MOC and high-low climate linkages on orbital and submillennial timescales since the Pliocene.*

The Drake Passage is the major geographic constriction for the ACC and forms an important pathway for the return of upper waters to the Atlantic through the cold-water route of the MOC (Gordon, 1986). Resolving changes in the flow of circumpolar water masses through the Drake Passage is crucial for advancing our understanding of the Southern Ocean's role in affecting ocean and climate change on a global scale. Surface and intermediate water masses flowing through the Drake Passage strongly affect the AMOC, together with the warm-water route inflow of Indian Ocean water masses through the Agulhas Current system (Beal et al., 2011; Knorr and Lohmann, 2003). Complementary sites below the warm-water route were drilled during IODP Expedition 361 (Hall et al., 2015). The potential role of the Drake Passage throughflow in driving changes in the global MOC on glacial–interglacial and millennial timescales is not well constrained (Knorr and Lohmann, 2003; McCave et al., 2014). For the last glacial cycle, Lamy et al. (2015) reconstructed Drake Passage throughflow based on a sediment record (MD07-3128) from the Chilean margin (corresponding to proposed Site CHI-4A) and another record from the southernmost Argentinean continental slope and found a significant glacial decrease in Drake Passage throughflow (Figure **F6**). This finding is consistent with generally reduced current velocities of the ACC during glacials and concomitant reduction in interbasin exchange in the Southern Ocean, most likely regulated by variations in the SWW field over the SAZ and changes in Antarctic sea ice extent.

The geographic locations and water depths of the sites will allow us (1) to compare the dynamics of the ACC *laterally* between the CSP in the vicinity of the EPR (bathymetric constraints) and the ESP before entering the Drake Passage and (2) to investigate the *vertical structure* of the ACC. The planned sites sample the major water masses of the ACC in the Pacific sector of the Southern Ocean from AAIW (proposed Sites CHI-4B, CHI-5A, CHI-7A, and CHI-8A) across the CDW/Pacific Deep Water (PDW) (proposed Sites CSP-1A, CSP-2B, CSP-4A, and CSP-6A) and potentially down to AABW (proposed Sites CSP-3A, ESP-1B, and ESP-2A) (at least for glacial times) (Ferrari et al., 2014).

Downstream from the Drake Passage, a meridional section of sediment records from the Scotia Sea revealed little overall bottom current speed variations between the Last Glacial Maximum (LGM) and the Holocene (McCave et al., 2014) (Figure **F6**). In contrast, a 500,000 y record from the Indian sector of the Southern Ocean suggests that the ACC was weak during warm stages and strong during glacial epochs (Mazaud et al., 2010). Likewise, in the southwest Pacific the deep western boundary current east of New Zealand intensified during glacial periods over the past 1.2 My (Hall et al., 2001), a process related to a northward extension of the ACC along the New Zealand continental margin. Finally, a recent density reconstruction (based on benthic foraminifers) across the ACC south of Australia suggests a moderate increase of the ACC flow during the LGM (Lynch-Stieglitz et al., 2016). Taken together, the substantial disagreement about the ACC flow speed and its potential impact on changes in Drake Passage throughflow in response to glacial–interglacial cycles prevents us from a more complete understanding of MOC dynamics.

Superimposed on the long-term glacial reduction of Drake Passage throughflow, prominent high-amplitude, millennial-scale variability was observed, implying a strong sensitivity of the northern ACC in the Southeast Pacific to suborbital climate variations (Lamy et al., 2015). Enhanced Drake Passage throughflow during Antarctic warm periods is consistent with the previously suggested impact of the bipolar seesaw mechanism on the Southern Ocean (e.g., Anderson et al., 2009; Lamy et al., 2007), leading to, for example, surface water warming, enhanced upwelling, and a stronger ACC caused by southward-shifted SWW. The glacial reduction of the cold-water route occurred in concert with the well-documented decrease of the warm-water route (Agulhas leakage; Beal et al., 2011). The presently available data thus indicate that both of these oceanographic corridors are critical for the South Atlantic contribution to glacial MOC strength changes.

Our planned CHI and ESP sites (Figure **F5**) provide a unique opportunity to extend the existing 60 ky record back into the early Pleistocene and Pliocene and address important questions such as the role of long-term, orbital-scale, and millennial-scale changes in ACC strength and Drake Passage throughflow in warmer-than-present interglacials (e.g., marine isotope stages [MISs] 5e, 11, and 31) or the Pliocene warm period and the link to Antarctic climate fluctuations over multiple glacial–interglacial cycles.

In the Pacific sector of the Southern Ocean, atmosphere-ocean changes between the high, mid, and low latitudes are strongly linked. Pronounced past changes in surface ocean properties at both millennial and orbital timescales, particularly SSTs, indicate an exceptional climate sensitivity to external and internal forcings on these timescales. Glacial–interglacial amplitudes in Subantarctic SSTs are generally >4°C in the Atlantic (Gersonde et al., 2005; Martínez-García et al., 2010), Indian (e.g., De Deckker et al., 2012; Lorrey et al., 2012), and Pacific Southern Ocean (Caniupán et al., 2011; Ho et al., 2012; Pahnke et al., 2003). Millennial-scale fluctuations with amplitudes of ~2–3°C are observed at continental margin sites in the Subantarctic Pacific (SAP) during the last glacial (Barrows et al., 2007; Caniupán et al., 2011; Lamy et al., 2004; Pahnke et al., 2003).

High-amplitude glacial–interglacial SST changes in the SAP Southern Ocean (Ho et al., 2012) are closely coupled to those observed in the subtropical ESP, implying large shifts of the northern ACC system and export of subantarctic surface water masses into the HCS. This variability is probably directly related to variations in the strength and position of the ACC fronts, the SWW, and Drake Passage throughflow (Lamy et al., 2015) (Figure **F6**).

Along the Chilean margin, the reconstructed glacial cooling implies a stronger northward extension of the Antarctic cold-water influence in the ESP during glacials (Ho et al., 2012) compared to the central Pacific (Figure **F6**). The significant glacial decrease in Drake Passage transport, accompanied by a reduction of the ACC transport, strongly reduced the interbasin water mass exchange in the Southern Ocean and enhanced the high-low latitude exchange within the Pacific Eastern Boundary Current System (Figure **F6**). The reacceleration of subantarctic Drake Passage transport matches the major deglacial warming in the subantarctic Southeast Pacific and South Atlantic (Barker and Diz, 2014), suggesting a close coupling of Drake Passage throughflow to the initiation of Southern Hemisphere warming.

Similar to the glacial–interglacial pattern, the inferred millennial-scale changes in Drake Passage throughflow (Lamy et al., 2015) are paralleled by SST changes in proxy records from the Southeast Pacific (Ocean Drilling Program [ODP] Site 1233) (Kaiser and

Lamy, 2010) extending north to the cold tongue in the eastern tropical Pacific (Lea et al., 2006). These data imply that substantial changes in the oceanographic dynamics of the South Pacific gyre are related to the northward deflection of ACC waters at millennial timescales. Paleoceanographic reconstructions based on our CHI and ESP sites, in combination with ODP Leg 202 sites (Figure **F5**) (e.g., Dekens et al., 2007; Lamy et al., 2004; Pena et al., 2008; Rincón-Martinez et al., 2009), will allow us to estimate changes in the coupling between the ACC and the tropical Pacific over various timescales and at warmer-than-present climate states. High-low latitude linkages (both modern and past) in the oceanographically little-explored ESP are important for global climate. The suggested enhanced glacial northward export of cold-water masses to the tropical Pacific reinforces earlier modeling studies that showed the importance of southerly derived surface and intermediate water masses in the tropical Pacific for global cooling during the LGM (Liu et al., 2002).

Expedition 383 drill sites will allow us to better constrain the latitudinal shifts of the Southern Ocean fronts over time to understand the resulting changes in ACC transport, intrabasin mixing, and AAIW production over a wider range of climate states. For example, reconstructions of past changes in the latitudinal position of the SAF suggest as much as 9° latitude northward shifts during glacials, whereas other areas suggest no shift at all (Kohfeld et al., 2013). Smaller shifts probably occurred where the front is bathymetrically confined, as in the vicinity of the EPR (CSP sites). Large shifts likely occurred in the eastern SAP, with the SAF potentially located north of the Drake Passage during peak glacials (Gersonde et al., 2003; Ho et al., 2012; Lamy et al., 2015). As stated above, these changes may substantially affect the Drake Passage throughflow and low-high latitude exchange of heat and nutrients with major implications for the global climate development. Further south, Benz et al. (2016) reconstructed a glacial WSI expansion by ~2°–3° in latitude in the western part of the Pacific sector and an even stronger shift (~5° in latitude) of both the SACCF and the WSI edge in the central part (Figure **F7**). This west–east differentiation in the winter SST pattern and sea ice extent can be related to differences in topographic and atmospheric forcing (Benz et al., 2016).

Despite the strong climate sensitivity of the Subantarctic Southern Ocean, only one available SST record (ODP Site 1090 in the Subantarctic Atlantic) reaches back to the Pliocene (Figure **F8**). Here, the major cooling phase after ~1.6 Ma coincides with the emergence of the eastern tropical Pacific cold tongue and an intensification of the meridional temperature gradients (Martínez-García et al., 2010) (Figure **F8**). The ANDRILL records suggest that high-latitude climate cooling between 3.0 and 2.5 Ma drove both the WAIS and EAIS toward their present expanded cold polar state (Naish et al., 2009). The intensification of Antarctic cooling resulted in strengthened SWW and northward migration of Southern Ocean fronts, which would restrict water exchange between ocean basins (reduced MOC) beginning after 3.3 Ma (McKay et al., 2012). Warm early Pleistocene and Pliocene SSTs are consistent with the poleward-expanded warm pool (Brierley et al., 2009).

Our CSP sites, located on a cross-frontal transect between the modern PF (proposed Site CSP-3A) and the southern SAZ (proposed Sites CSP-1A and CSP-2A) (Table **T1**), will allow a more comprehensive assessment of the temperature evolution of the Pacific Southern Ocean and its relation to atmospheric variations of the SWW, sea ice, and AIS variability during cold and warmer-than-present (e.g., MISs 5, 11, and 31 and the Pliocene warming) time periods. Information on warm periods is critical in assessing the Southern Ocean's role under future warming, especially for AIS melting and associated sea level rise, because ice sheet modeling together with modern observations show that oceanic forcing is the most important forcing mechanism (Pollard and DeConto, 2009; Paolo et al., 2015).

Moreover, temperature records from our high-resolution sites from the Chilean margin (particularly proposed Sites CHI-4A and CHI-5A) and CSP (proposed Sites CSP-2A and CSP-3A) will allow us to compare millennial-scale variations between the Pacific Southern Ocean and Antarctica and do so for a time interval that is well beyond the reach of ice cores. Even on a global scale, such millennial-scale temperature records back into the Pliocene are rare (e.g., Integrated Ocean Drilling Program Site U1313, Naafs et al., 2013; ODP Leg 980, McManus et al., 1999).

2. *Hypothesis H2: variations in the Pacific ACC determine the physical and biological characteristics of the oceanic carbon pump and atmospheric CO_2.*

Atmosphere-ocean-cryosphere interactions and teleconnections between high and low latitudes play an important role in understanding processes and feedbacks of past and future climate change, and the Subantarctic Southern Ocean provides the major link between Antarctica and the low latitudes. In the Southern Ocean, these interactions are believed to control sea ice cover, AIS dynamics, upper ocean stratification, biological nutrient utilization, and exposure rates of deepwater. They have been considered to play a key role in explaining the variability in atmospheric CO_2 concentration. At low latitudes, oceanic circulation changes have profound impacts on large-scale atmospheric circulation patterns, particularly in regard to trade and westerly winds. The SWW strongly impact the upwelling of carbon-rich deep-water masses in the Southern Ocean affecting atmospheric CO_2 (e.g., Anderson et al., 2009) and also control the return flow of intermediate waters to the tropics (Figure **F9**). Moreover, the SWW exert an important control on the upwelling of relatively warm deepwater onto the West Antarctic continental shelf in the Pacific sector, where it causes sub–ice shelf melting and mass loss of the WAIS (e.g., Steig et al., 2012). Thus, the SWW are thought to play a key role in past and future climate change, and yet their strength and position in colder and warmer climates relative to today remain a wide-open question (Kohfeld et al., 2013).

In the modern Southern Ocean, deep waters with high DIC and major nutrient concentrations are carried to the surface by wind-driven upwelling and density-driven overturning. However, phytoplankton growth is limited by the scarcity of iron, and these nutrients return to the subsurface before they are completely consumed. This incomplete utilization of nutrients represents a substantial leak in the modern global biological pump because it allows the escape of deeply sequestered carbon back to the atmosphere, keeping atmospheric CO_2 levels high during interglacial stages. An increase in the efficiency of the global biological pump can be accomplished either by decreasing the physical cycling of deepwater through the surface of the Southern Ocean or by increasing the degree to which surface nutrients are consumed by marine organisms (e.g., as a result of increasing iron availability relative to other nutrients) (Sigman and Boyle, 2000; Sigman et al., 2010).

Paleoceanographic records (mainly from the Atlantic sector of the Southern Ocean) indicate that ice age productivity was lower (Anderson et al., 2009; Kohfeld et al., 2005; Jaccard et al., 2013) in the AZ (i.e., south of the PF), whereas nutrient consumption was higher (Robinson and Sigman, 2008; Studer et al., 2015). These data indicate that the AZ was more strongly stratified during ice ages,

reducing the Antarctic leak in the biological pump and therefore contributing to the lowering of atmospheric CO_2 during glacial times.

In the Subantarctic Atlantic (SAA), higher dust flux, increased productivity and nutrient consumption, and lower atmospheric CO_2 covary during peak glacial times and millennial cold events, a process which has been associated with iron fertilization (e.g., Frank et al., 2000; Kumar et al., 1995; Martínez-García et al., 2009, 2011, 2014). Martinez-Garcia et al. (2009, 2014) suggested that around 40–50 parts per million by volume (ppmv) of the glacial atmospheric CO_2 decline can be attributed to iron fertilization (Figure **F10**), which is in good agreement with model estimates (Hain et al., 2010; Chalk et al., 2017; Brovkin et al., 2007). At ODP Site 1090, the first significant rise in ice age dust and iron deposition over the past 4 My occurred at ~2.7 Ma, whereas the most dramatic rise in dust deposition occurred across the mid-Pleistocene transition (Martínez-García et al., 2011).

For the past million years, higher dust deposition during glacial periods compared to interglacials has also been documented for the Pacific Southern Ocean, suggesting an eastward extension of the influence of Australian and/or New Zealand dust sources (Lamy et al., 2014). In this area, dust fluxes follow the same glacial–interglacial fluctuations, but absolute glacial fluxes in the SAP are about half of those in the Atlantic Southern Ocean (Figure **F11**). As in the Atlantic sector, export production in the SAZ of the Pacific sector over the past ~450 ky is higher during glacial times, but, in contrast to the SAA (Martínez-García et al., 2014), the relationship between productivity and nutrient consumption has not been evaluated in detail yet. Our preliminary data suggest that nutrient consumption increased in response to iron fertilization (A. Martinez-Garcia, unpubl. data).

The drill cores from the Pacific sector of the Southern Ocean will allow us to explore in more detail the glacial–interglacial changes in biological productivity both north and south of the Antarctic PF. Core records, including those from ODP Leg 177, have shown that the glacial-time biological productivity in the SAZ of the Atlantic sector of the Southern Ocean increased during the glacial periods of the Late Quaternary, whereas it decreased in the AZ of this sector (Diekmann, 2007; Jaccard et al., 2013). The glacial productivity decrease in the AZ is under debate and may have been caused either by stratification of the water column (Sigman et al., 2004; Jaccard et al., 2005) or expansion of Antarctic sea ice coverage (Hillenbrand and Cortese, 2006). The new drill core records proposed here will allow us to test whether this pattern is also observed in the Pacific sector of the Southern Ocean, as indicated by Bradtmiller et al. (2009), and help to identify the cause for the potential glacial productivity decrease south of the PF.

Our planned drill sites from the CSP will provide robust data to test to what extent processes found to be active in the Atlantic sector can be translated to the Pacific sector, thus allowing us to construct a more global picture of the Southern Ocean's role in nutrient distribution, biogenic export production, and their impact on CO_2 variations. It is necessary to solve these issues before we can model more realistically the impact on the ocean carbon cycle under different climate boundary conditions.

The ESP and CHI sites will also provide a long-term record of variability of the Patagonian Ice Sheet (PIS). Both terrestrial records from Patagonia and records of ice-rafted debris (IRD) in marine sediment cores from the Chilean margin (Core MD07-3128 at proposed Site CHI-4A) indicate substantial millennial-scale variability of the PIS paralleling dust input changes recorded in Antarctic ice cores. This covariance implies a causal link between ice sheet advances and dust availability (Caniupán et al., 2011; Sudgen et al., 2009). Thus, the CHI sites will provide important baseline information for dust variability in the Atlantic sector of the ACC.

Our two hypotheses contain a large number of challenging research targets critical for paleoceanography and paleoclimatology on a global scale. Our sites in the CSP contain the first drilling transect across the ACC fronts in the Pacific sector of the Southern Ocean. Through comparison to the ESP site, we include a particularly sensitive ocean area where glacial–interglacial changes are strongly amplified. Finally, the CHI sites will provide information on changes at a shallower water depth together with changes in the PIS and potential links to dust input in the Atlantic sector of the Southern Ocean.

The development of reliable, high-resolution age models will be a major effort. Initial low-resolution age models will be generated with traditional biostratigraphy combined with geomagnetic polarity/intensity stratigraphies. Based on previous work on piston cores in the Pacific Southern Ocean, such low-resolution age models can be substantially improved by tuning selected core scanner records to Antarctic ice core data (e.g., dust; Lamy et al., 2014). Figure **F12** shows the correlation of iron content fluctuations (dust) in the site survey cores of our CSP transect from the calcareous sediments north of the SAF (proposed Site CSP-1A) to the opal belt (proposed Site CSP-3A). This figure also illustrates the potential of transferring benthic oxygen isotope stratigraphies from the carbonate sediments into the opal belt, which will be particularly important in obtaining reliable age models for the time interval beyond the reach of the Antarctic ice cores. Additionally, Figure **F12** shows the correlation of SST records based on different proxies (Mg/Ca, TEX-86, and diatom transfer functions) along the transect as an alternative correlation tool across the oceanic fronts. High-resolution TEX-86 SST records have been, for example, used to derive a detailed age model for ODP Site 1094 in the AZ of the South Atlantic (Hayes et al., 2014). Based on the excellent correlation of the different proxies to global climate records, we will also include orbital tuning strategies for older time intervals. Water depths and carbonate preservation at the sites of the Chile margin will likewise allow for oxygen isotope stratigraphies. Core scanner records such as Zr/Rb ratios can be tuned to ice cores and global isotope stacks and will allow for a close intercorrelation among the sites.

Operations plan/drilling strategy

Expedition 383 aims to achieve an ambitious coring program that prioritizes six primary sites and eight alternate sites in 1110–5130 m of water (Tables **T1**, **T2**). Three sites are located in the CSP between the modern PF and the SAZ at water depths ranging from 5100 to 3600 m. Three sites are located in a depth transect along the Chilean margin close to the Drake Passage in ~1110 to ~3900 m of water across the major Southern Ocean water masses. The planned drilling strategy is designed for recovering sediment sequences suitable for high-resolution studies. The sites are located at latitudes and water depths where sediments will allow the application of a wide range of siliciclastic, carbonate, and opal-based proxies for reconstructing surface to deep-ocean variations and their relation to atmosphere and cryosphere changes with unprecedented stratigraphic detail.

The final operations plan and number of sites to be cored is contingent upon the *JOIDES Resolution* operations schedule, operational risks (see below), and the outcome of requests for territorial permission to occupy these sites. The long transit to the central Pacific Ocean is of particular relevance because, should ship speed be less than the estimated average of 10.5 kt, the drilling schedule could be significantly impacted.

Coring strategy will consist of advanced piston corer (APC) coring using nonmagnetic core barrels in three holes (A, B, and C) at each site to ~300 meters below seafloor (mbsf) or APC refusal with the exception of proposed Sites CHI-4B and ESP-1B, which have deeper depth objectives (500 and 400 mbsf, respectively), and proposed Site CSP-1A, which has a shallower depth objective (180 mbsf). As described below, and pending further discussions, at this point only Hole A cores at each site will be oriented.

For planning purposes, the APC refusal depth is estimated at 300 mbsf, although this may vary depending on the formation. APC refusal is conventionally defined as a complete stroke (determined from the standpipe pressure after the shot) not being achieved because the formation is too hard and/or excess force (>100,000 lb) is required to pull the core barrel out of the formation because the sediment is too cohesive or "sticky." In cases where a significant stroke can be achieved but excessive force cannot retrieve the barrel, the core barrel can be "drilled over" (i.e., after the core barrel is successfully shot into the formation, the bit is advanced to some depth to free the core barrel). When APC refusal occurs in a hole before the target depth is reached, the half-length APC (HLAPC) system may be used to deepen the hole before switching to the extended core barrel (XCB) system.

According to the current primary operations plan, Expedition 383 will core ~5740 m of sediment and potentially recover ~5600 m of core. The estimated amount of core recovered is based on 100% recovery with the APC system and 65% recovery with the XCB system. Considering the significant transit time to cover the distances between the Chilean margin sites and the Central Pacific sites (~1290 nmi) and from the Central Pacific to Valparaiso, Chile (~2578 nmi), this coring schedule within the remaining time of the expedition is indeed ambitious and will require tight operational planning and flexibility.

By the time of the publication of this scientific prospectus, proposed primary Site CHI-1C and alternate sites CHI-6A–CHI-8A, ESP-2A, and CSP-4A–CSP-7A are contingent on Environmental Protection and Safety Panel approval.

Downhole measurements strategy

Formation temperature measurements

We plan to use the advanced piston corer temperature tool (APCT-3) to measure formation temperature in the first hole of each site to reconstruct the thermal gradient. This tool can only be deployed with the APC system. The operations plan includes four temperature measurements per site, typically beginning with the fourth core. Should the first three measurements be successful, we may opt not to take a fourth measurement to save time.

Core orientation

We plan to orient all APC cores in one hole per site with the Icefield MI-5 core orientation tool. This tool will be used in conjunction with nonmagnetic coring hardware to the maximum extent possible.

Downhole wireline logging

The downhole wireline logging plan aims to provide a broad set of physical property measurements that can be used for characterization of in situ formation properties (e.g., lithology, structure, and petrophysics) and orbital- and millennial-scale cyclicities. The plan includes deploying two standard IODP tool strings in the final and deepest hole at proposed Sites CHI-4B, CHI-1C, and ESP-1B (Table **T1**). Coring is the top priority at all of the sites, and the scheduled logging program may be modified or abandoned if the coring objectives cannot be met in the allotted time.

The first logging run will be the triple combination (triple combo) tool string, which logs formation resistivity (High-Resolution Laterolog Array [HRLA]/Phasor Dual Induction-Spherically Focused Resistivity Tool [DIT]), density (Hostile Environment Litho-Density Sonde [HLDS]), porosity (Accelerator Porosity Sonde [APS]), natural gamma radiation (NGR; Hostile Environment Natural Gamma Ray Sonde [HNGS]/Enhanced Digital Telemetry Cartridge [EDTC]), and borehole diameter. The magnetic susceptibility sonde (MSS) may be added to the triple combo tool string in place of the porosity tool to provide magnetic field and magnetic susceptibility information. The borehole diameter log provided by the caliper on the density tool will allow assessment of hole conditions (e.g., washouts of sandy beds), log quality, and the potential for success of the following run(s).

Proposed drill sites

Chile margin (Sites CHI-1C and CHI-4B) and eastern South Pacific (Site ESP-1B)

The southern Chile margin is the southernmost area of the South American continent intersecting the northern ACC. It provides the unique opportunity to drill intermediate and deep-water sediment sequences in the Subantarctic ACC, a task that has otherwise been impossible in the ACC (except for the New Zealand margin). We propose to drill sites from ~1100 to ~2100 m water depth at the continental margin off southern Chile (proposed Sites CHI-4B through CHI-1C) and at ~3900 m water depth at the deep southeast Pacific basin west of the Peru-Chile Trench (proposed Site ESP-1B) (Table **T1**; Figure **F13**). The water depths covered by the planned sites sample the major water masses of the northern ACC from AAIW, across CDW/PDW, and potentially down to AABW (Figure **F13**). The sites are located underneath the southward-flowing CHC (Figure **F2**), a northern branch of the ACC that continues toward the Drake Passage and provides a major fraction of the present-day northern Drake Passage transport (Well et al., 2003).

Based on the proximity to South American sediment sources and the available information from site survey cores, we expect very high sedimentation rates (10–50 cm/ky) for the CHI sites. These rates will provide intermediate to deep-water Pleistocene sediment records beyond the reach of Antarctic ice cores with unprecedented time resolution for Southern Ocean records. Despite the high glacial terrigenous input, $CaCO_3$ content in Chile margin sediments (Lamy et al., 2015) is sufficiently high to allow us to utilize the entire suite of carbonate-based paleoceanographic proxies.

Fore-arc basin (Site CHI-1C)

The two major fore-arc basins at ~53°S–54.5°S and 55°S–56.5°S off southern Chile (Polonia et al., 2007) are characterized by sediment infill as thick as ~3 km (Figure **F4**). We propose a primary site

from the southern fore-arc basin (Site CHI-1C). Seismic lines document ~3 km of undeformed sediments in this basin, which most likely formed after the ridge consumption (10–14 Ma) when accretion resumed and constructed the outer high that provided the barrier for the accumulation of continent-derived sediments.

Proposed Site CHI-1C is located at 2091 m water depth (Figure **F2**). Several attempts to obtain longer sediment cores with gravity and piston corers during Cruise PS97 recovered only relatively short cores with a maximum length of ~3 m (Core PS97/109; Lamy, 2016). Core PS97/109 consists of Holocene foraminiferal ooze at the top that grades into silty clay with occasional sandy layers, most likely representing glacial sediments. IRD is occasionally present in small quantities. The lowermost part is again composed of primarily calcareous sediments. Based on several other cores from outside the fore-arc basin, calcareous sediments are confined to interglacials and occur at 6–10 m core depth at more distal locations (Core PS97/111), and they are beyond the reach of conventional gravity and piston coring at proximal sites such as MD07-3128 (proposed Site CHI-4B) (Lamy et al., 2015; Lamy, 2016). Thus, given these overall high glacial sedimentation rates, the biogenic sequence at the base of PS97-109 is most likely a turbidite. The seismic data include as much as ~3 km of thick sediment infill in the fore-arc basin. Assuming a late Miocene age for the basins (Polonia et al., 2007), the thickness of the sediment fill is consistent with high sedimentation rates. Although we are aware that the occurrence of turbidites might interrupt the continuity of the targeted sediment sequences, we expect that the main part of the drilled sediment sequence will be undisturbed, allowing us to address our paleoceanographic targets on high-resolution sediment records from relatively shallow water depths in the core of southward-flowing PDW (Figure **F2**) and to obtain a proximal record of PIS variability. We propose one alternate site (CHI-6A) in the eastern part of the fore-arc basin at a similar water depth.

Sediment drift (Site CHI-4B)

North of ~53°S, subduction in the Chile Trench is more orthogonal and results in a steep slope incised by canyons that run perpendicular to the trench axis. Recent sediment cover is minor at the lower slope, but a relatively small-scale sediment depocenter has been localized at the upper continental slope. This sediment drift (proposed Site CHI-4B at 1111 water depth) is located at the upper continental margin ~30 nmi off the entrance to the Strait of Magellan and contains a sediment sequence as thick as ~700 m. Proposed Site CHI-4B is a shallow drill site at the thickest upper sediment coverage of the drift located close to survey Core MD07-3128 (Lamy et al., 2015). The basement age of the sediment drift is unknown, but a maximum age of ~10 Ma can be derived from the end of the tectonic erosion and start of subsidence at the continental margin (Polonia et al., 2007). Given the high sedimentation rates in Core MD07-3128 (~0.5m/ky in average over the past 60 ky), we expect a younger basal age for the proposed drilling depth of 500 mbsf in the order of ~1–2 Ma.

Piston Core MD07-3128, taken close to the position of proposed Site CHI-4B, provided excellent high-resolution paleoceanographic records (e.g., Caniupán et al., 2011; Lamy et al., 2015). It is located in the major modern AAIW formation area (e.g., Bostock et al., 2013). Sediments at proposed Site CHI-4B are foraminiferal oozes (~30 and 55 wt% $CaCO_3$) during the Holocene underlain by glacial, primarily siliciclastic sediments (~1 to 12 wt% $CaCO_3$). Biogenic opal contents range from 1 to 4 wt%. The lower glacial biogenic carbonate and opal content are primarily due to dilution by enhanced terrigenous sediment supply from the glaciated hinterland, absence of sediment trapping in the fjords, and reduced winnowing by the overlying CHC. We propose three alternate sites, CHI-5A, CHI-7A, and CHI-8A, located on the same sediment drift.

Pelagic eastern South Pacific (Site ESP-1B)

Proposed primary Site ESP-1B is located 95 nmi off Chile at ~3900 m water depth (Figure **F2**) west of the Chile Trench on a topographically elevated ridge with thick sediment cover. Proposed Site ESP-1B lies close to the intersection of two seismic lines and has a sediment thickness of 500–600 m. The oceanic basement age at proposed Site ESP-1B is ~20 Ma (Eagles et al., 2006). Site survey Core PS97/114-1 provided a ~22 m sediment record reaching back to ~475 ky that indicates average sedimentation rates of ~5 cm/ky. Extrapolating this value to depth would result in an age of ~6 Ma for the envisaged drilling to 400 mbsf. Core scanner and bulk sediment data from Core PS97/114-1 indicate strong fluctuations in carbonate versus siliciclastic sediment components. High $CaCO_3$ values are found during interglacials (as high as 50% for MIS 5 and 95% for MIS 11). Glacial sediments are dominated by clay with $CaCO_3$ content below 1 wt%. Remarkably similar fluctuations in grain size most likely relate to variations in currents. Consistent with shallower sediment records (Core MD07-3128 at proposed Site CHI-4B), these data strongly suggest reduced glacial currents (Lamy et al., 2015) with fluctuations following the Antarctic temperature record in great detail. We propose an alternate site, ESP-2A, northeast of the primary site on the same seismic line (Figure **F13**).

Pelagic central South Pacific sites (CSP-1A, CSP -2B, and CSP -3A)

The CSP sites are located along a cross-frontal transect across the ACC in the central Pacific Southern Ocean from north of the present-day SAF to the modern PF (Figure **F2**). The arrangement of the sites provides depth transects between 5100 and 3600 m covering AABW and CDW. The northern sites are located at the outer reaches of the EPR but are ~160 nmi west (proposed Site CSP-1A) and ~210 nmi east (proposed Site CSP-2B), respectively, from the crest (Figure **F14**) and thus not affected by volcanic processes.

Proposed Site CSP-1A (water depth = ~3621 m) provides ~180 m thick sediments that reach back to the late Miocene. An ~14 m long piston core from this site contains primarily $CaCO_3$ (>90 wt% during interglacials and 30–60 wt% during glacials when opal and lithogenic contents reach 10–20 wt% and 30–50 wt%, respectively). Based on the excellent benthic oxygen isotope stratigraphy (Lamy et al., 2014; Ullermann et al., 2016), the core reaches back to ~450 ka (sedimentation rates ~3 cm/ky) (Figure **F12**). Lithogenic content and paleoproductivity estimates based on Core PS75/059-2 have a remarkable similarity to dust content fluctuations in Antarctic ice cores (Lamy et al., 2014). We will drill a 180 m long sequence from this site down to basement.

Proposed Site CSP-2B (water depth = ~4111 m) is located at the eastern flank of the southernmost EPR, ~100 nmi north of the modern average SAF. The seismic cross profiles indicate ~650 m thick sediments that reach back to the Miocene. We propose to drill to 300 mbsf to recover the Plio-Pleistocene section. A ~22 m long piston core (PS75/054-1) covering the past ~165 ky at proposed Site CSP-2A contains an alternation of diatom ooze (glacials; ~12–20 wt% $CaCO_3$) and diatomaceous calcareous ooze (interglacials; ~50–70 wt% $CaCO_3$) deposited at high sedimentation rates (~5–25

cm/ky) (Figure **F12**). Siliciclastic content and terrestrial biomarker data indicate significant dust input that largely follow the variability pattern observed in the lower resolution central Pacific Southern Ocean (Lamy et al., 2014) and Antarctic ice core dust records. Preliminary SST reconstructions indicate fluctuations generally in phase with ice core records (Figure **F12**). We propose two alternate sites nearby: CSP-4A, CSP-6A, and CSP-7A (Figure **F14**).

Proposed Site CSP-3A (water depth = ~5130 m) is located in the northern Bellingshausen Sea ~80 nmi north of the PF. Bathymetric and PARASOUND surveys around proposed Site CSP-3A document the presence of packages of sediment (diatom ooze) as thick as 100 m above a more densely acoustically stratified sediment section (diatomaceous mud). Together with the high sedimentation rates documented in piston Cores PS58/271-1 (Figure **F12**) and PS75/52-3, these data suggest that the site is located on a regional sediment drift active since ~250 ka. Before, sedimentation rates were anticipated to be lower. We propose to drill to ~300 mbsf to recover a complete Plio-Pleistocene sequence. The available seismic information and the projected basement ages (Eagles, 2006) suggest that oldest sediments at the site at ~600 mbsf reach around the Oligocene/Miocene boundary at deep-water proposed Site CSP-3A. Paleoceanographic records from survey Core PS58/271-1 document millennial-scale changes in SST and WSI (Figure **F12**). Stratigraphically, the records can be tied to the Subantarctic carbonate records further north (Figure **F12**). We propose one alternate site (CSP-5A) on the same drift, southwest of the primary site.

Risks and contingency

We will operate in areas of the South Pacific Ocean that are in the range of the maximum wind speeds of the SWW. Average wind speeds reach maximum values during austral summer (October through February). Although Expedition 383 is scheduled during austral winter (June through September), when winds speeds in the Pacific Southern Ocean are substantially reduced, encountering rough weather and seas during transit or while on site could result in the loss of substantial operational time.

Other potential risks identified:

- We have to obtain approval from Chile to conduct drilling and coring operations in their territorial waters.
- Penetration rates are an estimate only. Slower penetration rates will require more time to meet depth objectives.
- Unstable hole conditions can impact coring and downhole logging operations.
- The presence of sand beds can be detrimental to core recovery.
- The operations plan is ambitious for the time available. Good time management will be extremely important to mitigate this risk.
- Even though the southernmost Site CSP-3A is located significantly north of the WSI margin, very occasional passing icebergs are possible.

All of these factors may affect drilling, coring, and downhole logging operations. In addition to operational risks, the remote location of half of the drill sites presents a risk to personnel in the event of illness/injury. All expedition members should ensure they are physically and mentally healthy to sail.

Sampling and data sharing strategy

Shipboard and shore-based researchers should refer to the *IODP Sample, Data, and Obligations Policy and Implementation Guidelines* (**http://www.iodp.org/top-resources/program-documents/policies-and-guidelines**). This document outlines the policy for distributing IODP samples and data to research scientists, curators, and educators. The document also defines the obligations that sample and data recipients incur. The Sample Allocation Committee (SAC) will work with the entire scientific party to formulate a formal expedition-specific sampling plan for shipboard and postexpedition sampling. The SAC is composed of the Co-Chief Scientists, Expedition Project Manager/Staff Scientist, and IODP Curator on shore or curatorial representative on board the ship.

Every member of the science party is obligated to carry out scientific research for the expedition and publish the results. Shipboard and potential shore-based scientists are expected to submit a research plan accompanied by a sample and/or data request using the Sample and Data Request Database (**http://iodp.tamu.edu/sdrm**) at least 4–5 months before the beginning of the expedition. Based on shipboard and shore-based research plans submitted by this deadline, the SAC will prepare a tentative sampling plan, which will be revised on the ship as dictated by recovery and expedition objectives. The sampling plan will be subject to modification depending upon the actual material recovered and collaborations that may evolve between scientists during the expedition. The SAC must approve any modifications of the sampling strategy during the expedition. Given the specific objectives of Expedition 383, great care will be taken to maximize shared sampling to promote integration of data sets and enhance scientific collaboration among members of the scientific party so that our scientific objectives are met and each scientist has the opportunity to contribute.

All sample sizes and frequencies must be justified on a scientific basis and will depend on core recovery, the full spectrum of other requests, and the expedition objectives. Some redundancy of measurement is unavoidable, but minimizing the duplication of measurements among the shipboard party and identified shore-based collaborators will be a major factor in evaluating sample requests.

If critical intervals are recovered, there may be considerable demand for samples from a limited amount of cored material. These intervals may require special handling, a higher sampling density, reduced sample size, or continuous core sampling by a single investigator. A sampling plan coordinated by the SAC may be required before critical intervals are sampled. Substantial collaboration and cooperation will be required.

Shipboard sampling will be restricted to acquiring ephemeral data types and shipboard measurements. Whole-round samples may be taken for interstitial water measurements and physical property measurements as dictated by the shipboard sampling plan that will be finalized during the first few days of the expedition. At the discretion of the SAC, limited low-resolution sampling for personal research that is required to define plans for the postexpedition sampling meeting may be approved. The majority of the sampling for postexpedition research will be postponed until a shore-based sampling party that will be implemented approximately ~3–5 months after the end of the Expedition 383 at the IODP Gulf Coast Repository in College Station, Texas (USA). The data collected during the expedition will be used to produce stratigraphic spliced sections

and age models for each site, which are critical to the overall objectives of the expedition and for planning for higher resolution sampling postexpedition.

Expedition scientists and scientific participants

The current list of participants for Expedition 383 can be found at **http://iodp.tamu.edu/scienceops/expeditions/dynamics_of_pacific_ACC.html**.

References

Anderson, R.F., Ali, S., Bradtmiller, L.I., Nielsen, S.H.H., Fleisher, M.Q., Anderson, B.E., and Burckle, L.H., 2009. Wind-driven upwelling in the Southern Ocean and the deglacial rise in atmospheric CO_2. *Science,* 323(5920):1443–1448. **https://doi.org/10.1126/science.1167441**

Anderson, R.F., Barker, S., Fleisher, M., Gersonde, R., Goldstein, S.L., Kuhn, G., Mortyn, P.G., Pahnke, K., and Sachs, J.P., 2014. Biological response to millennial variability of dust and nutrient supply in the Subantarctic South Atlantic Ocean. *Philosophical Transactions of the Royal Society A: Mathematical, Physical and Engineering Sciences,* 372(219):20130054. **https://doi.org/10.1098/rsta.2013.0054**

Barker, S., and Diz, P., 2014. Timing of the descent into the last ice age determined by the bipolar seesaw. *Paleoceanography and Paleoclimatology,* 29(6):489–507. **https://doi.org/10.1002/2014PA002623**

Barrows, T.T., Juggins, S., De Deckker, P., Calvo, E., and Pelejero, C., 2007. Long-term sea surface temperature and climate change in the Australian–New Zealand region. *Paleoceanography and Paleoclimatology,* 22(2):PA2215. **https://doi.org/10.1029/2006PA001328**

Beal, L.M., De Ruijter, W.P.M., Biastoch, A., Zahn, R., and SCOR/WCRP/IAPSO Working Group 136, 2011. On the role of the Agulhas system in ocean circulation and climate. *Nature,* 472(7344):429–436. **https://doi.org/10.1038/nature09983**

Benz, V., Esper, O., Gersonde, R., Lamy, F., and Tiedemann, R., 2016. Last Glacial Maximum sea surface temperature and sea-ice extent in the Pacific sector of the Southern Ocean. *Quaternary Science Reviews,* 146:216–237. **https://doi.org/10.1016/j.quascirev.2016.06.006**

Bostock, H.C., Sutton, P.J., Williams, M.J.M., and Opdyke, B.N., 2013. Reviewing the circulation and mixing of Antarctic Intermediate Water in the South Pacific using evidence from geochemical tracers and Argo float trajectories. *Deep Sea Research, Part I: Oceanographic Research Papers,* 73:84–98. **https://doi.org/10.1016/j.dsr.2012.11.007**

Bradtmiller, L.I., Anderson, R.F., Fleisher, M.Q., and Burckle, L.H., 2009. Comparing glacial and Holocene opal fluxes in the Pacific sector of the Southern Ocean. *Paleoceanography and Paleoclimatology,* 24(2):PA2214. **https://doi.org/10.1029/2008PA001693**

Brierley, C.M., Fedorov, A.V., Liu, Z., Herbert, T.D., Lawrence, K.T., and LaRiviere, J.P., 2009. Greatly expanded tropical warm pool and weakened Hadley circulationin the early Pliocene. *Science,* 323(5922):1714–1718. **https://doi.org/10.1126/science.1167625**

Brovkin, V., Ganopolski, A., Archer, D., and Rahmstorf, S., 2007. Lowering of glacial atmospheric CO_2 in response to changes in oceanic circulation and marine biogeochemistry. *Paleoceanography and Paleoclimatology,* 22(4):PA4202. **https://doi.org/10.1029/2006PA001380**

Callahan, J.E., 1972. The structure and circulation of deep water in the Antarctic. *Deep-Sea Research and Oceanographic Abstracts,* 19(8):563–575. **https://doi.org/10.1016/0011-7471(72)90040-X**

Caniupán, M., Lamy, F., Lange, C.B., Kaiser, J., Arz, H., Kilian, R., Baeza Urrea, O., et al., 2011. Millennial-scale sea surface temperature and Patagonian Ice Sheet changes off southernmost Chile (53°S) over the past ~60 kyr. *Paleoceanography and Paleoclimatology,* 26(3):PA3221. **https://doi.org/10.1029/2010PA002049**

Chaigneau, A., and Pizarro, O., 2005. Surface circulation and fronts of the South Pacific Ocean, east of 120°W. *Geophysical Research Letters,* 32(8):L08605. **https://doi.org/10.1029/2004GL022070**

Chalk, T.B., Hain, M.P., Foster, G.L., Rohling, E.J., Sexton, P.F., Badger, M.P.S., Cherry, S.G., et al., 2017. Causes of ice age intensification across the Mid-Pleistocene Transition. *Proceedings of the National Academy of Sciences of the United States of America,* 114(50):13114–13119. **https://doi.org/10.1073/pnas.1702143114**

Chase, Z., Anderson, R.F., Fleisher, M.Q., and Kubik, P.W., 2003. Accumulation of biogenic and lithogenic material in the Pacific sector of the Southern Ocean during the past 40,000 years. *Deep Sea Research, Part II: Topical Studies in Oceanography,* 50(3–4):799–832. **https://doi.org/10.1016/S0967-0645(02)00595-7**

Chase, Z., Kohfeld, K.E., and Matsumoto, K., 2015. Controls on biogenic silica burial in the Southern Ocean. *Global Biogeochemical Cycles,* 29(10):1599–1616. **https://doi.org/10.1002/2015GB005186**

Cook, C.P., van de Flierdt, T., Williams, T., Hemming, S.R., Iwai, M., Kobayashi, M., Jimenez-Espejo, F.J., et al., 2013. Dynamic behaviour of the East Antarctic Ice Sheet during Pliocene warmth. *Nature Geoscience,* 6(9):765–769. **https://doi.org/10.1038/ngeo1889**

Cortese, G., Gersonde, R., Hillenbrand, C.-D., and Kuhn, G., 2004. Opal sedimentation shifts in the world ocean over the last 15 Myr. *Earth and Planetary Science Letters,* 224(3–4):509–527. **https://doi.org/10.1016/j.epsl.2004.05.035**

de Baar, H.J.W., de Jong, J.T.M., Bakker, D.C.E., Löscher, B.M., Veth, C., Bathmann, U., and Smetacek, V., 1995. Importance of iron for plankton blooms and carbon dioxide drawdown in the Southern Ocean. *Nature,* 373(6513):412–415. **https://doi.org/10.1038/373412a0**

De Deckker, P., Moros, M., Perner, K., and Jansen, E., 2012. Influence of the tropics and southern westerlies on glacial interhemispheric asymmetry. *Nature Geoscience,* 5(4):266–269. **https://doi.org/10.1038/ngeo1431**

Deacon, G.E.R., 1937. *Discovery Reports* (Volume 15): *The Hydrology of the Southern Ocean:* Cambridge, United Kingdom (Cambridge University Press).

Dekens, P.S., Ravelo, A.C., and McCarthy, M.D., 2007. Warm upwelling regions in the Pliocene warm period. *Paleoceanography and Paleoclimatology,* 22(3):PA3211. **https://doi.org/10.1029/2006PA001394**

Diekmann, B., 2007. Sedimentary patterns in the late Quaternary Southern Ocean. *Deep Sea Research, Part II: Topical Studies in Oceanography,* 54(21–22):2350–2366. **https://doi.org/10.1016/j.dsr2.2007.07.025**

Eagles, G., 2006. Deviations from an ideal thermal subsidence surface in the southern Pacific Ocean. *Terra Antarctica Reports,* 12:109–118.

Eagles, G., Livermore, R., and Morris, P., 2006. Small basins in the Scotia Sea: the Eocene Drake Passage gateway. *Earth and Planetary Science Letters,* 242(3–4):343–353. **https://doi.org/10.1016/j.epsl.2005.11.060**

Esper, O., and Gersonde, R., 2014. Quaternary surface water temperature estimations: new diatom transfer functions for the Southern Ocean. *Palaeogeography, Palaeoclimatology, Palaeoecology,* 414:1–19. **https://doi.org/10.1016/j.palaeo.2014.08.008**

Expedition 318 Scientists, 2010. *Expedition 318 Preliminary Report: Wilkes Land Glacial History*. Integrated Ocean Drilling Program. **https://doi.org/10.2204/iodp.pr.318.2010**

Ferrari, R., Provost, C., Park, Y.-H., Sennéchael, N., Koenig, Z., Sekma, H., Garric, G., and Bourdallé-Badie, R., 2014. Heat fluxes across the Antarctic Circumpolar Current in Drake Passage: mean flow and eddy contributions. *Journal of Geophysical Research: Oceans,* 119(9):6381–6402. **https://doi.org/10.1002/2014JC010201**

Florindo, F., Nelson, A.E., and Haywood, A.M., 2008. Introduction to "Antarctic cryosphere and Southern Ocean climate evolution (Cenozoic–Holocene)." *Palaeogeography, Palaeoclimatology, Palaeoecology,* 260(1–2):1–7. **https://doi.org/10.1016/j.palaeo.2007.12.001**

Frank, M., Gersonde, R., van der Loeff, M.R., Bohrmann, G., Nürnberg, C.C., Kubik, P.W., Suter, M., and Mangini, A., 2000. Similar glacial and interglacial export bioproductivity in the Atlantic sector of the Southern Ocean: multiproxy evidence and implications for glacial atmospheric CO_2. *Paleoceanography and Paleoclimatology,* 15(6):642–658. **https://doi.org/10.1029/2000PA000497**

Gersonde, R., 2011. The Expedition of the Research Vessel "*Polarstern*" to the Polar South Pacific Sea in 2009/2010 (ANT-XXVI/2 - BIPOMAC). *Berichte zur Polar und Meeresforschung,* 632. **http://epic.awi.de/29941/**

Gersonde, R., Abelmann, A., Brathauer, U., Becquey, S., Bianchi, C., Cortese, G., Grobe, H., Kuhn, G., Niebler, H.-S., Segl, M., Sieger, R., Zielinski, U., and Fütterer, D.K., 2003. Last glacial sea surface temperatures and sea-ice extent in the Southern Ocean (Atlantic-Indian sector): a multiproxy approach. *Paleoceanography,* 18(3):1061. **https://doi.org/10.1029/2002PA000809**

Gersonde, R., Crosta, X., Abelmann, A., and Armand, L., 2005. Sea-surface temperature and sea ice distribution of the Southern Ocean at the EPILOG Last Glacial Maximum—a circum-Antarctic view based on siliceous microfossil records. *Quaternary Science Reviews,* 24(7–9):869–896. **https://doi.org/10.1016/j.quascirev.2004.07.015**

Gordon, A.L., 1986. Interocean exchange of thermocline water. *Journal of Geophysical Research: Oceans,* 91(C4):5037–5046. **https://doi.org/10.1029/JC091iC04p05037**

Hain, M.P., Sigman, D.M., and Haug, G.H., 2010. Carbon dioxide effects of Antarctic stratification, North Atlantic Intermediate Water formation, and subantarctic nutrient drawdown during the last ice age: diagnosis and synthesis in a geochemical box model. *Global Biogeochemical Cycles,* 24(4):GB4023. **https://doi.org/10.1029/2010GB003790**

Hall, I.R., Hemming, S.R., and LeVay, L.J., 2015. *Expedition 361 Scientific Prospectus: South African Climates (Agulhas LGM Density Profile).* International Ocean Discovery Program. **https://doi.org/10.14379/iodp.sp.361.2015**

Hall, I.R., McCave, I.N., Shackleton, N.J., Weedon, G.P., and Harris, S.E., 2001. Intensified deep Pacific inflow and ventilation in Pleistocene glacial times. *Nature,* 412(6849):809–812. **https://doi.org/10.1038/35090552**

Hayes, C.T., Martínez-García, A., Hasenfratz, A.P., Jaccard, S.L., Hodell, D.A., Sigman, D.M., Haug, G.H., and Anderson, R.F., 2014. A stagnation event in the deep South Atlantic during the last interglacial period. *Science,* 346(6216):1514–1517. **https://doi.org/10.1126/science.1256620**

Hillenbrand, C.-D., and Cortese, G., 2006. Polar stratification: a critical view from the Southern Ocean. *Palaeogeography, Palaeoclimatology, Palaeoecology,* 242(3–4):240–252. **https://doi.org/10.1016/j.palaeo.2006.06.001**

Ho, S.L., Mollenhauer, G., Lamy, F., Martínez-Garcia, A., Mohtadi, M., Gersonde, R., Hebbeln, D., Nunez-Ricardo, S., Rosell-Melé, A., and Tiedemann, R., 2012. Sea surface temperature variability in the Pacific sector of the Southern Ocean over the past 700 kyr. *Paleoceanography and Paleoclimatology,* 27(4):PA4202. **https://doi.org/10.1029/2012PA002317**

Jaccard, S.L., Haug, G.H., Sigman, D.M., Pedersen, T.F., Thierstein, H.R., and Röhl, U., 2005. Glacial/interglacial changes in subarctic North Pacific stratification. *Science,* 308(5724):1003–1006. **https://doi.org/10.1126/science.1108696**

Jaccard, S.L., Hayes, C.T., Martínez-García, A., Hodell, D.A., Anderson, R.F., Sigman, D.M., and Haug, G.H., 2013. Two modes of change in Southern Ocean productivity over the past million years. *Science,* 339(6126):1419–1423. **https://doi.org/10.1126/science.1227545**

Kaiser, J., and Lamy, F., 2010. Links between Patagonian Ice Sheet fluctuations and Antarctic dust variability during the last glacial period (MIS 4–2). *Quaternary Science Reviews,* 29(11–12):1464–1471. **https://doi.org/10.1016/j.quascirev.2010.03.005**

Kanfoush, S.L., Hodell, D.A., Charles, C.D., Janecek, T.R., and Rack, F.R., 2002. Comparison of ice-rafted debris and physical properties in ODP Site 1094 (South Atlantic) with the Vostok ice core over the last four climate cycles. *Palaeogeography, Palaeoclimatology, Palaeoecology,* 182(3–4):329–349. **https://doi.org/10.1016/S0031-0182(01)00502-8**

Kawabe, M., and Fujio, S., 2010. Pacific Ocean circulation based on observation. *Journal of Oceanography,* 66(3):389–403. **https://doi.org/10.1007/s10872-010-0034-8**

Knorr, G., and Lohmann, G., 2003. Southern Ocean origin for the resumption of Atlantic thermohaline circulation during deglaciation. *Nature,* 424(6948):532–536. **https://doi.org/10.1038/nature01855**

Koenig, Z., Provost, C., Ferrari, R., Sennéchael, N., and Rio, M.-H., 2014. Volume transport of the Antarctic Circumpolar Current: production and validation of a 20 year long time series obtained from in situ and satellite observations. *Journal of Geophysical Research: Oceans,* 119(8):5407–5433. **https://doi.org/10.1002/2014JC009966**

Kohfeld, K.E., Graham, R.M., de Boer, A.M., Sime, L.C., Wolff, E.W., Le Quéré, C., and Bopp, L., 2013. Southern Hemisphere westerly wind changes during the Last Glacial Maximum: paleo-data synthesis. *Quaternary Science Reviews,* 68:76–95. **https://doi.org/10.1016/j.quascirev.2013.01.017**

Kohfeld, K.E., Le Quéré, C., Harrison, S.P., and Anderson, R.F., 2005. Role of marine biology in glacial–interglacial CO_2 cycles. *Science,* 308(5718):74–78. **https://doi.org/10.1126/science.1105375**

Kuhlbrodt, T., Griesel, A., Montoya, M., Levermann, A., Hofmann, M., and Rahmstorf, S., 2007. On the driving processes of the Atlantic meridional overturning circulation. *Reviews of Geophysics,* 45(2):RG2001. **https://doi.org/10.1029/2004RG000166**

Kumar, N., Anderson, R.F., Mortlock, R.A., Froelich, P.N., Kubik, P., Dittrich-Hannen, B., and Suter, M., 1995. Increased biological productivity and export production in the glacial Southern Ocean. *Nature,* 378(6558):675–680. **https://doi.org/10.1038/378675a0**

Lamy, F., 2016. The Expedition PS97 of the Research Vessel *POLARSTERN* to the Drake Passage in 2016. *Berichte zur Polar und Meeresforschung,* 701. **http://epic.awi.de/41674/**

Lamy, F., Arz, H.W., Kilian, R., Lange, C.B., Lembke-Jene, L., Wengler, M., Kaiser, J., Baeza-Urrea, O., Hall, I.R., Harada, N., and Tiedemann, R., 2015. Glacial reduction and millennial-scale variations in Drake Passage throughflow. *Proceedings of the National Academy of Sciences of the United States of America,* 112(44):13496–13501. **https://doi.org/10.1073/pnas.1509203112**

Lamy, F., Gersonde, R., Winckler, G., Esper, O., Jaeschke, A., Kuhn, G., Ullermann, J., Martinez-Garcia, A., Lambert, F., and Kilian, R., 2014. Increased dust deposition in the Pacific Southern Ocean during glacial periods. *Science,* 343(6169):403–407. **https://doi.org/10.1126/science.1245424**

Lamy, F., Kaiser, J., Arz, H.W., Hebbeln, D., Ninnemann, U., Timm, O., Timmermann, A., and Toggweiler, J.R., 2007. Modulation of the bipolar seesaw in the southeast Pacific during Termination 1. *Earth and Planetary Science Letters,* 259(3–4):400–413. **https://doi.org/10.1016/j.epsl.2007.04.040**

Lamy, F., Kaiser, J., Ninnemann, U., Hebbeln, D., Arz, H.W., and Stoner, J., 2004. Antarctic timing of surface water changes off Chile and Patagonian Ice Sheet response. *Science,* 304(5679):1959–1962. **https://doi.org/10.1126/science.1097863**

Lea, D.W., Pak, D.K., Belanger, C.L., Spero, H.J., Hall, M.A., and Shackleton, N.J., 2006. Paleoclimate history of Galápagos surface waters over the last 135,000 yr. *Quaternary Science Reviews,* 25(11–12):1152–1167. **https://doi.org/10.1016/j.quascirev.2005.11.010**

Liu, Z., Shin, S.-I., Otto-Bliesner, B., Kutzbach, J.E., Brady, E.C., and Lee, D.E., 2002. Tropical cooling at the Last Glacial Maximum and extratropical ocean ventilation. *Geophysical Research Letters,* 29(10):48-1–48-4. **https://doi.org/10.1029/2001GL013938**

Lorrey, A.M., Vandergoes, M., Almond, P., Renwick, J., Stephens, T., Bostock, H., Mackintosh, A., et al., 2012. Palaeocirculation across New Zealand during the Last Glacial Maximum at ~21 ka. *Quaternary Science Reviews,* 36:189–213. **https://doi.org/10.1016/j.quascirev.2011.09.025**

Lynch-Stieglitz, J., Ito, T., and Michel, E., 2016. Antarctic density stratification and the strength of the circumpolar current during the Last Glacial Maximum. *Paleoceanography and Paleoclimatology,* 31(5):539–552. **https://doi.org/10.1002/2015PA002915**

Maksym, T., Stammerjohn, S.E., Ackley, S., and Massom, R., 2012. Antarctic sea ice—a polar opposite? *Oceanography,* 25(3):140–151. **https://doi.org/10.5670/oceanog.2012.88**

Marshall, J., and Speer, K., 2012. Closure of the meridional overturning circulation through Southern Ocean upwelling. *Nature Geoscience,* 5(3):171–180. **https://doi.org/10.1038/ngeo1391**

Martin, J.H., 1990. Glacial–interglacial CO_2 change: the iron hypothesis. *Paleoceanography and Paleoclimatology,* 5(1):1–13. **https://doi.org/10.1029/PA005i001p00001**

Martínez-Garcia, A., Rosell-Melé, A., Geibert, W., Gersonde, R., Masqué, P., Gaspari, V., and Barbante, C., 2009. Links between iron supply, marine productivity, sea surface temperature, and CO_2 over the last 1.1 Ma. *Paleoceanography and Paleoclimatology,* 24(1):PA1207. **https://doi.org/10.1029/2008PA001657**

Martínez-Garcia, A., Rosell-Melé, A., Jaccard, S.L., Geibert, W., Sigman, D.M., and Haug, G.H., 2011. Southern Ocean dust–climate coupling over the past four million years. *Nature,* 476(7360):312–315. **https://doi.org/10.1038/nature10310**

Martínez-Garcia, A., Rosell-Melé, A., McClymont, E.L., Gersonde, R., and Haug, G.H., 2010. Subpolar link to the emergence of the modern equatorial Pacific cold tongue. *Science,* 328(5985):1550–1553. **https://doi.org/10.1126/science.1184480**

Martínez-Garcia, A., Sigman, D.M., Ren, H., Anderson, R.F., Straub, M., Hodell, D.A., Jaccard, S.L., Eglinton, T.I., and Haug, G.H., 2014. Iron fertilization of the Subantarctic Ocean during the Last Ice Age. *Science,* 343(6177):1347–1350. **https://doi.org/10.1126/science.1246848**

Mazaud, A., Michel, E., Dewilde, F., and Turon, J.L., 2010. Variations of the Antarctic Circumpolar Current intensity during the past 500 ka. *Geochemistry, Geophysics, Geosystems,* 11(8):Q08007. **https://doi.org/10.1029/2010GC003033**

McCartney, M.S., 1977. Subantarctic mode water. *In* Angel, M. (Ed.), *A Voyage of Discovery: George Deacon 70th Anniversary Volume.* Deep-Sea Research and Oceanographic Abstracts, 24:103–119.

McCave, I.N., Crowhurst, S.J., Kuhn, G., Hillenbrand, C.D., and Meredith, M.P., 2014. Minimal change in Antarctic Circumpolar Current flow speed between the last glacial and Holocene. *Nature Geoscience,* 7(2):113–116. **https://doi.org/10.1038/ngeo2037**

McKay, R., Naish, T., Carter, L., Riesselman, C., Dunbar, R., Sjunneskog, C., Winter, D., et al., 2012. Antarctic and Southern Ocean influences on late Pliocene global cooling. *Proceedings of the National Academy of Sciences of the United States of America,* 109(17):6423–6428. **https://doi.org/10.1073/pnas.1112248109**

McManus, J.F., Oppo, D.W., and Cullen, J.L., 1999. A 0.5-million-year record of millennial-scale climate variability in the North Atlantic. *Science,* 283(5404):971–975. **https://doi.org/10.1126/science.283.5404.971**

Meijers, A.J.S., 2014. The Southern Ocean in the Coupled Model Intercomparison Project Phase 5. *Philosophical Transactions of the Royal Society, A: Mathematical, Physical & Engineering Sciences,* 372(2019):20130296. **https://doi.org/10.1098/rsta.2013.0296**

Meredith, M.P., Woodworth, P.L., Chereskin, T.K., Marshall, D.P., Allison, L.C., Bigg, G.R., Donohue, K., et al., 2011. Sustained monitoring of the Southern Ocean at Drake Passage: past achievements and future priorities. *Reviews of Geophysics,* 49(4):RG4005. **https://doi.org/10.1029/2010RG000348**

Naafs, B.D.A., Hefter, J., and Stein R., 2013. Millennial-scale ice rafting events and Hudson Strait Heinrich(-like) events during the late Pliocene and Pleistocene: a review. *Quaternary Science Reviews,* 80:1–28. **https://doi.org/10.1016/j.quascirev.2013.08.014**

Naish, T.R., Powell, R., Levy, R., Wilson, G., Scherer, R., Talarico, F., Krissek, L., et al., 2009. Obliquity-paced Pliocene West Antarctic Ice Sheet oscillations. *Nature,* 458(7236):322–329. **https://doi.org/10.1038/nature07867**

Orsi, A.H., Johnson, G.C., and Bullister, J.L., 1999. Circulation, mixing, and production of Antarctic bottom water. *Progress in Oceanography,* 43(1):55–109. **https://doi.org/10.1016/S0079-6611(99)00004-X**

Orsi, A.H., Whitworth III, T., and Nowlin, W.D., Jr., 1995. On the meridional extent and fronts of the Antarctic Circumpolar Current. *Deep-Sea Research, Part I,* 42(5):641–673. **https://doi.org/10.1016/0967-0637(95)00021-W**

Pahnke, K., Zahn, R., Elderfield, H., and Schulz, M., 2003. 340,000-year centennial-scale marine record of Southern Hemisphere climatic oscillation. *Science,* 301(5635):948–952. **https://doi.org/10.1126/science.1084451**

Paolo, F.S., Fricker, H.A., and Padman, L., 2015. Volume loss from Antarctic ice shelves is accelerating. *Science,* 348(6232):327–331. **https://doi.org/10.1126/science.aaa0940**

Parrenin, F., Masson-Delmotte, V., Köhler, P., Raynaud, D., Paillard, D., Schwander, J., Barbante, C., Landais, A., Wegner, A., and Jouzel, J., 2013. Synchronous change of atmospheric CO_2 and Antarctic temperature during the Last Deglacial Warming. *Science,* 339(6123):1060–1063. **https://doi.org/10.1126/science.1226368**

Pena, L.D., Cacho, I., Ferretti, P., and Hall, M.A., 2008. El Niño-Southern Oscillation-like variability during glacial terminations and interlatitudinal teleconnections. *Paleoceanography and Paleoclimatology,* 23(3):PA3101. **https://doi.org/10.1029/2008PA001620**

Pollard, D., and DeConto, R.M, 2009. Modelling West Antarctic Ice Sheet growth and collapse through the past five million years. *Nature,* 458(7236):329–332. **https://doi.org/10.1038/nature07809**

Polonia, A., Torelli, L., Brancolini, G., and Loreto, M.-F., 2007. Tectonic accretion versus erosion along the southern Chile Trench: oblique subduction and margin segmentation. *Tectonics,* 26(3):TC1983. **https://doi.org/10.1029/2006TC001983**

Reid, J.L., and Lynn, R.J., 1971. On the influence of the Norwegian-Greenland and Weddell Seas upon the bottom waters of the Indian and Pacific Oceans. *Deep Sea Research and Oceanographic Abstracts,* 18(11):1063–1088. **https://doi.org/10.1016/0011-7471(71)90094-5**

Renault, A., Provost, C., Sennéchael, N., Barré, N., and Kartavtseff, A., 2011. Two full-depth velocity sections in the Drake Passage in 2006—transport estimates. *Deep Sea Research, Part II: Topical Studies in Oceanography,* 58(25–26):2572–2591. **https://doi.org/10.1016/j.dsr2.2011.01.004**

Reynolds, R.W., Rayner, N.A., Smith, T.M., Stokes, D.C., and Wang, W., 2002. An improved in situ and satellite SST analysis for climate. *Journal of Climate,* 15(13):1609–1625. **https://doi.org/10.1175/1520-0442(2002)015<1609:AIISAS>2.0.CO;2**

Reynolds, R.W., Smith, T.M., Liu, C., Chelton, D.B., Casey, K.S., and Schlax, M.G., 2007. Daily high-resolution-blended analyses for sea surface temperature. *Journal of Climate,* 20(22):5473–5496. **https://doi.org/10.1175/2007JCLI1824.1**

Rincon-Martinez, D., Contreras, S., Lamy, F., and Tiedemann, R., 2009. Are glacials (interglacial) in the easternmost Pacific Ocean drier (wetter) during the last 300 000 years? In *Awards Ceremony Speeches and Abstracts of the 19th Annual V.M. Goldschmidt Conference.* Geochimica et Cosmochimica Acta, 73(13S):A1102. **https://doi.org/10.1016/j.gca.2009.05.014**

Robinson, R.S., and Sigman, D.M., 2008. Nitrogen isotopic evidence for a poleward decrease in surface nitrate within the ice age Antarctic. *Quaternary Science Reviews,* 27(9–10):1076–1090. **https://doi.org/10.1016/j.quascirev.2008.02.005**

Ronge, T.A., Tiedemann, R., Lamy, F., Köhler, P., Alloway, B.V., De Pol-Holz, R., Pahnke, K., Southon, J., and Wacker, L., 2016. Radiocarbon constraints on the extent and evolution of the South Pacific glacial carbon pool. *Nature Communications,* 7:11487. **https://doi.org/10.1038/ncomms11487**

Sigman, D.M., and Boyle, E.A., 2000. Glacial/interglacial variations in atmospheric carbon dioxide. *Nature,* 407(6806):859–869. **https://doi.org/10.1038/35038000**

Sigman, D.M., Hain, M.P., and Haug, G.H., 2010. The polar ocean and glacial cycles in atmospheric CO_2 concentration. *Nature,* 466(7302)47–55. **https://doi.org/10.1038/nature09149**

Sigman, D.M., Jaccard, S.L., and Haug, G.H., 2004. Polar ocean stratification in a cold climate. *Nature,* 428(6978):59–63. **https://doi.org/10.1038/nature02357**

Sloyan, B.M., and Rintoul, S.R., 2001. Circulation, renewal, and modification of Antarctic Mode and Intermediate Water. *Journal of Physical Oceanography,* 31(4):1005–1030. **https://doi.org/10.1175/1520-0485(2001)031<1005:CRAMOA>2.0.CO;2**

Sokolov, S., and Rintoul, S.R., 2009. Circumpolar structure and distribution of the Antarctic Circumpolar Current fronts: 1. Mean circumpolar paths. *Journal of Geophysical Research: Oceans,* 114(C11):C11018. **https://doi.org/10.1029/2008JC005108**

Stammerjohn, S., Massom, R., Rind, D., and Martinson, D., 2012. Regions of rapid sea ice change: an inter-hemispheric seasonal comparison. *Geophysical Research Letters,* 39(6):L06501. **https://doi.org/10.1029/2012GL050874**

Steig, E.J., Ding, Q., Battisti, D.S., and Jenkins, A., 2012. Tropical forcing of Circumpolar Deep Water inflow and outlet glacier thinning in the

Amundsen Sea Embayment, West Antarctica. *Annals of Glaciology,* 53(60):19–28. **https://doi.org/10.3189/2012AoG60A110**

Studer, A.S., Sigman, D.M., Martínez-García, A., Benz, V., Winckler, G., Kuhn, G., Esper, O., et al., 2015. Antarctic Zone nutrient conditions during the last two glacial cycles. *Paleoceanography and Paleoclimatology,* 30(7):845–862. **https://doi.org/10.1002/2014PA002745**

Sugden, D.E., McCulloch, R.D., Bory, A.J-M., and Hein, A.S., 2009. Influence of Patagonian glaciers on Antarctic dust deposition during the last glacial period. *Nature Geoscience,* 2(4):281–285. **https://doi.org/10.1038/ngeo474**

Talley, L.D., 2013. Closure of the global overturning circulation through the Indian, Pacific, and Southern Oceans: schematics and transports. *Oceanography,* 26(1):80–97. **https://doi.org/10.5670/oceanog.2013.07**

Teitler, L., Florindo, F., Warnke, D.A., Filippelli, G.M., Kupp, G., and Taylor, B., 2015. Antarctic Ice Sheet response to a long warm interval across marine isotope Stage 31: a cross-latitudinal study of iceberg-rafted debris. *Earth and Planetary Science Letters,* 409:109–119. **https://doi.org/10.1016/j.epsl.2014.10.037**

Teitler, L., Warnke, D.A., Venz, K.C., Hodell, D.A., Becquey, S., Gersonde, R., and Teitler, W., 2010. Determination of Antarctic Ice Sheet stability over the last ~500 ka through a study of iceberg-rafted debris. *Paleoceanography and Paleoclimatology,* 25(1). **https://doi.org/10.1029/2008PA001691**

Thompson, D.W.J., Solomon, S., Kushner, P.J., England, M.H., Grise, K.M., and Karoly, D.J., 2011. Signatures of the Antarctic ozone hole in Southern Hemisphere surface climate change. *Nature Geoscience,* 4(11):741–749. **https://doi.org/10.1038/ngeo1296**

Turner, J., Comiso, J.C., Marshall, G.J., Lachlan-Cope, T.A., Bracegirdle, T., Maksym, T., Meredith, M.P., Wang, Z., and Orr, A., 2009. Non-annular atmospheric circulation change induced by stratospheric ozone depletion and its role in the recent increase of Antarctic sea ice extent. *Geophysical Research Letters,* 36(8):L08502. **https://doi.org/10.1029/2009GL037524**

Ullermann, J., Lamy, F., Ninnemann, U., Lembke-Jene, L., Gersonde, R., and Tiedemann, R., 2016. Pacific-Atlantic Circumpolar Deep Water coupling during the last 500 ka. *Paleoceanography and Paleoclimatology,* 31(6):639–650. **https://doi.org/10.1002/2016PA002932**

Venz, K.A., and Hodell, D.A., 2002. New evidence for changes in Plio–Pleistocene deep water circulation from Southern Ocean ODP Leg 177 Site 1090. *Palaeogeography, Palaeoclimatology, Palaeoecology,* 182(3–4):197–220. **https://doi.org/10.1016/S0031-0182(01)00496-5**

WAIS Divide Project Members, 2013. Onset of deglacial warming in West Antarctica driven by local orbital forcing. *Nature,* 500(7463):440–444. **https://doi.org/10.1038/nature12376**

Well, R., Roether, W., and Stevens, D.P., 2003. An additional deep-water mass in Drake Passage as revealed by ^{3}He data. *Deep Sea Research, Part I: Oceanographic Research Papers,* 50(9):1079–1098. **https://doi.org/10.1016/S0967-0637(03)00050-5**

Yuan, X., 2004. ENSO-related impacts on Antarctic sea ice: a synthesis of phenomenon and mechanisms. *Antarctic Science,* 16(4): 415–425. **https://doi.org/10.1017/S0954102004002238**

Table T1. Primary and alternate proposed site locations, Expedition 383. EPSP = Environmental Protection and Safety Panel. mbsf = meters below seafloor.

Proposed site	Priority	Latitude	Longitude	Water depth (m)	Proposed penetration (mbsf)	EPSP approved penetration (mbsf)	Jurisdiction
CHI-1C	Primary	–55.53667	–71.59306	2091	300	Pending	Chile
CHI-4B	Primary	–52.7048	–75.5965	1111	500	500	Chile
ESP-1B	Primary	–54.5844	–76.6765	3881	400	400	Chile
CSP-1A	Primary	–54.2126	–125.4258	3621	180	230	International
CSP-2B	Primary	–56.151	–115.1341	4111	300	300	International
CSP-3A	Primary	–60.7361	–115.9063	5141	300	300	Antarctic Treaty
CHI-5A	Alternate	–52.7227	–75.6077	1170	500	500	Chile
CHI-6A	Alternate	–55.6036111	–71.4647222	2100	300	Pending	Chile
CHI-7A	Alternate	–52.74481	–75.6232	1250	500	Pending	Chile
CHI-8A	Alternate	–52.69288	–75.58817	1060	200	Pending	Chile
ESP-2A	Alternate	–54.55337	–76.52128	3850	400	Pending	Chile
CSP-4A	Alternate	–56.1859	–115.1922	4110	300	Pending	International
CSP-5A	Alternate	–60.7786	–116.0003	5130	300	Pending	Antarctic Treaty
CSP-6A	Alternate	–55.15816	–114.7887	3570	125	Pending	International
CSP-7A	Alternate	–55.14111	–114.84197	3540	150	Pending	International

Table T2. Operations and time estimates for Expedition 383.

Site	Location (latitude, longitude)	Seafloor depth (mbrf)	Operations description	Transit (days)	Drilling/ Coring (days)	LWD/ MWD log (days)
Punta Arenas, Chile			Begin expedition 5.0	Port call days		
			Transit ~235 nmi @ 10.0 kt to CHI-4B	0.9		
CHI-4B	52°42.2880'S	1111	Hole A - APC to 300 mbsf with APCT-3		1.5	
EPSP	75°35.7900'W		Hole B - APC to 300 mbsf		0.9	
to 500 mbsf			Hole C - APC/XCB to 500 mbsf and log with modified triple combo		1.9	0.5
			Subtotal days on site: 4.8			
			Transit ~221 nmi to CHI-1C @ 10.5 kt	0.9		
CHI-1C	55°32.2002'S	2091	Hole A - APC to 300 mbsf with APCT-3		1.5	
EPSP	71°35.5836'W		Hole B - APC to 300 mbsf		1.2	
to TBD			Hole C - APC to 300 mbsf and log with modified triple combo		1.4	0.4
			Subtotal days on site: 4.5			
			Transit ~147 nmi to ESP-1B @ 10.5 kt	0.6		
ESP-1B	54°35.0640'S	3881	Hole A - APC/HLAPC to 400 mbsf with APCT-3		2.9	
EPSP	76°40.5900'W		Hole B - APC/HLAPC to 400 mbsf		2.4	
to 400 mbsf			Hole C - APC/HLAPC to 400 mbsf and log with modified triple combo		2.6	0.5
			Subtotal days on site: 8.4			
			Transit ~1290 nmi to CSP-3A @ 10.5 kt	5.1		
CSP-3A	60°44.1660'S	5141	Hole A - APC to 300 mbsf with APCT-3		2.7	
EPSP	115°54.3780'W		Hole B - APC to 300 mbsf		2.1	
to 300 mbsf			Hole C - APC to 300 mbsf		2.6	
			Subtotal days on site: 7.4			
			Transit ~276 nmi to CSP-2B @ 10.5 kt	1.1		
CSP-2B	56°9.0600'S	4111	Hole A - APC to 300 mbsf with APCT-3		2.4	
EPSP	115°8.0460'W		Hole B - APC to 300 mbsf		1.8	
to 300 mbsf			Hole C - APC to 300 mbsf		2.2	
			Subtotal days on site: 6.4			
			Transit ~371 nmi to CSP-1A @ 10.5 kt	1.5		
CSP-1A	54°12.7560'S	3621	Hole A - APC to 180 mbsf with APCT-3		1.5	
EPSP	125°25.5480'W		Hole B - APC to 180 mbsf		1.1	
to 230 mbsf			Hole C - APC to 180 mbsf		1.6	
			Subtotal days on site: 4.2			
			Transit ~2578 nmi to Valparaiso @ 10.5 kt	10.2		
Valparaiso, Chile			End expedition	20.3	34.3	1.4

Port call:	5.0	Total operating days:	56.0
Subtotal on site:	35.7	Total expedition:	61.0

Figure F1. Antarctic Circumpolar Current (from Marshall and Speer, 2012) and the DYNAPACC drill sites. The climatological positions of the Subantarctic Front (SAF) and Polar Front (PF) are marked in orange; line thickness represents the variability in the latitudinal position of the corresponding front. Green arrows indicate the observed speed and direction of surface ocean currents as measured by drifters floating at a depth of 15 m. Red shaded area indicates estimated glacial dust supply, based on reconstructions from Lamy et al. (2014). Red dots indicate the planned drill sites for Expedition 383; the six primary sites are noted in a larger font.

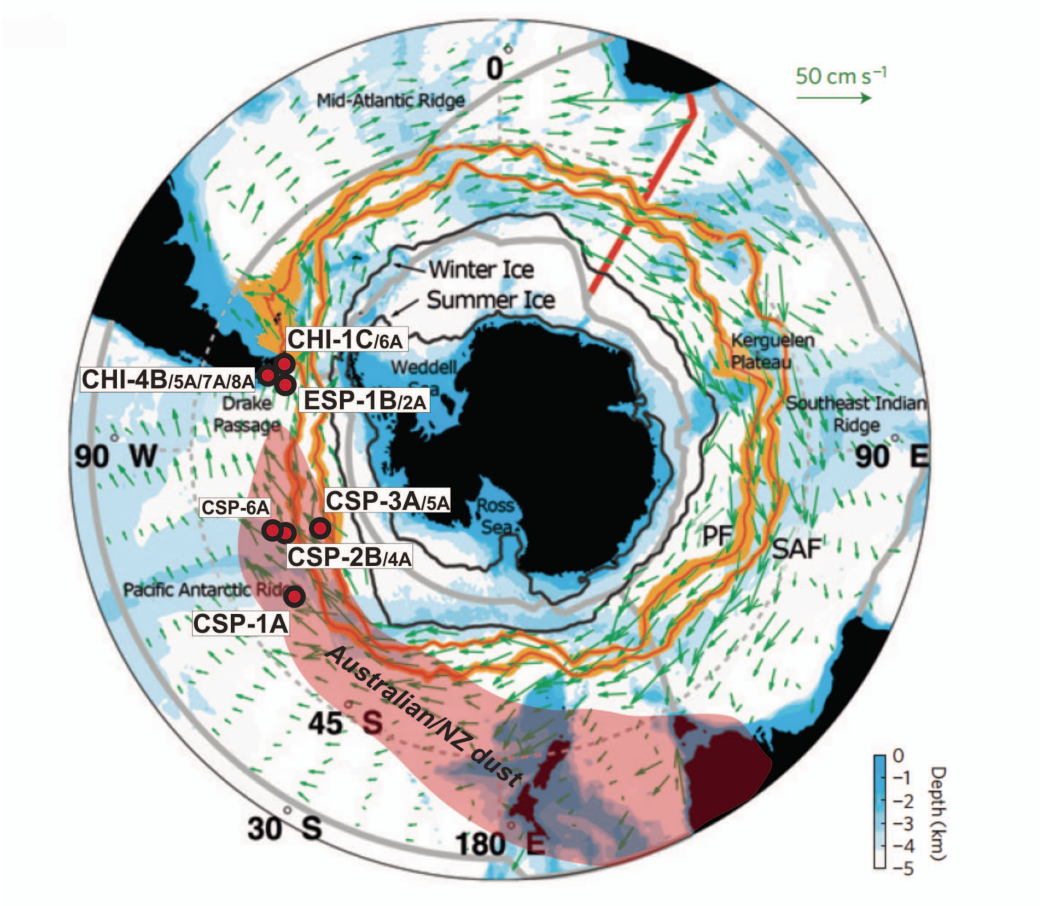

Figure F2. Examples of surface buoy trajectories (dots = 30-day positions) indicating northeast flow of northern Antarctic Circumpolar Current (ACC) water after crossing the East Pacific Rise. Also shown is the bifurcation of surface waters close to the Chilean coast (at ~45°S) with northward flowing water in the Humboldt Current System (HCS) and strongly accelerated southward flow in the Cape Horn Current (CHC) toward the Drake Passage. West–east drifting buoys follow the South Pacific Current (SPC). Modified from Chaigneau and Pizzaro (2005) and Lamy et al. (2015).

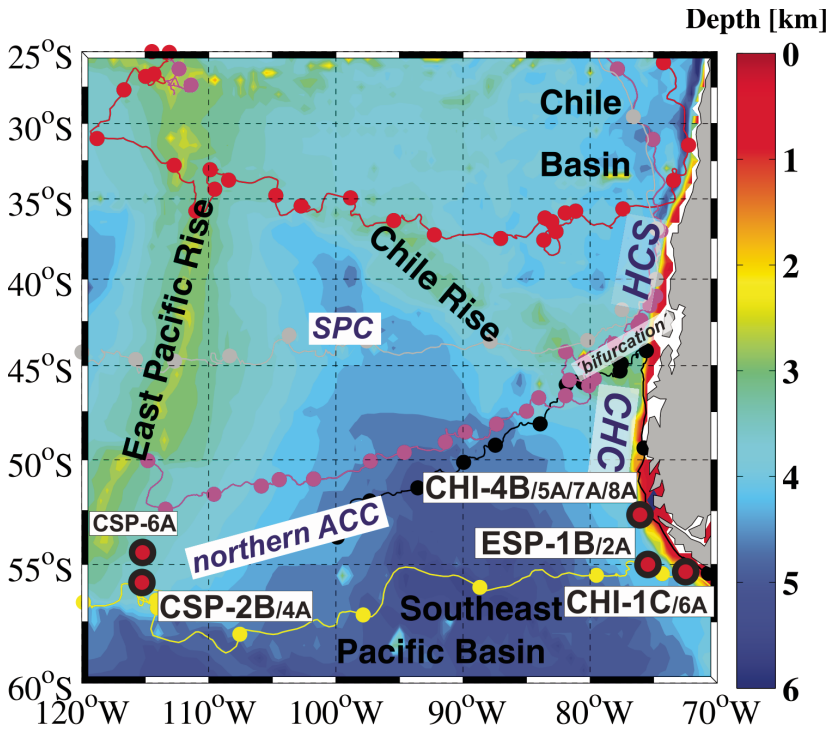

Figure F3. Basement ages of South Pacific oceanic crust (from Eagles, 2006; number indicates age in Ma). Locations of Expedition 383 sites are indicated.

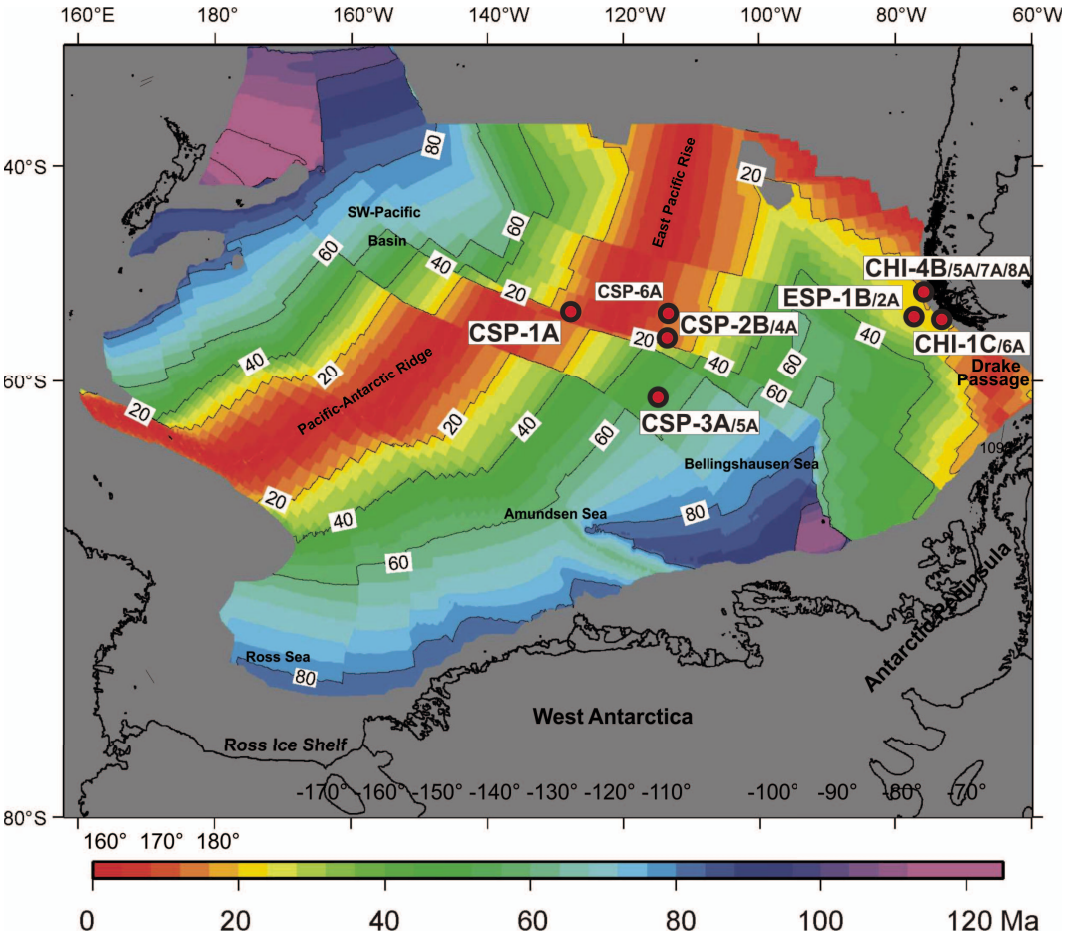

Figure F4. Tectonic setting of Chile margin sites. Seismic Line IT95-171 across the southern Chilean continental margin. Site CHI-1C and alternate Site CHI-6A are located in the fore-arc basin at the upper margin. PSDM = prestack depth migration. Figures modified from Polonia et al. (2007).

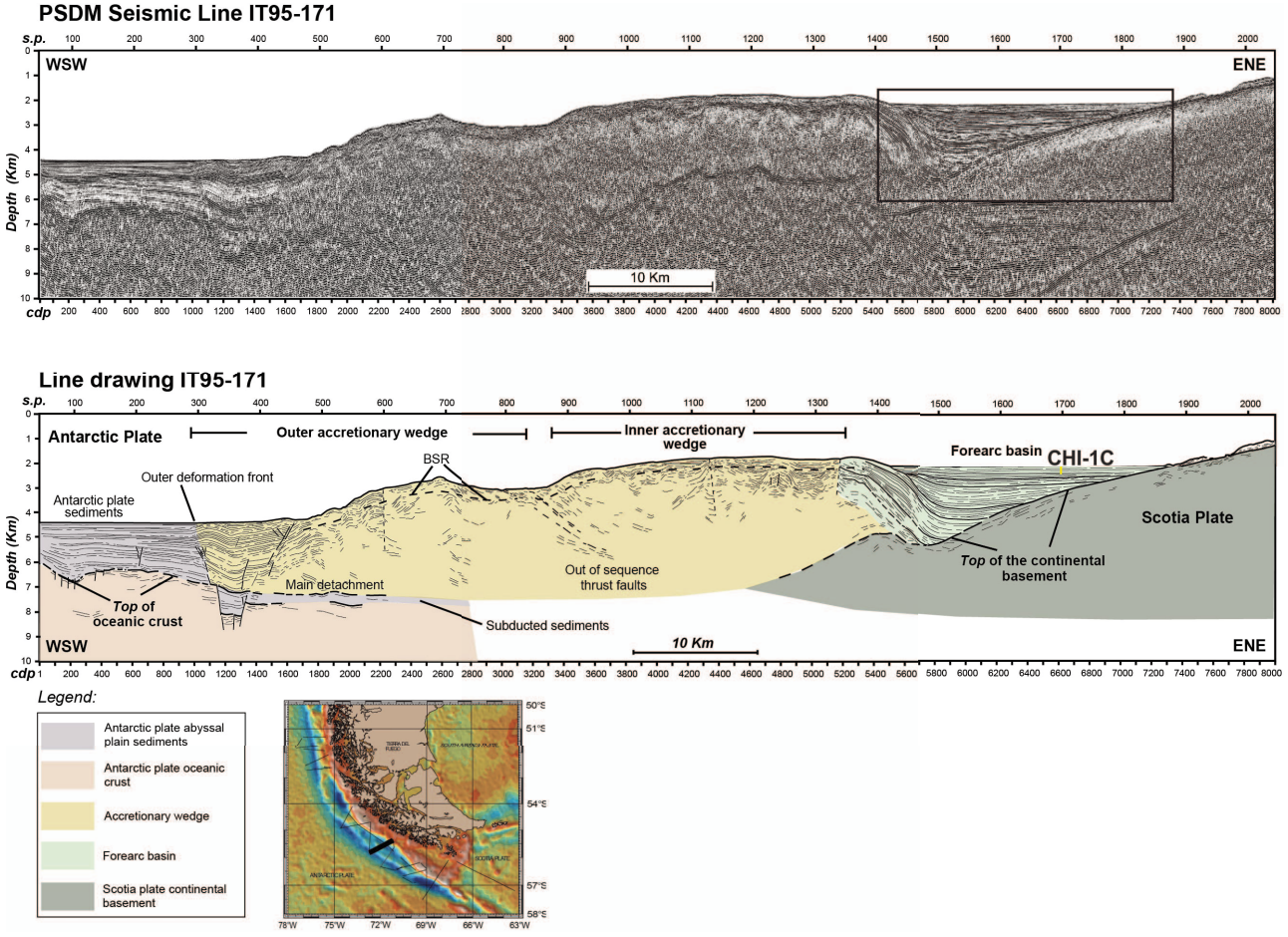

Figure F5. Location of the proposed drilling sites in the Pacific Antarctic Circumpolar Current (ACC) (red dots = proposed sites with site survey cores) and cores collected previously during various expeditions in the eastern Pacific (see text; white dots = ODP Leg 202, Sites 1232–1240; ODP Leg 178, Sites 1095–1102) in the context of the modern oceanography. Modern locations after Orsi et al. (1995) and Reynolds et al. (2002, 2007). Dotted lines = inferred Last Glacial Maximum (LGM) positions. WSI = winter sea ice, SAF = Subantarctic Front, PF = Polar Front, SPC = South Pacific Current, HCS = Humboldt Current System, CHC = Cape Horn Current, EPR = East Pacific Rise. Small inset figures show vertical water mass structure along two transects in the central and eastern South Pacific (oxygen content). AABW = Antarctic Bottom Water, AAIW = Antarctic Intermediate Water, CDW = Circumpolar Deep Water, PDW = Pacific Deep Water. See Scientific objectives for a discussion of the geographic locations and water depths.

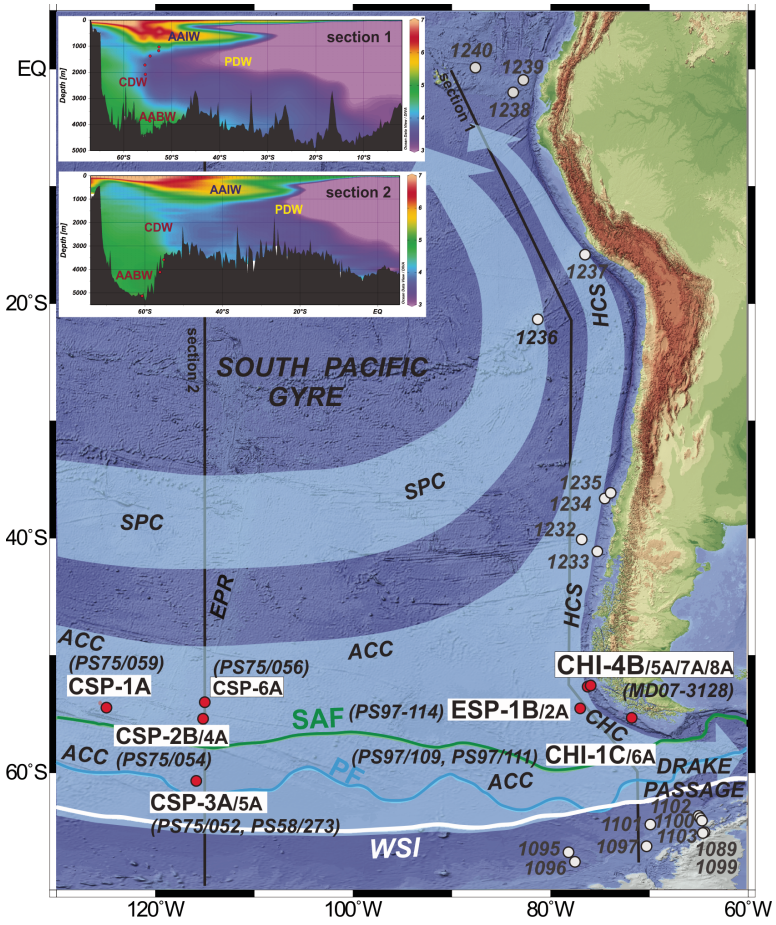

Figure F6. Central and eastern South Pacific paleoceanography and Drake Passage (DP) throughflow (modified from Lamy et al., 2015). A. Reconstructed Drake Passage throughflow during the Last Glacial Maximum (LGM) compared to modern setting. B. Drake Passage region showing major surface and intermediate water circulation. C. LGM sea surface temperature anomalies. The pronounced glacial cooling in the eastern Subantarctic Pacific is consistent with a northward extension of Antarctic cold-water influence. Reduced Cape Horn Current (CHC) and more sluggish glacial northern Drake Passage transport decreases the export of Pacific Antarctic Circumpolar Current (ACC) water into the South Atlantic (cold-water route). Reduced strong westerly winds (SWW) core and extended sea ice diminish the wind forcing on the ACC and thus the Drake Passage transport. Stronger winds in the northern SWW enhance the South Pacific Gyre and the export of northern ACC water into the Humboldt Current System (HCS). APF = Antarctic Polar Front, SACCF = Southern ACC Front, SAF = Subantarctic Front, SPC = South Pacific Current, WSI = winter sea ice.

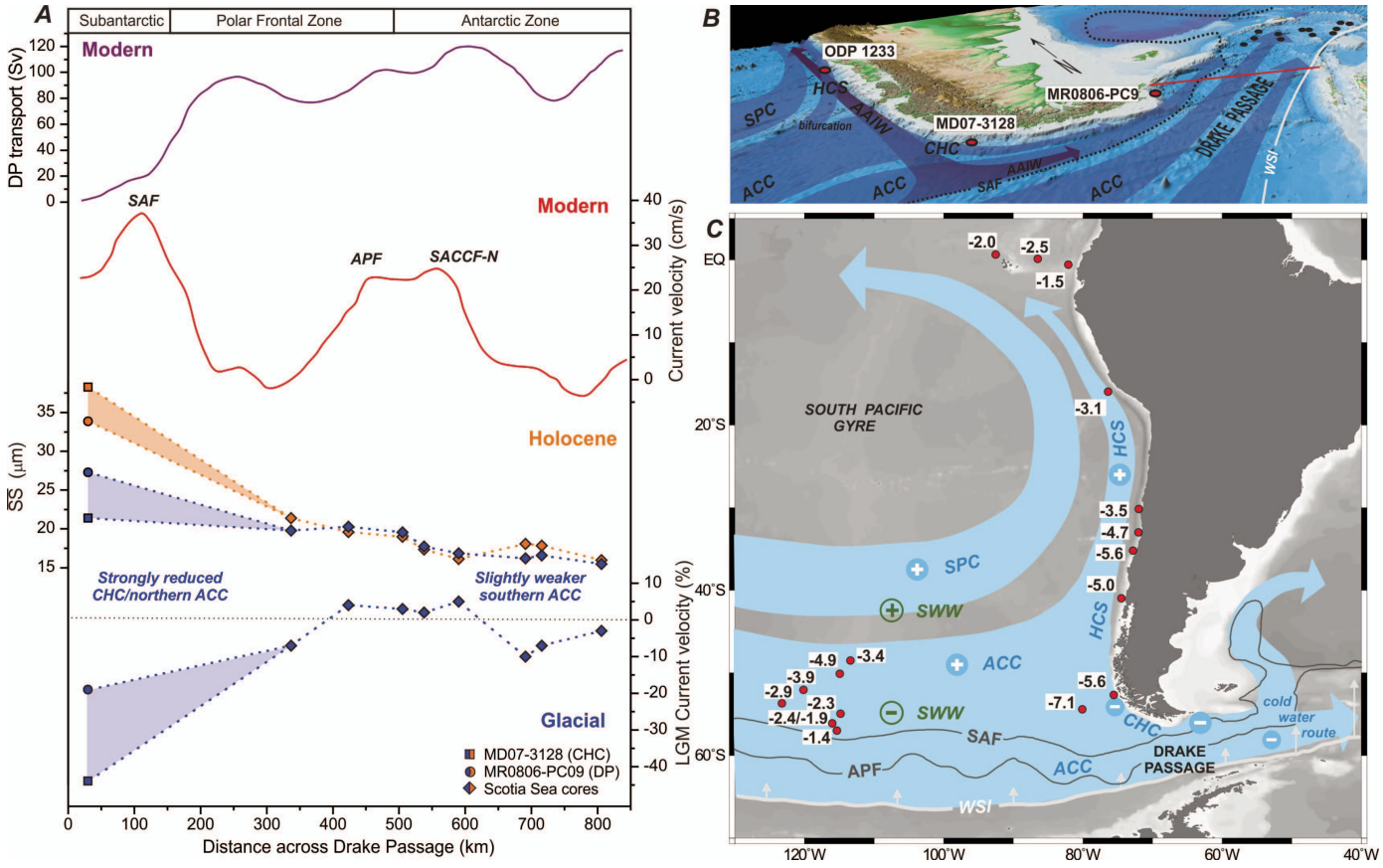

Figure F7. Last Glacial Maximum (LGM) winter sea surface temperatures and sea ice extent in the Pacific Southern Ocean (from Benz et al., 2016). GSSTF = Glacial Southern Subtropical Front. Color scale of core symbols is the same color code as the World Ocean Atlas 09 winter sea surface temperature. E-LGM winter sea ice (WSI) estimates include the maximum WSI extent (>15% September concentration) and the average sea ice concentration (40% concentration). Modern WSI edges after Reynolds et al. (2007).

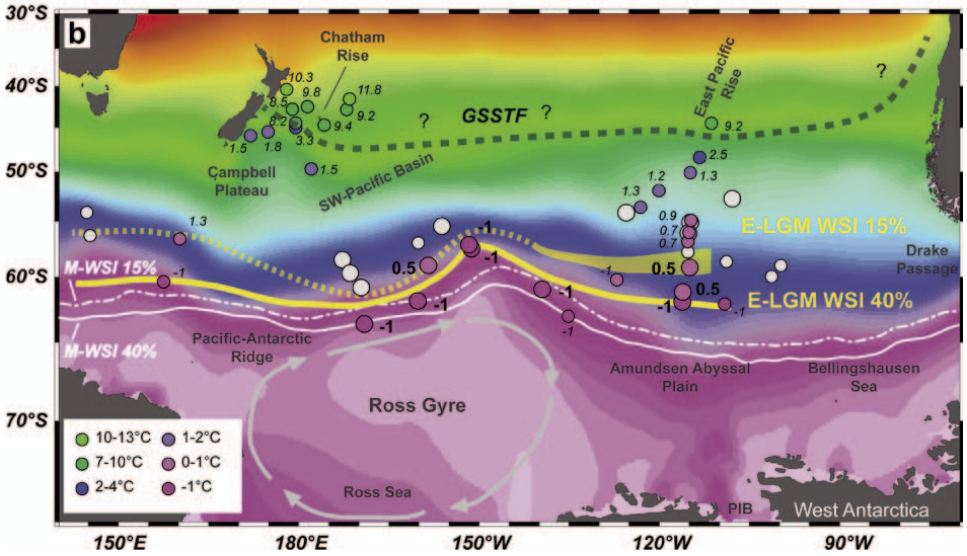

Figure F8. Plio-Pleistocene sea surface temperature (SST) changes in the subpolar North Pacific (Site 882) and Atlantic Southern Ocean (Site 1090) compared to records from the western equatorial Pacific (WEP; Site 806) and eastern equatorial Pacific (EEP; Site 847). Strong enhancement of meridional SST gradients and shift in orbital frequencies at Site 1090 coincide with the strengthening of the "cold tongue" between 1.2 and 1.8 Ma (from Martinez-Garcia et al., 2010). SAP = Subantarctic Pacific, SAA = Subantarctic Atlantic.

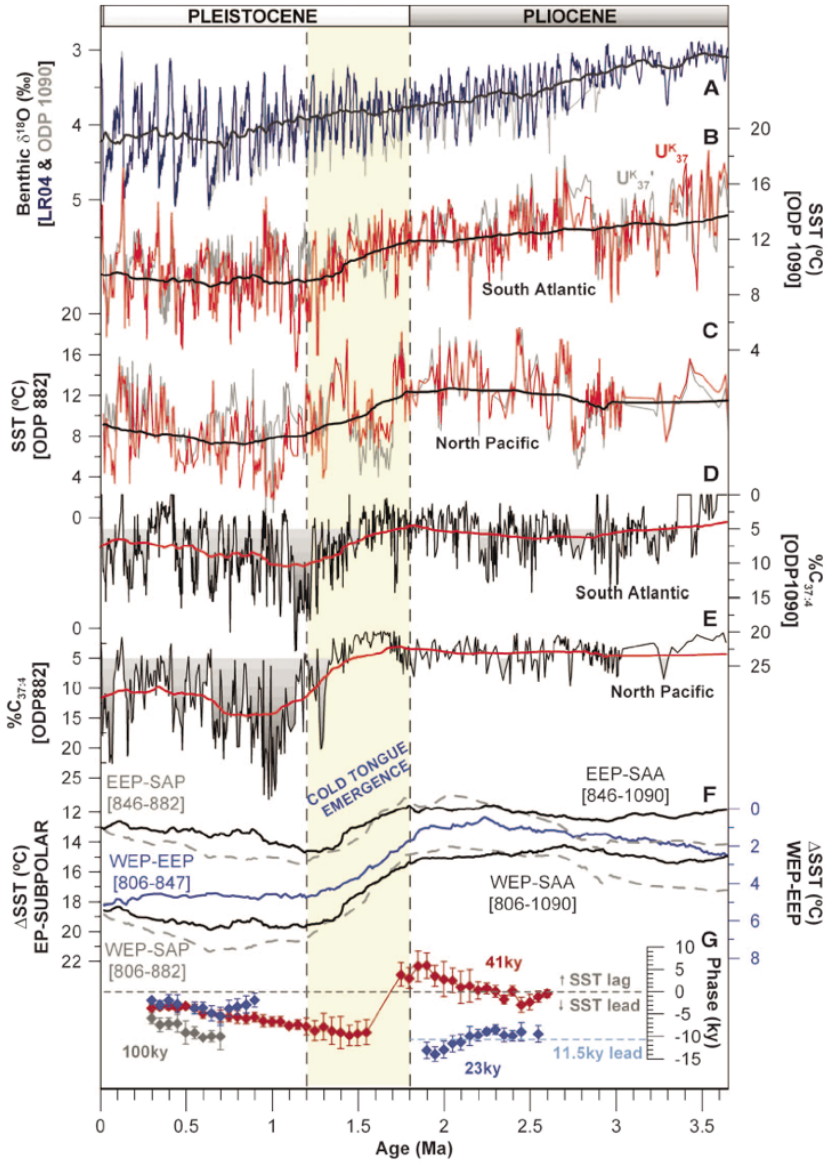

Figure F9. Antarctic Circumpolar Current (ACC) overturning circulation in the Pacific sector of the Southern Ocean (modified from Ronge et al., 2016). Glacial pattern (left): northernmost extent of sea ice and strong westerly winds (SWW). Increased Antarctic Bottom Water (AABW) salinity by brine rejection and reduced Southern Ocean upwelling favors stratification. Increased dust input promotes primary production and drawdown of CO_2. Modern and deglacial pattern (right): upwelling induced by southward shift of Antarctic sea ice and SWW. The erosion of the deep-water carbon pool releases ^{14}C-depleted CO_2 toward the atmosphere. Following air–sea gas exchange, the outgassing signal is incorporated into newly formed Antarctic Intermediate Water (AAIW; light-blue shading). Blue shading = poorly ventilated old and CO_2-rich waters, darkest shading = 2,500–3,600 m water level influenced by hydrothermal CO_2. Green arrows = intermediate water, orange arrows = deepwater, light-blue areas = sea ice; circular arrows = diffusional and diapycnal mixing.

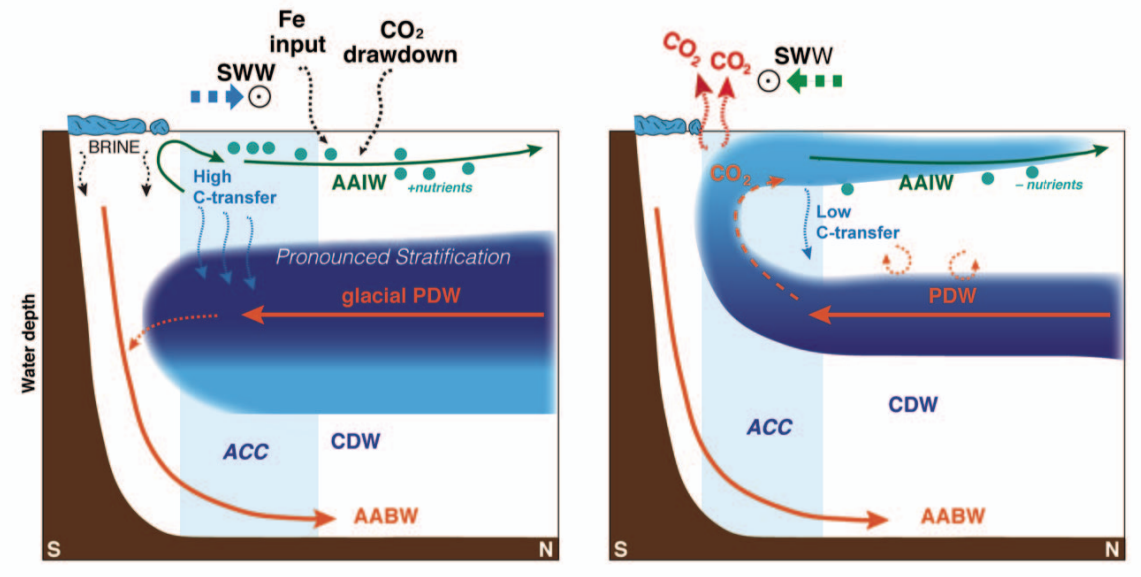

Figure F10. Left: contrasting paleoproductivity pattern in the Antarctic Zone (AZ; ODP Site 1094) versus the Subantarctic Zone (SAZ; ODP Site 1090) over the past 1 My (from Jaccard et al., 2013). Red and blue shading highlights intervals where AZ and SAZ processes, respectively, are dominantly controlling the partitioning of CO_2 between the ocean interior and the atmosphere. During glacial inceptions, the first half of the pCO_2 reduction is essentially accomplished by decreasing vertical mixing and upwelling in the AZ (red shading). The second portion of the pCO_2 reduction (blue shading), initiated around 225 ppmv, is achieved by enhancing carbon sequestration resulting from increased Fe fertilization in the SAZ, thereby leading the climate system to reach full glacial conditions. Right: records of Subantarctic dust-borne iron flux, phytoplankton productivity, surface nitrate consumption, and atmospheric CO_2 over the last glacial cycle (from Martinez-Garcia et al., 2014). The gray vertical bars highlight maxima in dust flux that correspond to minima in atmospheric CO_2.

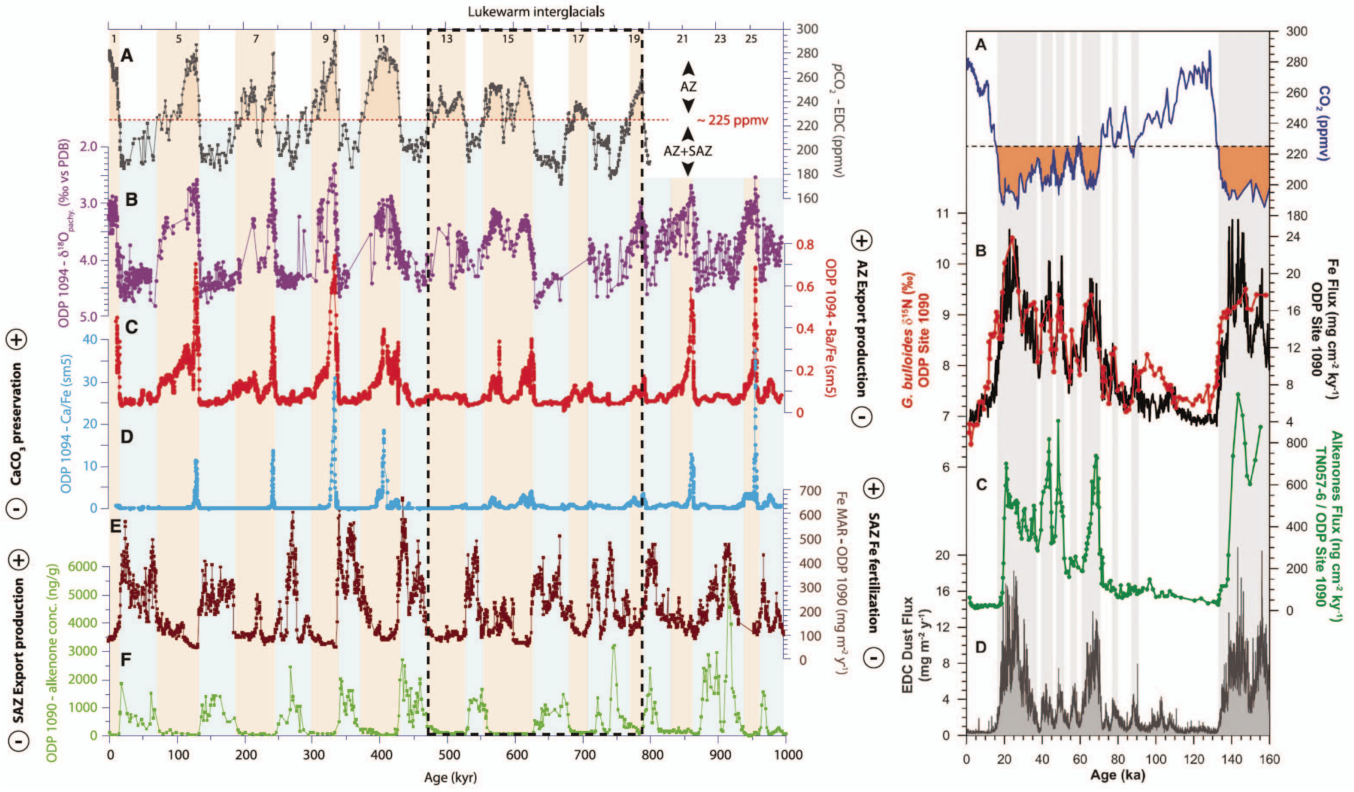

Figure F11. Changes in lithogenic mass accumulation rates (Litho. MAR) in the Pacific Southern Ocean (SO; from Lamy et al., 2014). B–D. Open diamonds = ^{230}Th-normalized Litho. MAR. E–G. Values are ^{230}Th-normalized.

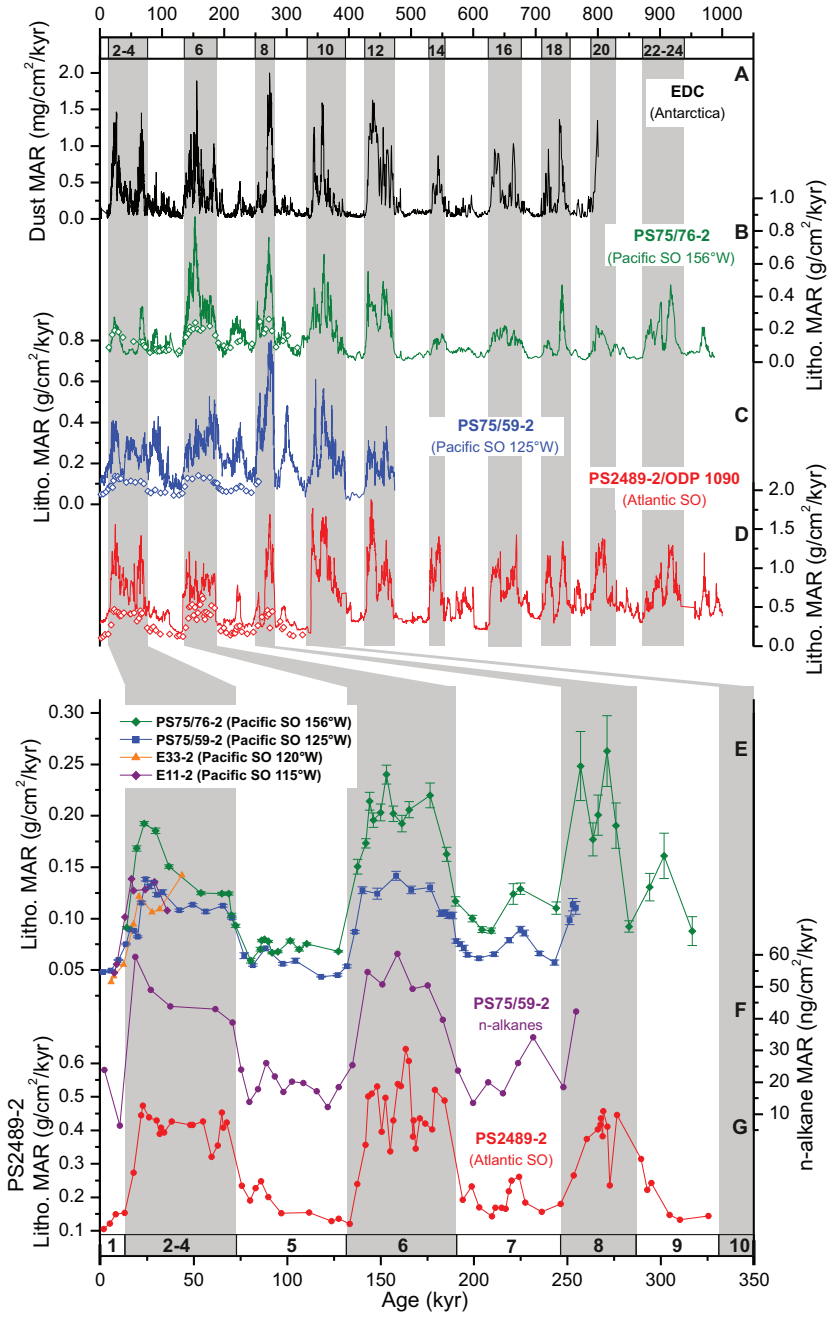

Figure F12. Site survey core records from the proposed central South Pacific transect extending from the calcareous sediments of the Subantarctic Zone (SAZ; Sites CSP-1A and CSP-2A) into the opal belt in vicinity of the Polar Front (Site CSP-3A). Left: consistent iron content (dust) fluctuations. Right: benthic oxygen isotope records (northern sites) and sea surface temperature (SST) records (all sites; Mg/Ca, TEX-86, and diatom assemblages; data from Esper et al., 2014a; Lamy et al., 2014; Ullermann et al., 2016; J. Ullermann, unpubl. data; D. Tapia, unpubl. data; Jaeschke, unpubl. data; G. Kuhn, unpubl. data). Note that absolute Mg/Ca and TEX-86 SST values are not yet regionally calibrated.

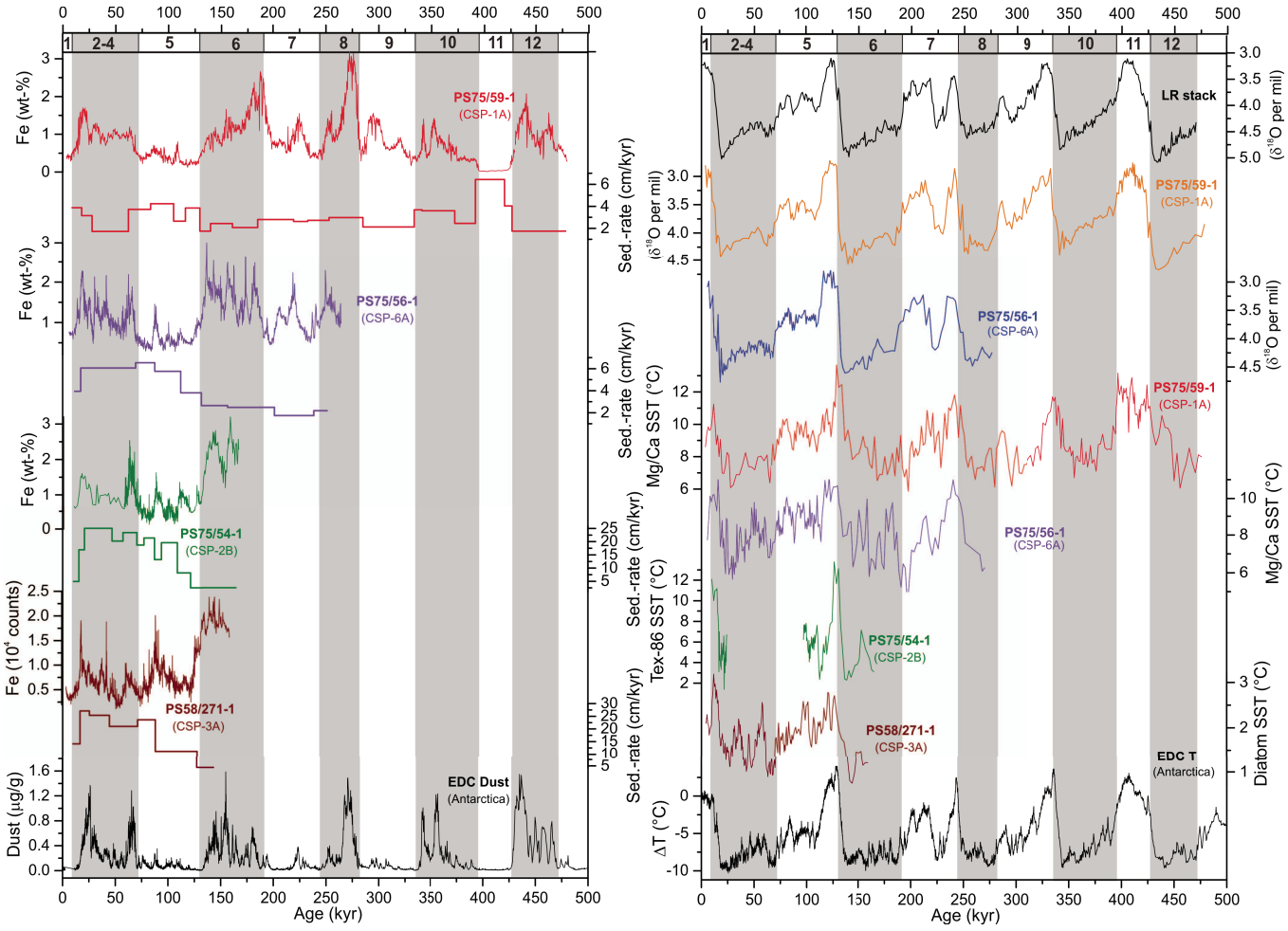

Figure F13. Chile margin and adjacent eastern South Pacific with locations of primary sites (CHI-4B, CHI-1C, and ESP-1B) and alternate sites (CHI-5A, CHI-6A, CHI-7A, CHI-8A, and ESP-2A).

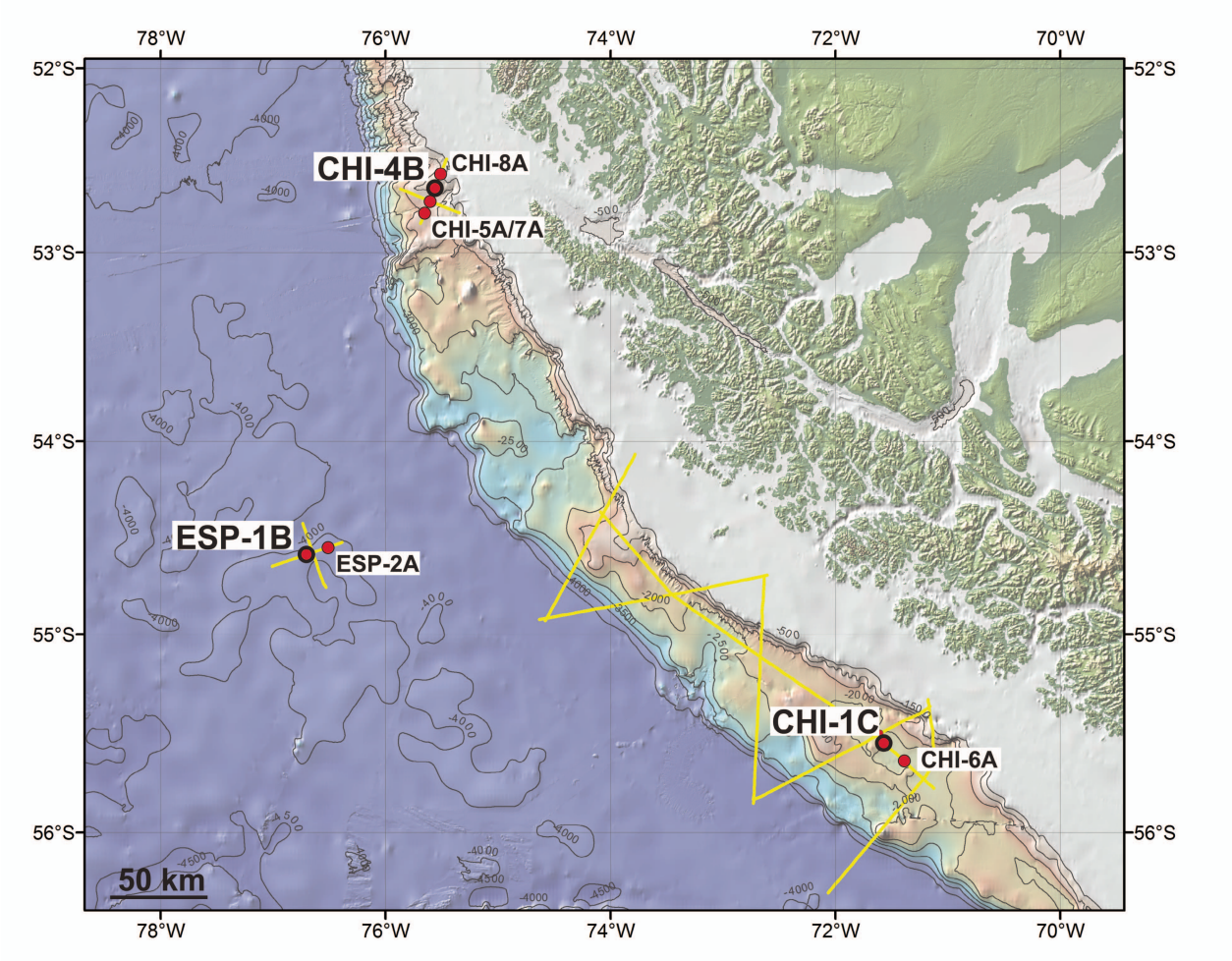

Figure F14. Central South Pacific (CSP) with location of primary and alternate sites. Green line = modern Subantarctic Front, blue line = modern Polar Front.

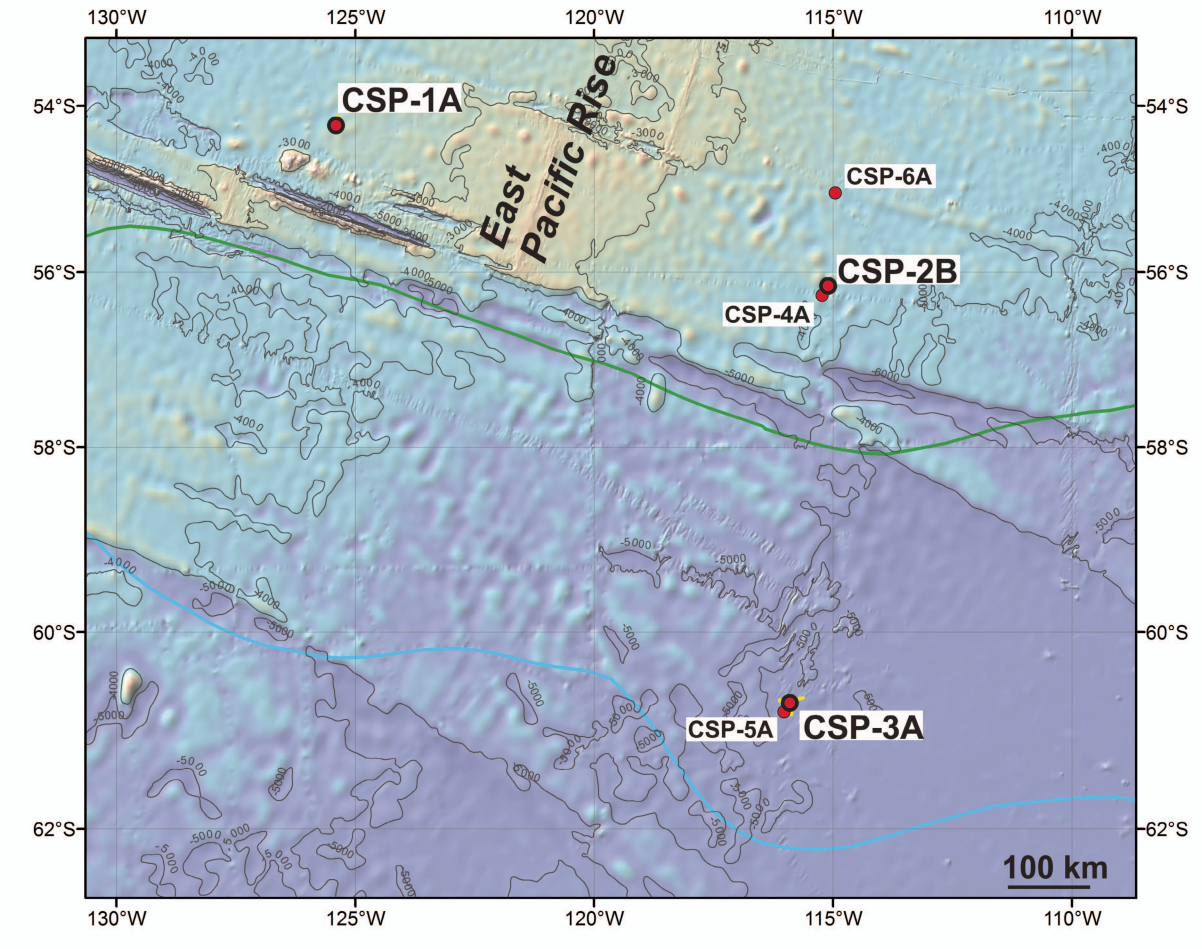

Site summaries

Site CHI-1C

Priority:	Primary
Position:	55°32.2002'S, 71°35.5836'W
Jurisdiction	Chile
Water depth (m):	2093
Target drilling depth (mbsf):	300
Approved maximum penetration (mbsf):	Pending EPSP approval
Survey coverage (track map; seismic profile):	Site is located in a fore-arc basin, ~60 km from land. Bathymetry is very flat. Site is selected proximal to South American sediment sources avoiding pathways of turbidity currents. • One MSC line over site (IT95-171) • Crossing line (IT95-181) is located ~2 km WSW
Objective(s):	• High-resolution Pleistocene paleoceanographic records • Northern ACC strength before entering Drake Passage, Cape Horn Current • Core of Pacific Deep Water, transition to Circumpolar Deep Water • Patagonian ice sheet dynamics
Coring program:	Triple APC to 300 m or refusal, HAPC if required to reach target depth
Logging/downhole measurements program:	Temperature measurements (with APCT-3)
Nature of rock anticipated:	Calcareous clayey silts; minor IRD during glacials. Fine-grained turbidites possible.

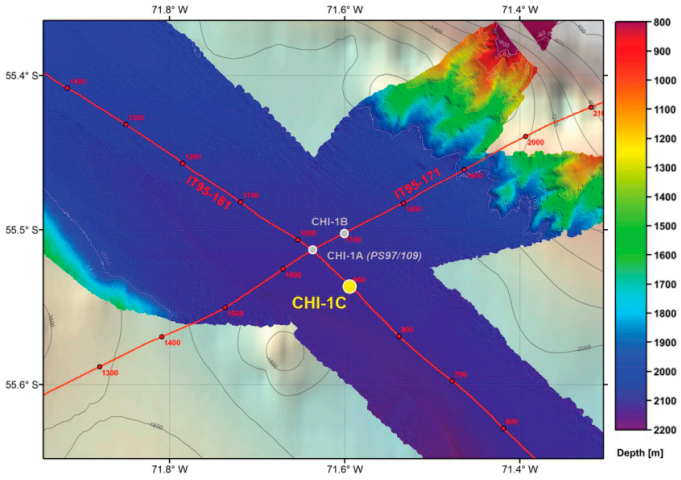

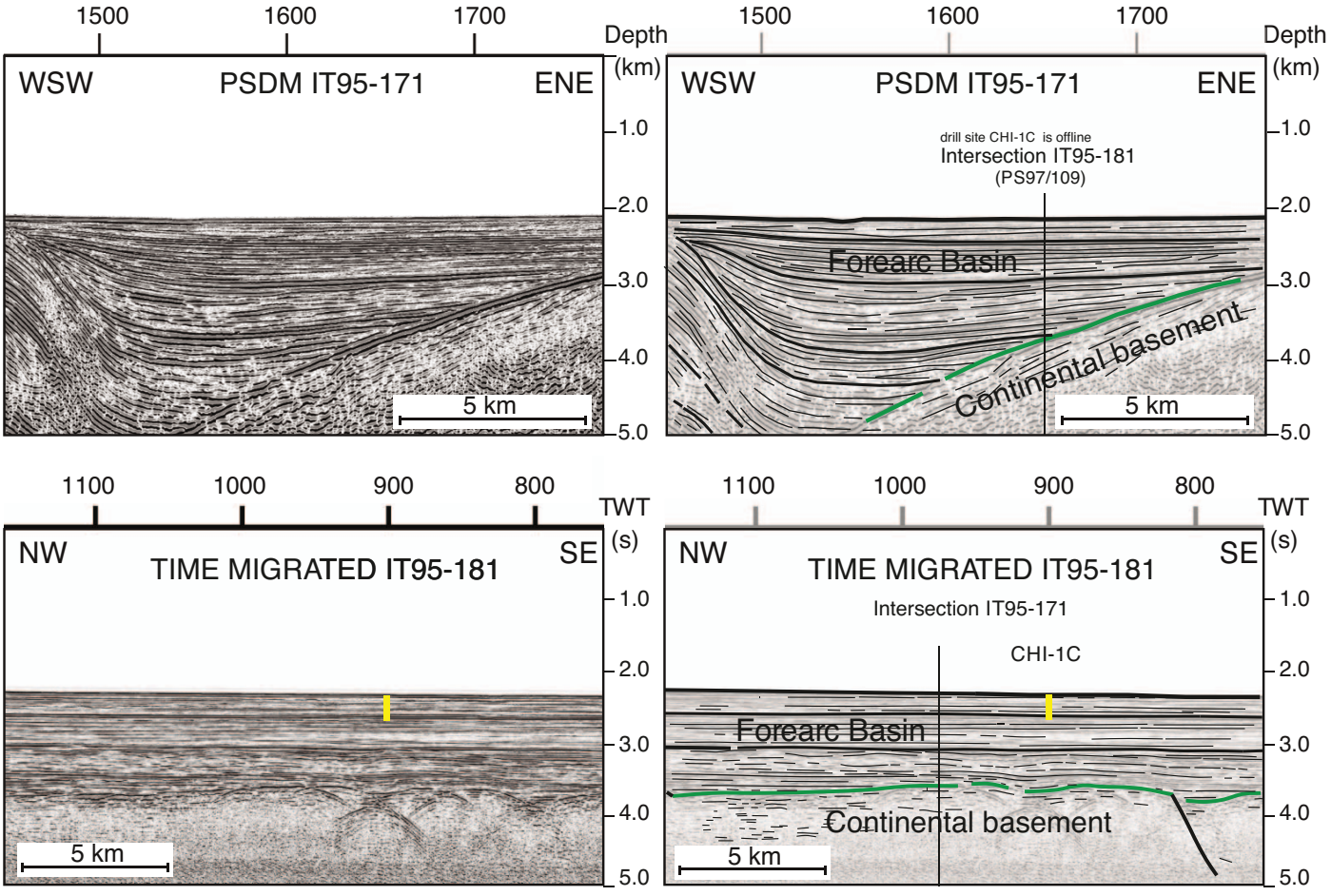

Site CHI-4B

Priority:	Primary
Position:	52°42.2880′S, 75°35.7900′W; Chilean waters
Jurisdiction	Chile
Water depth (m):	1100
Target drilling depth (mbsf):	500
Approved maximum penetration (mbsf):	500
Survey coverage (track map; seismic profile):	Site is located with a sediment drift at the upper continental slope, ~50 km from land. Bathymetry within the sediment drift is slightly inclined (dip < 1.5%). Site is selected proximal to South American sediment sources avoiding pathways of turbidity currents. • One MSC line over site (AWI-20160511) • Crossing line (AWI-2016513) is located ~3 km SW
Objective(s):	• High-resolution Pleistocene paleoceanographic records • Northern ACC strength before entering Drake Passage, Cape Horn Current • Reconstruction of intermediate water mass properties • Patagonian ice sheet dynamics
Coring program:	• Triple APC to 300 m or refusal, HAPC if required • XCB to reach target depth of 500 m in one hole
Logging/downhole measurements program:	• Temperature measurements (with APCT-3) • Downhole logging with modified triple combo
Nature of rock anticipated:	Site is located with a sediment drift at the upper continental slope, ~50 km from land. Calcareous clayey silts; minor IRD during glacials. Fine-grained turbidites possible.

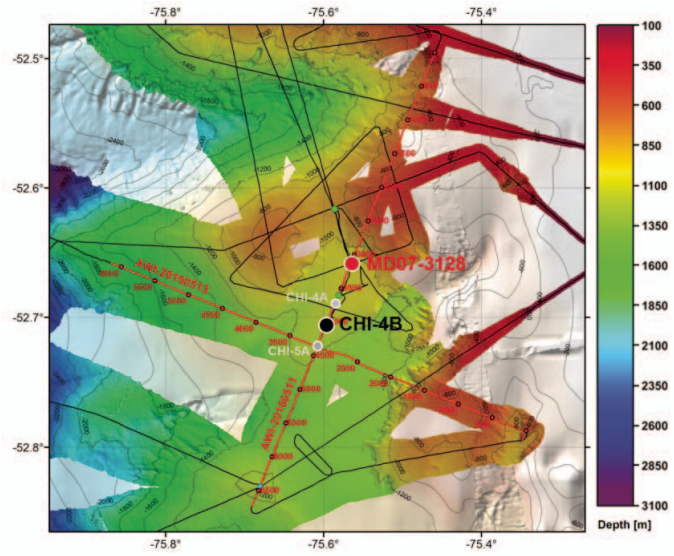

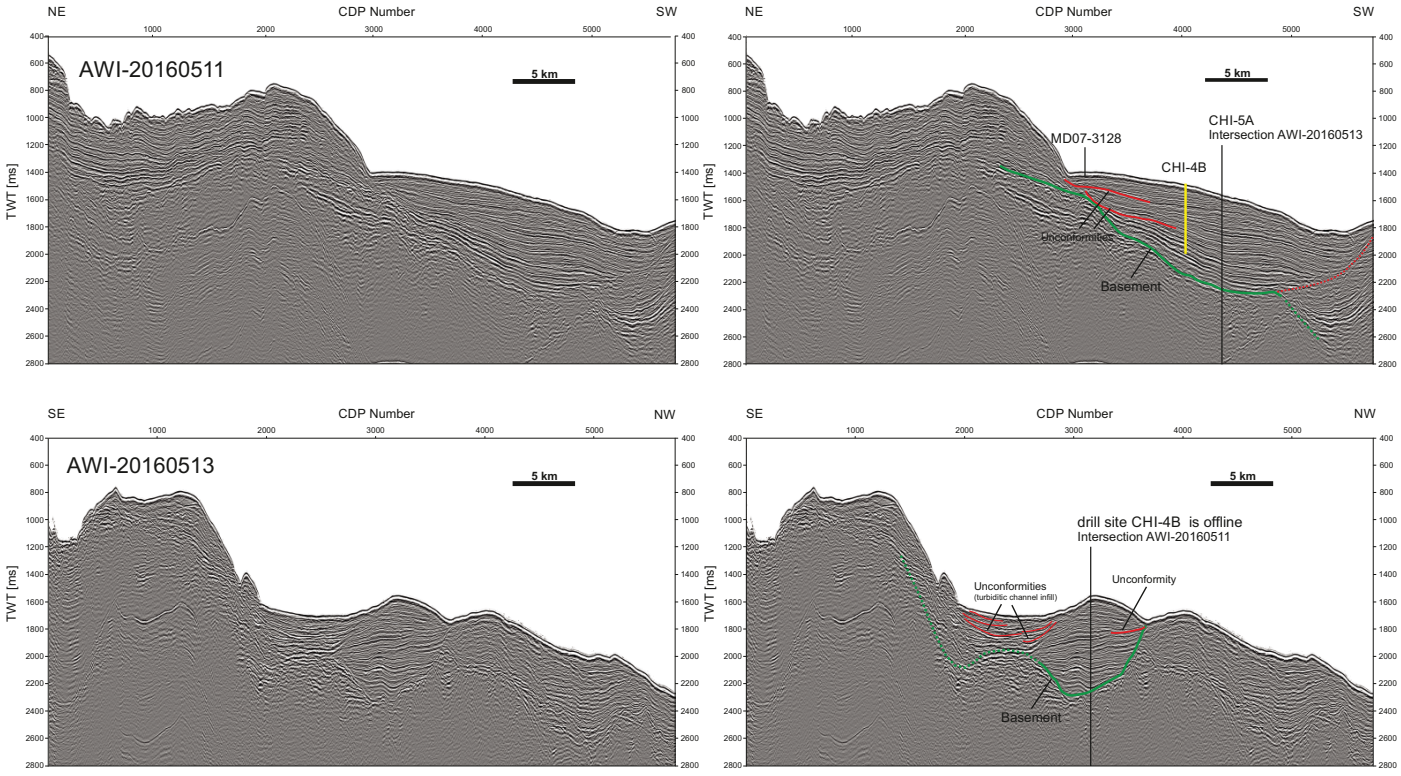

Site ESP-1B

Priority:	Primary
Position:	54°35.0640′S, 76°40.5900′W
Jurisdiction	Chile
Water depth (m):	3870
Target drilling depth (mbsf):	400
Approved maximum penetration (mbsf):	400
Survey coverage (track map; seismic profile):	Site is located at the deep southeast Pacific basin, west of the Peru-Chile Trench (~210 km from land), west of the Chile Trench on a topographically elevated ridge with thick sediment cover. Bathymetry is very flat (dip < 1%). Site is selected more distal to South American sediment. Site is selected proximal to South American sediment sources. • One MSC line over site (AWI-20160501) • Crossing line (AWI-2016503) is located ~1.5 km NE
Objective(s):	• Plio-Pleistocene (Miocene) paleoceanographic records • Northern ACC strength before entering Drake Passage, Cape Horn Current • Potential record of Antarctic Bottom Water during glacials • Long-term Patagonian ice sheet dynamics
Coring program:	Triple APC to 400 m or refusal, HAPC if required to reach target depth
Logging/downhole measurements program:	• Temperature measurements (with APCT-3) • Downhole logging with modified triple combo
Nature of rock anticipated:	Calcareous ooze and clay; minor IRD during glacials

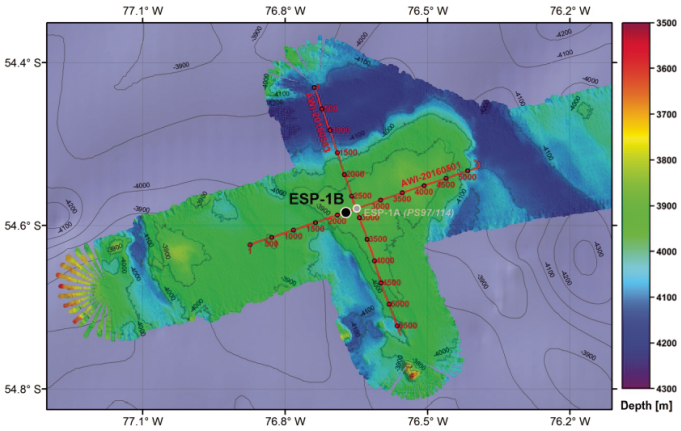

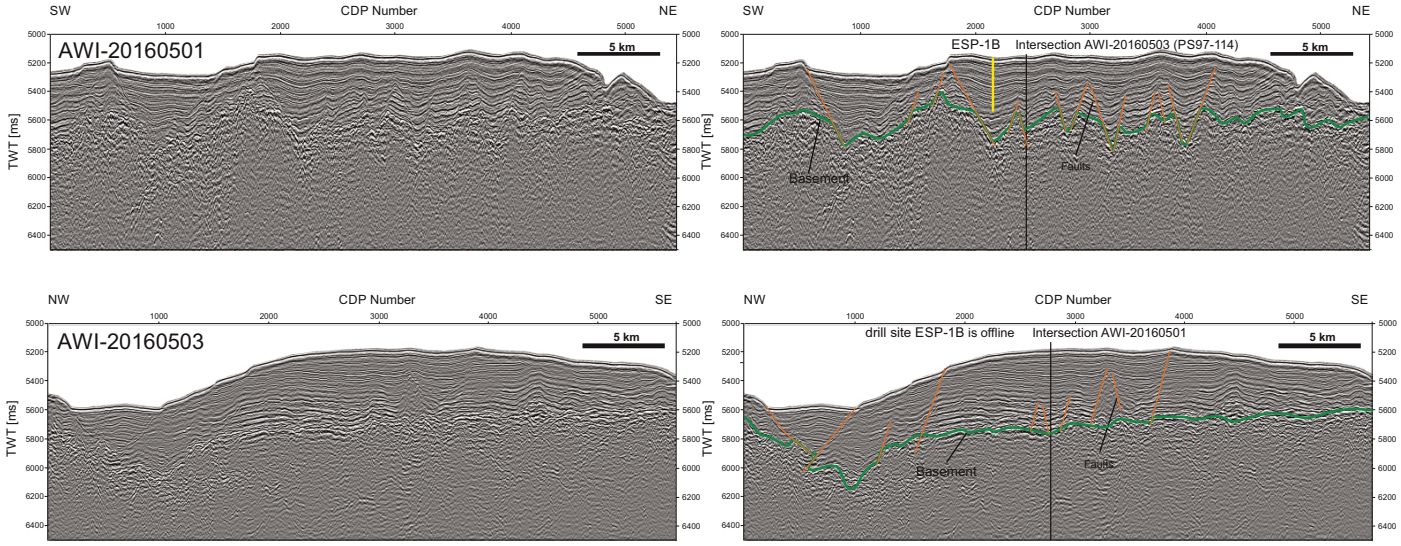

Site CSP-1A

Priority:	Primary
Position:	54°12.7560′S, 125°25.5480′W
Jurisdiction	International waters
Water depth (m):	3610
Target drilling depth (mbsf):	180
Approved maximum penetration (mbsf):	230
Survey coverage (track map; seismic profile):	Site is located in the central South Pacific at the outer reaches of the EPR, ~160 nmi west of the crest. Distance to land is ~2200 km. Site is located at intersection of MSC Lines AWI-2010014 and AWI-2010016.
Objective(s):	• Moderate-resolution subantarctic late Miocene–Quaternary carbonate record from CDW depth • Subantarctic SST, water mass, pCO_2, productivity record • Northernmost site of cross-frontal transect
Coring program:	Triple APC to 180 m or refusal
Logging/downhole measurements program:	Temperature measurements (with APCT-3)
Nature of rock anticipated:	Diatom bearing calcareous ooze, with occasional nannofossil ooze

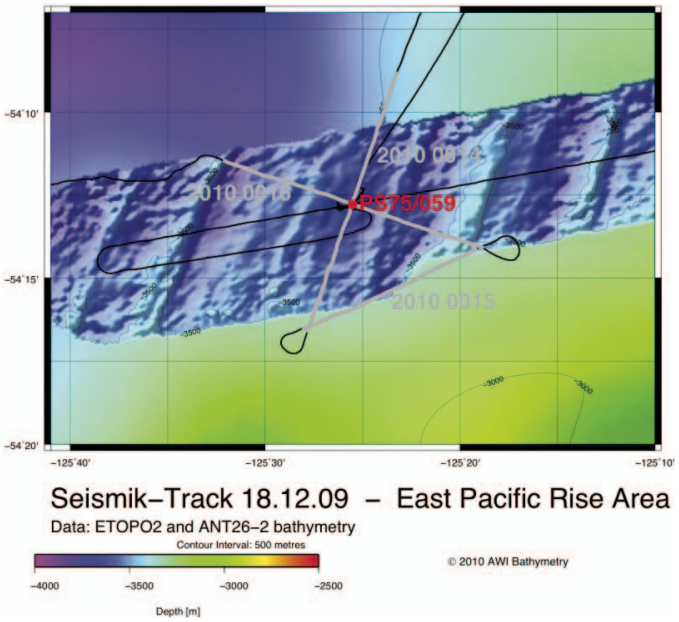

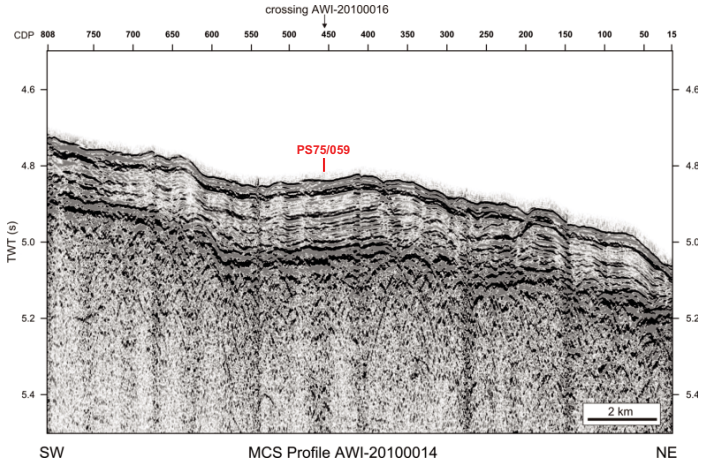

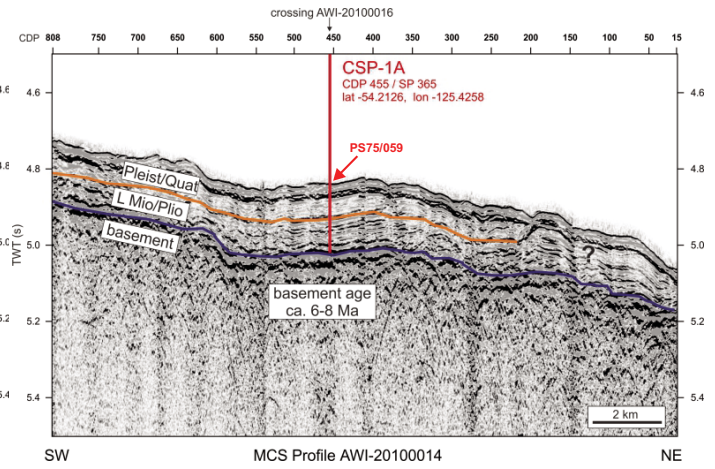

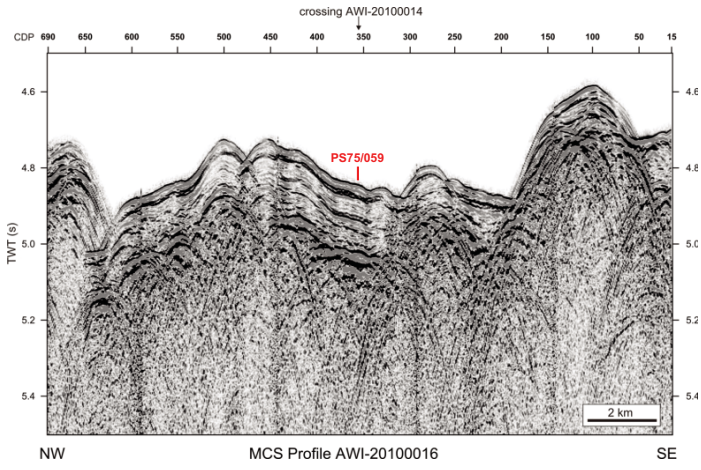

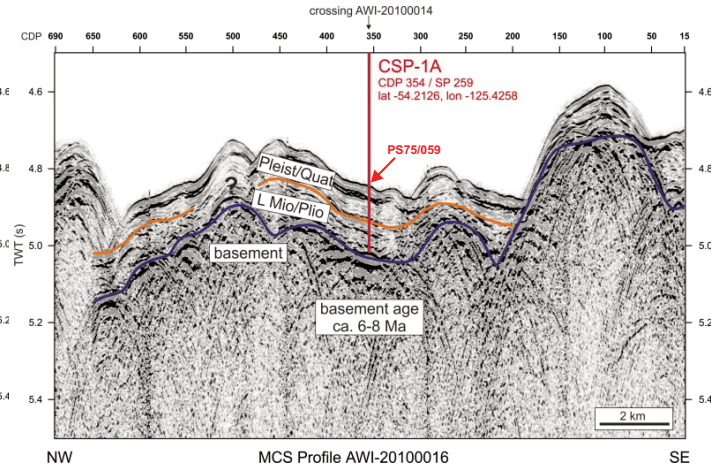

Site CSP-2B

Priority:	Primary
Position:	56°9.0600′S, 115°8.0460′W
Jurisdiction	International waters
Water depth (m):	4110
Target drilling depth (mbsf):	300
Approved maximum penetration (mbsf):	300
Survey coverage (track map; seismic profile):	Site is located in the central South Pacific at the outer reaches of the EPR, ~210 nmi east of the crest. Distance to land is ~2200 km. Site is located at intersection of MSC Lines AWI-2010011 and AWI-2010013.
Objective(s):	• Moderate to high-resolution subantarctic late Miocene–Quaternary carbonate record from lower CDW depth. • Subantarctic SST, water mass, pCO_2, productivity record • Central site of cross-frontal transect
Coring program:	Triple APC to 300 m or refusal
Logging/downhole measurements program:	Temperature measurements (with APCT-3)
Nature of rock anticipated:	Calcareous-biosiliceous ooze

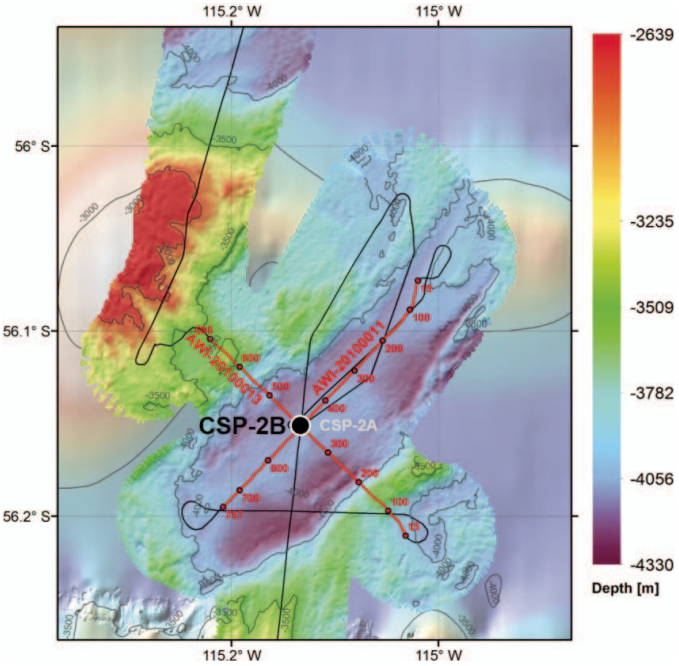

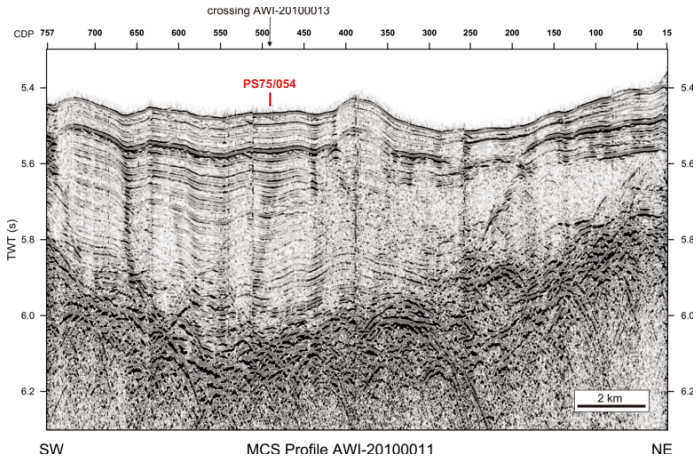

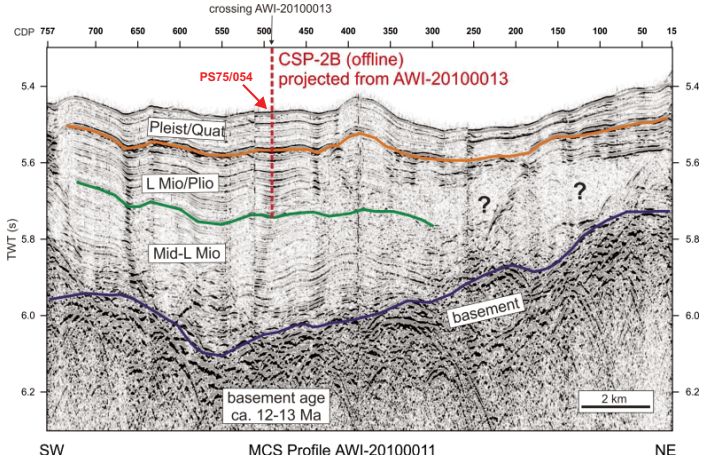

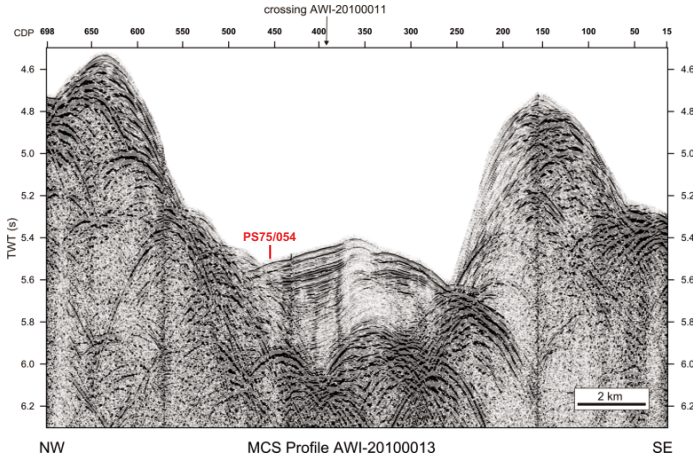

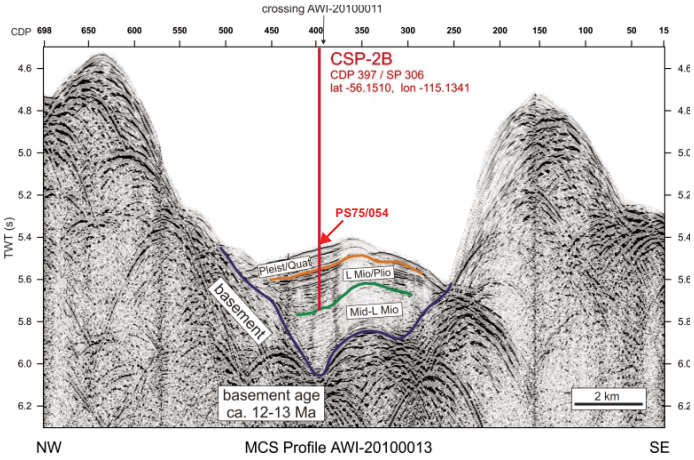

Site CSP-3A

Priority:	Primary
Position:	60°44.1660′S, 115°54.3780′W
Jurisdiction	Antarctic Treaty
Water depth (m):	5141
Target drilling depth (mbsf):	300
Approved maximum penetration (mbsf):	300
Survey coverage (track map; seismic profile):	Site is located in the central South Pacific at the outer reaches of the EPR, ~210 nmi east of the crest. Distance to land is ~2200 km. Site is located at intersection of MSC Lines AWI-2010011 and AWI-2010013.
Objective(s):	• Moderate to high-resolution subantarctic late Miocene-Quaternary carbonate record from lower CDW depth • Subantarctic SST, water mass, pCO_2, productivity record • Southernmost site of cross-frontal transect
Coring program:	Triple APC to 300 m or refusal
Logging/downhole measurements program:	Temperature measurements (with APCT-3)
Nature of rock anticipated:	Calcareous-biosiliceous ooze

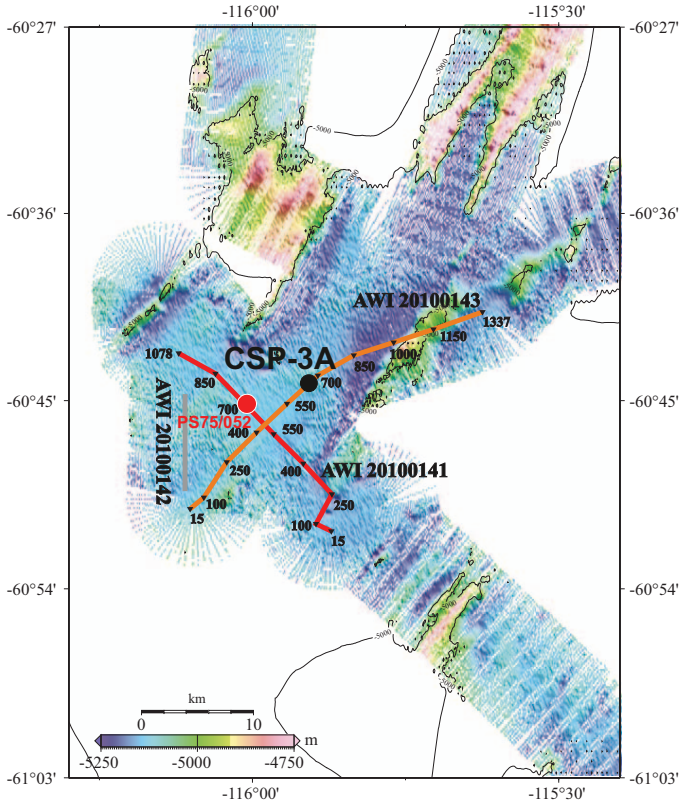

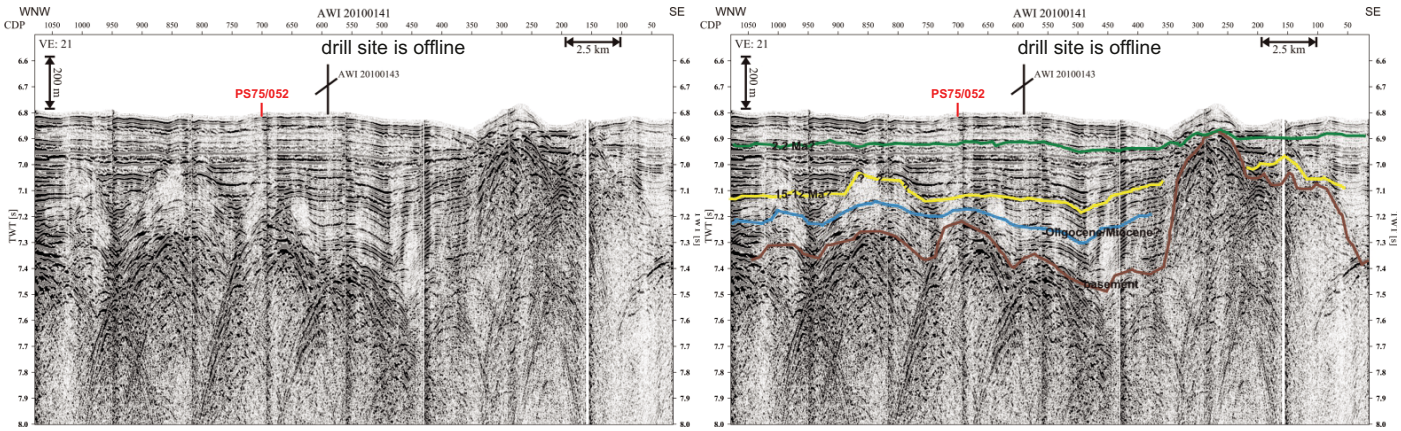

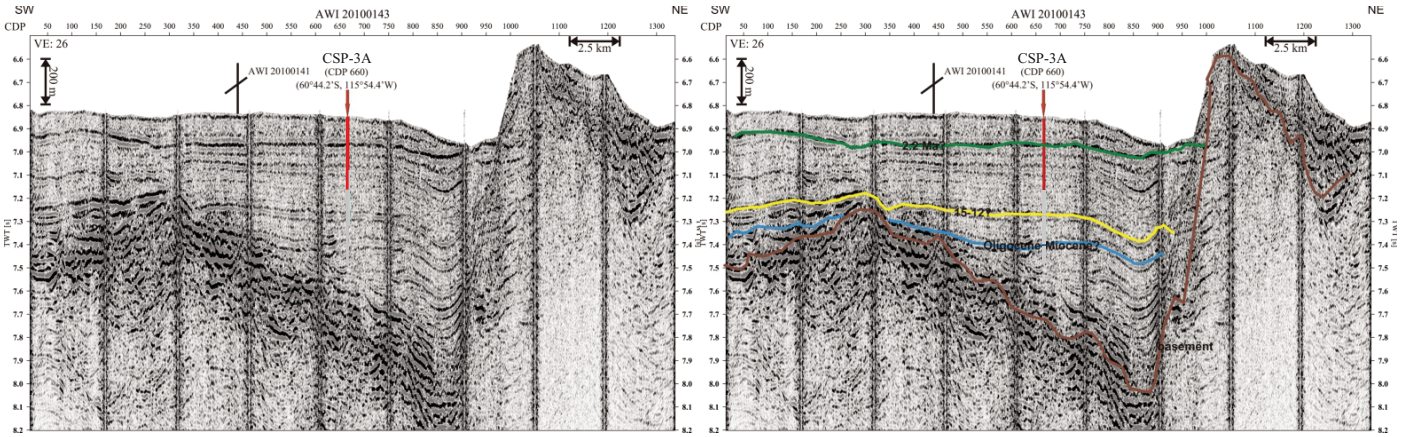

Site CHI-5A

Priority:	Alternate
Position:	52°43.362′S, 75°36.462′W; Chilean waters
Jurisdiction	Chile
Water depth (m):	1170
Target drilling depth (mbsf):	500
Approved maximum penetration (mbsf):	Pending EPSP approval
Survey coverage (track map; seismic profile):	Site is located with a sediment drift at the upper continental slope, ~50 km from land. Bathymetry within the sediment drift is slightly inclined (dip < 1.5%). Site is selected proximal to South American sediment sources avoiding pathways of turbidity currents. Site is located at intersection of MSC Lines AWI-20160511.
Objective(s):	• High-resolution Pleistocene paleoceanographic records • Northern ACC strength before entering Drake Passage, Cape Horn Current • Reconstruction of intermediate water mass properties • Patagonian ice sheet dynamics
Coring program:	• Triple APC to 300 m or refusal, HAPC if required • XCB to reach target depth of 500 m in one hole
Logging/downhole measurements program:	• Temperature measurements (with APCT-3) • Downhole logging with modified triple combo
Nature of rock anticipated:	Site is located within a sediment drift at the upper continental slope, ~50 km from land. Calcareous clayey silts; minor IRD during glacials. Fine-grained turbidites possible.

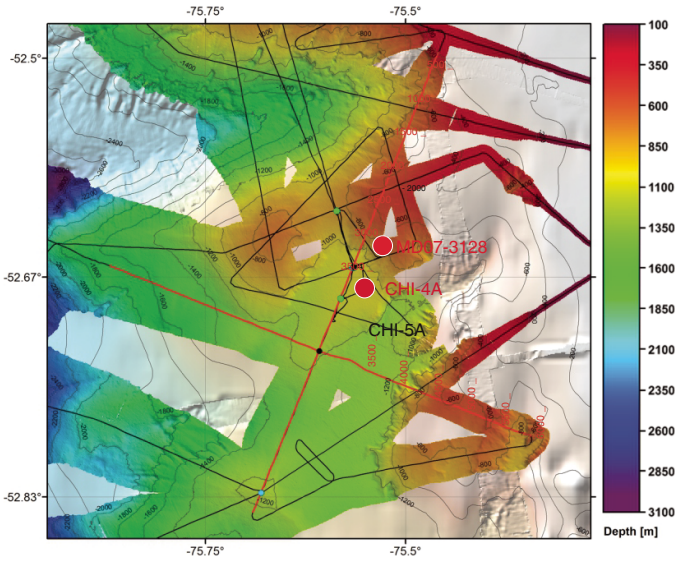

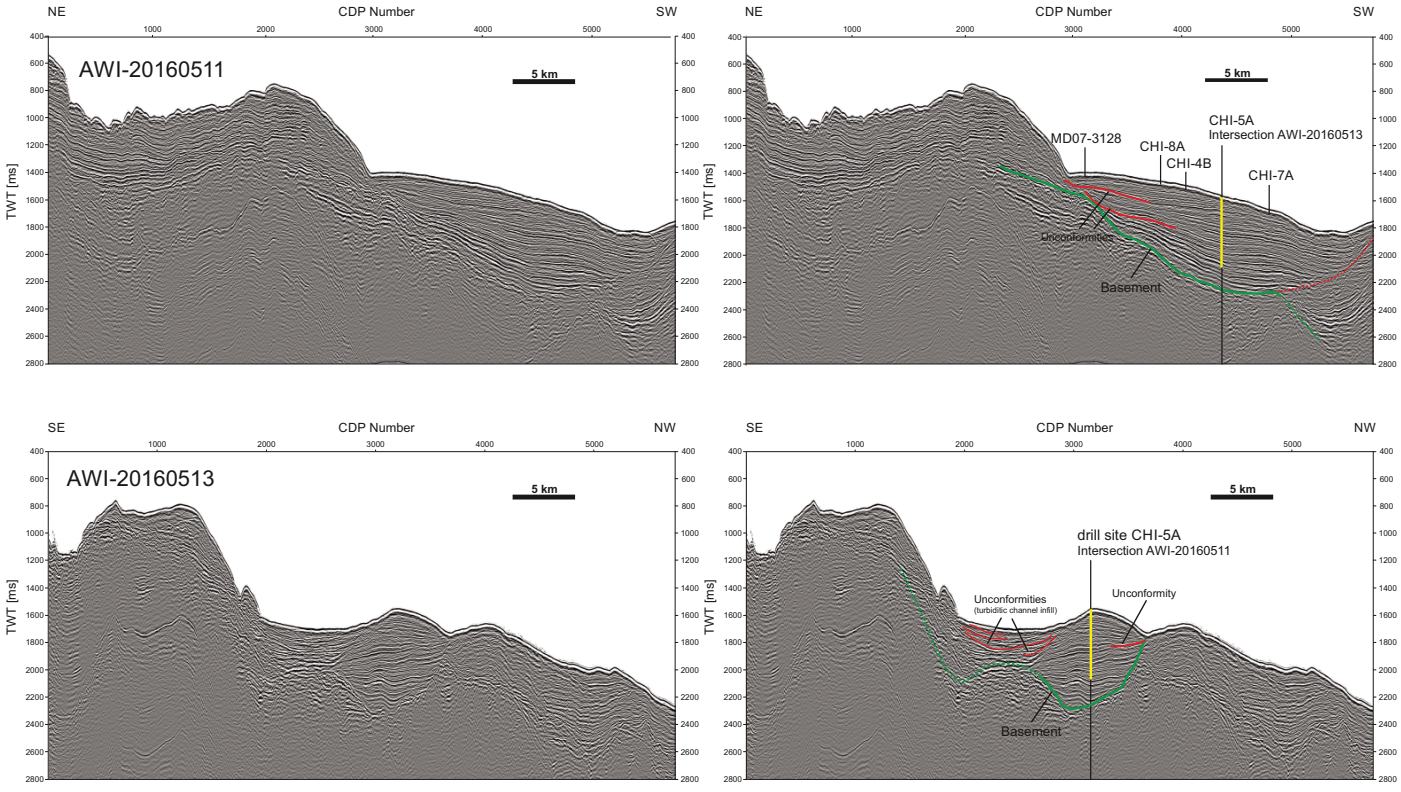

Site CHI-6A

Priority:	Alternate
Position:	55°36.2166′S, 71°27.8832′W
Jurisdiction	Chile
Water depth (m):	2100
Target drilling depth (mbsf):	300
Approved maximum penetration (mbsf):	Pending EPSP approval
Survey coverage (track map; seismic profile):	• CDP 680 • Seismic Line IT95-181
Objective(s):	• High-resolution Pleistocene paleoceanographic records • Northern ACC strength before entering Drake Passage, Cape Horn Current • Core of Pacific Deep Water, transition to Circumpolar Deep Water • Patagonian ice sheet dynamics
Coring program:	Triple APC to 300 m or refusal, HAPC if required to reach target depth
Logging/downhole measurements program:	Temperature measurements (with APCT-3)
Nature of rock anticipated:	Calcareous clayey silts; minor IRD during glacials. Fine-grained turbidites possible.

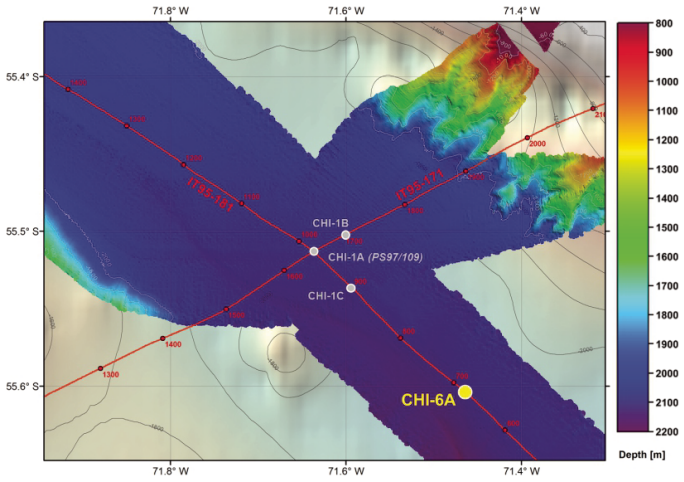

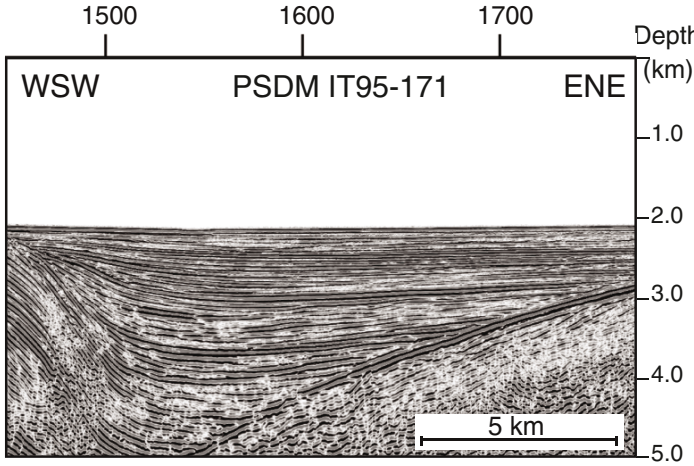

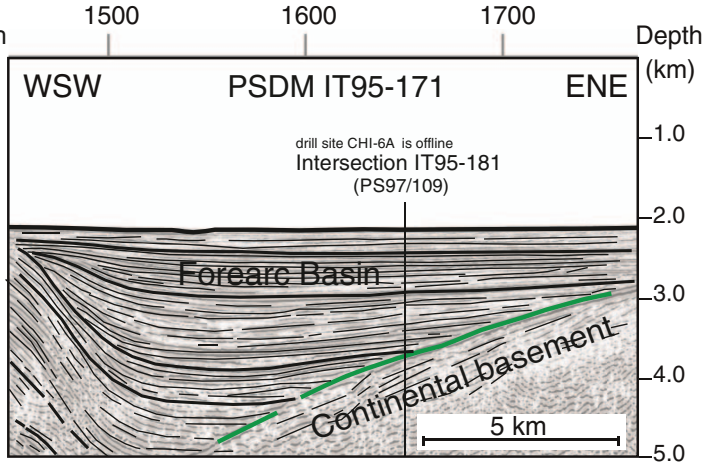

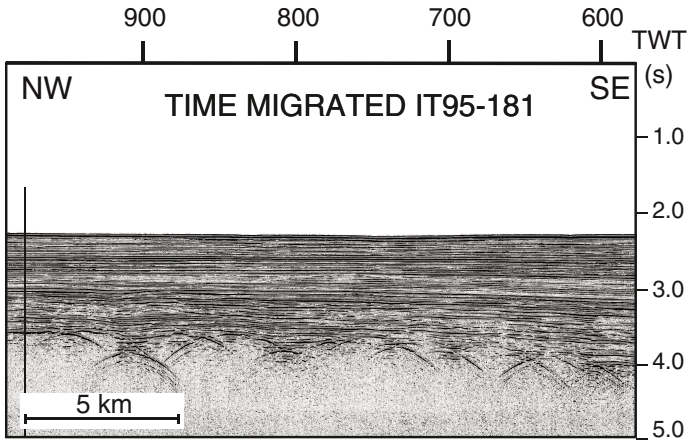

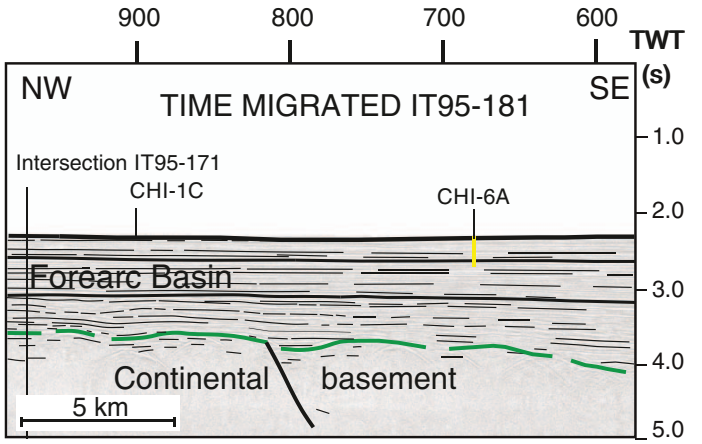

Site CHI-7A

Priority:	Alternate
Position:	52°44.6887′S, 75°37.3938′W
Jurisdiction	Chile
Water depth (m):	1250
Target drilling depth (mbsf):	500
Approved maximum penetration (mbsf):	Pending EPSP approval
Survey coverage (track map; seismic profile):	4800 AWI-20160511
Objective(s):	• High-resolution Pleistocene paleoceanographic records • Northern ACC strength before entering Drake Passage, Cape Horn Current • Reconstruction of intermediate water mass properties • Patagonian ice sheet dynamics
Coring program:	• Triple APC to 300 m or refusal, HAPC if required • XCB to reach target depth of 500 m in one hole
Logging/downhole measurements program:	• Temperature measurements (with APCT-3) • Downhole logging with modified triple combo
Nature of rock anticipated:	Site is located with a sediment drift at the upper continental slope, ~50 km from land. Calcareous clayey silts; minor IRD during glacials. Fine-grained turbidites possible.

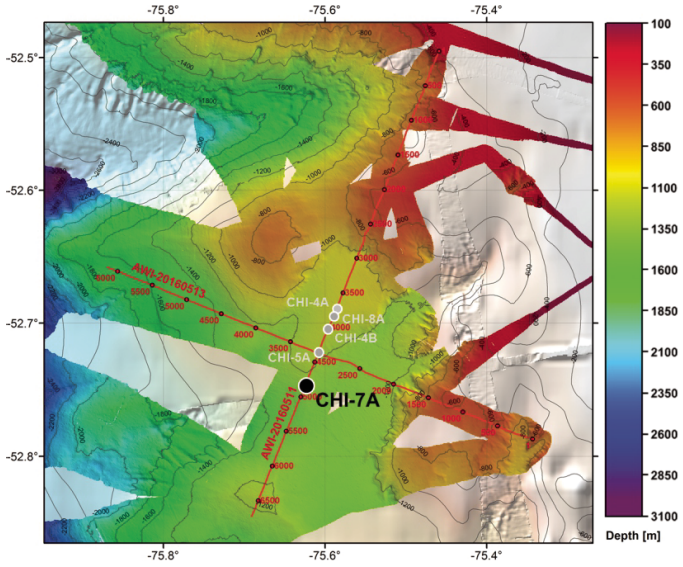

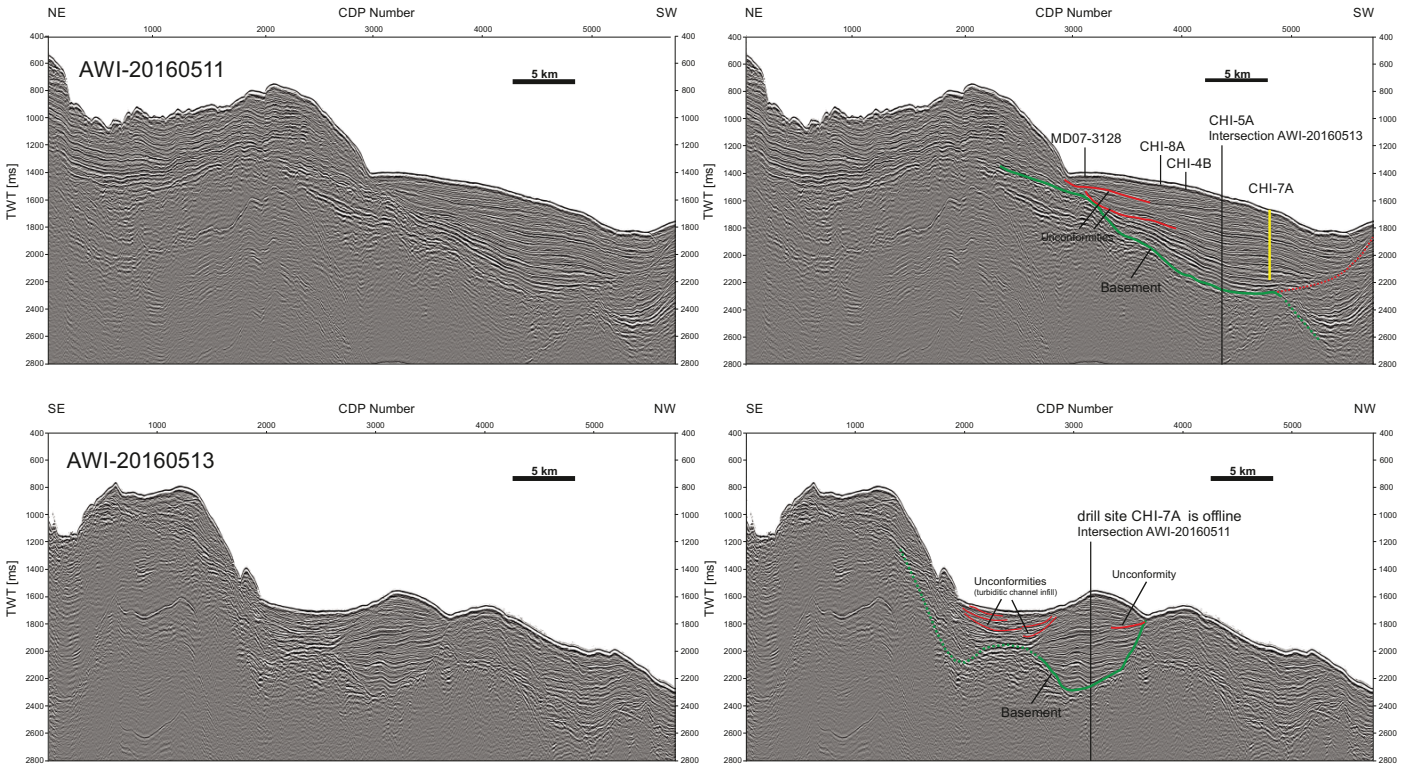

Site CHI-8A

Priority:	Alternate
Position:	52°41.5728′S, 75°35.2902′W
Jurisdiction	Chile
Water depth (m):	1060
Target drilling depth (mbsf):	200
Approved maximum penetration (mbsf):	Pending EPSP approval
Survey coverage (track map; seismic profile):	3800 AWI-20160511
Objective(s):	• High-resolution Pleistocene paleoceanographic records • Northern ACC strength before entering Drake Passage, Cape Horn Current • Reconstruction of intermediate water mass properties • Patagonian ice sheet dynamics
Coring program:	• Triple APC to 300 m or refusal, HAPC if required • XCB to reach target depth of 500 m in one hole
Logging/downhole measurements program:	• Temperature measurements (with APCT-3) • Downhole logging with modified triple combo
Nature of rock anticipated:	Site is located with a sediment drift at the upper continental slope, ~50 km from land. Calcareous clayey silts; minor IRD during glacials. Fine-grained turbidites possible.

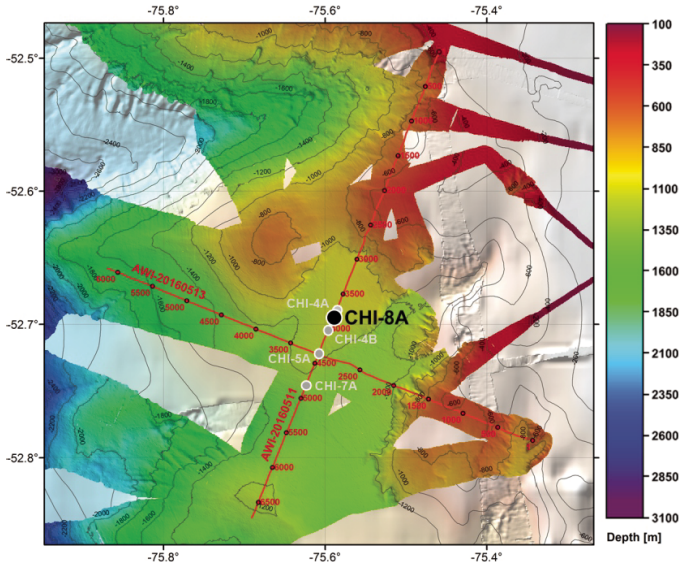

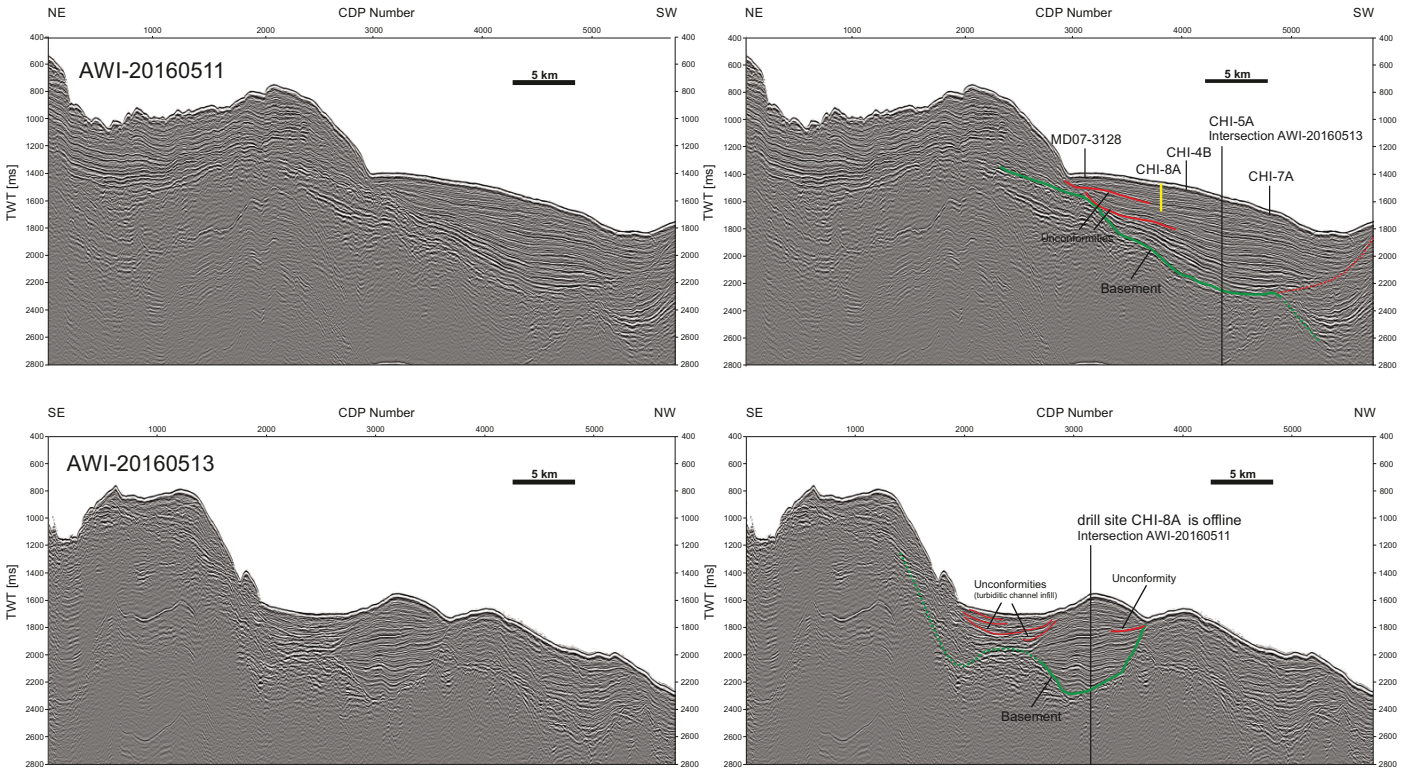

Site ESP-2A

Priority:	Alternate
Position:	54°33.2022′S, 76°31.2768′W
Jurisdiction	Chile
Water depth (m):	3850
Target drilling depth (mbsf):	400
Approved maximum penetration (mbsf):	Pending EPSP approval
Survey coverage (track map; seismic profile):	3850 AWI-20160501
Objective(s):	• Plio/Pleistocene (Miocene) paleoceanographic records • Northern ACC strength before entering Drake Passage, Cape Horn Current • Potential record of Antarctic Bottom Water during glacials • Long-term Patagonian ice sheet dynamics
Coring program:	Triple APC to 400 m or refusal, HAPC if required to reach target depth
Logging/downhole measurements program:	• Temperature measurements (with APCT-3) • Downhole logging with modified triple combo
Nature of rock anticipated:	Calcareous ooze and clay; minor IRD during glacials

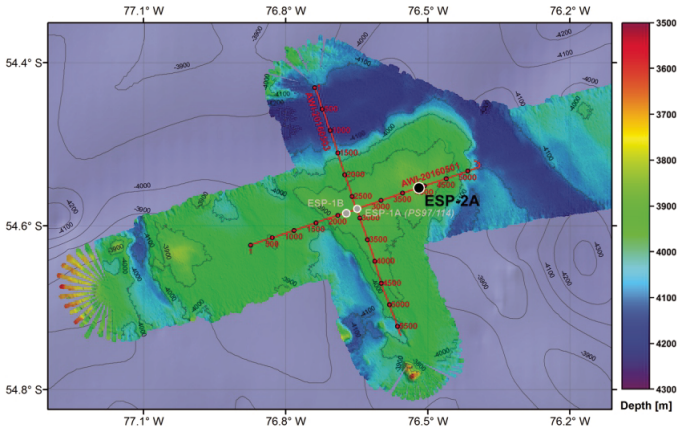

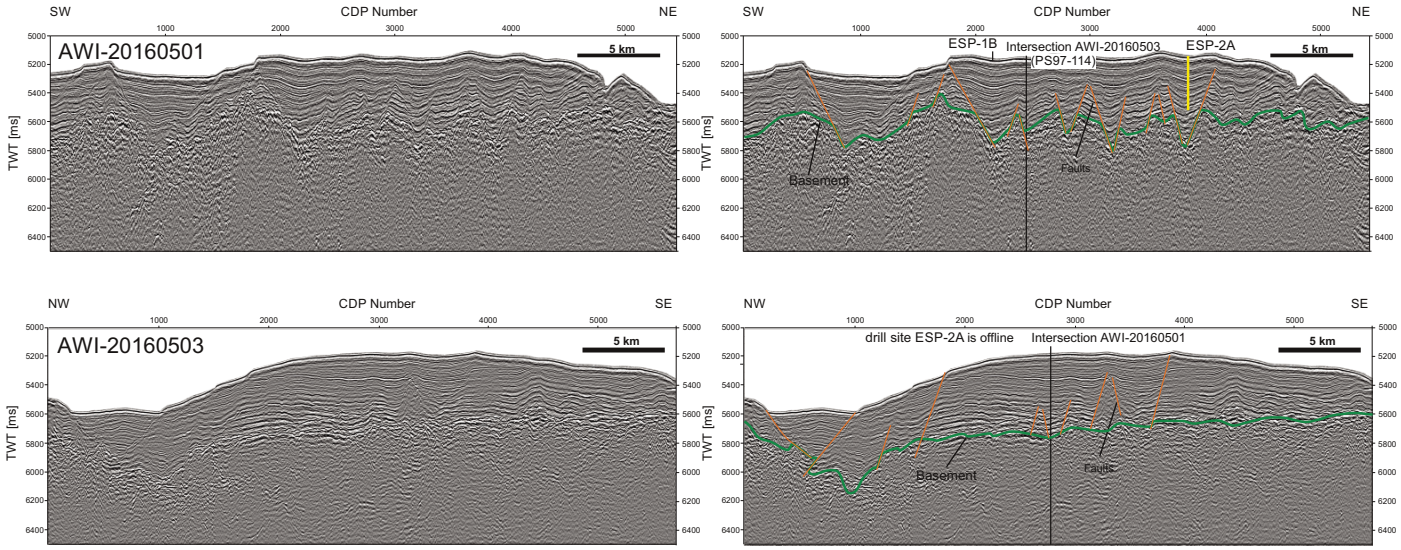

Site CSP-4A

Priority:	Alternate
Position:	56°11.154′S, 115°11.532′W
Jurisdiction	
Water depth (m):	4110
Target drilling depth (mbsf):	300
Approved maximum penetration (mbsf):	Pending EPSP approval
Survey coverage (track map; seismic profile):	700 AWI-20100011
Objective(s):	• Moderate to high-resolution subantarctic late Miocene-Quaternary carbonate record from lower CDW depth. • Subantarctic SST, water mass, pCO_2, productivity record • Central site of cross-frontal transect
Coring program:	Triple APC to 300 m or refusal
Logging/downhole measurements program:	Temperature measurements (with APCT-3)
Nature of rock anticipated:	Calcareous-biosiliceous ooze

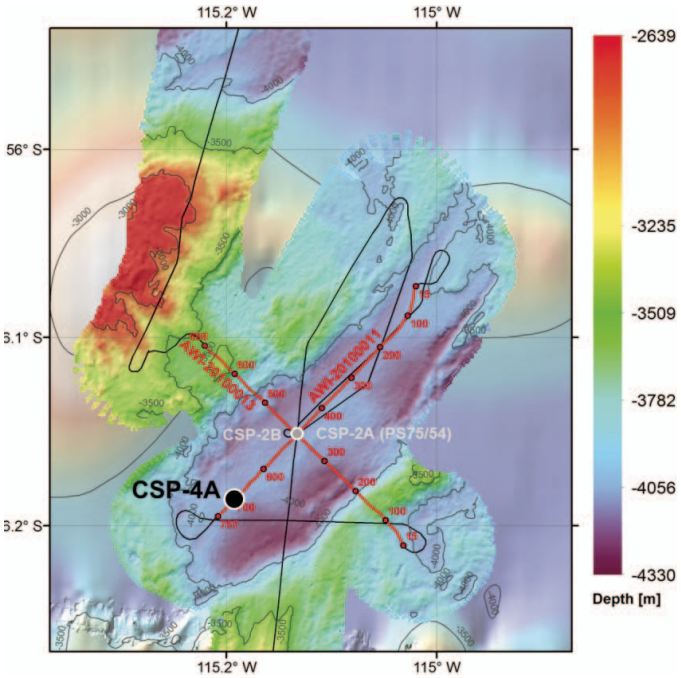

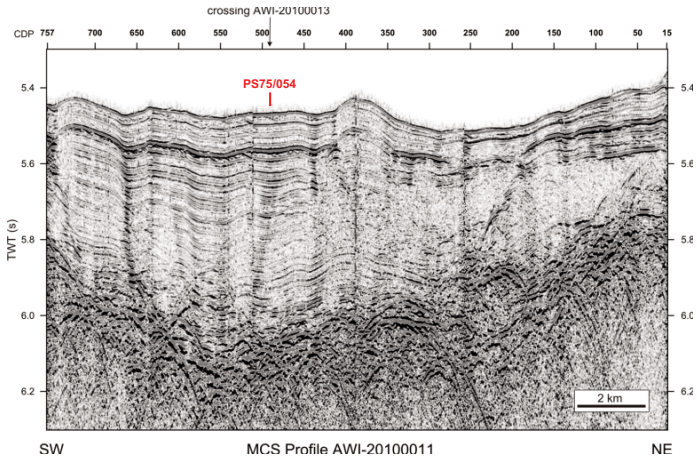

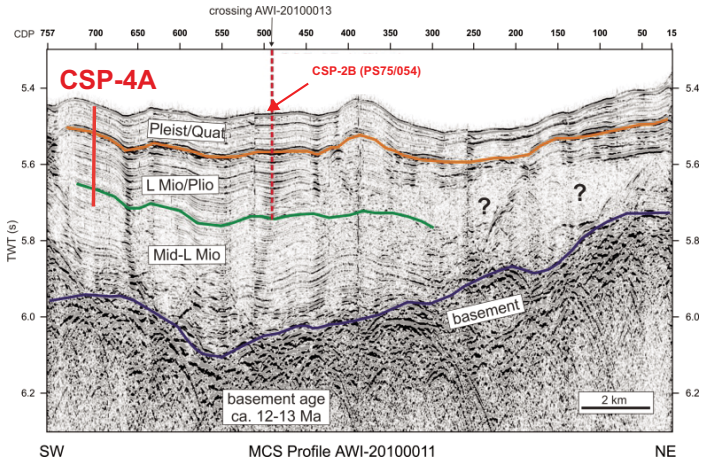

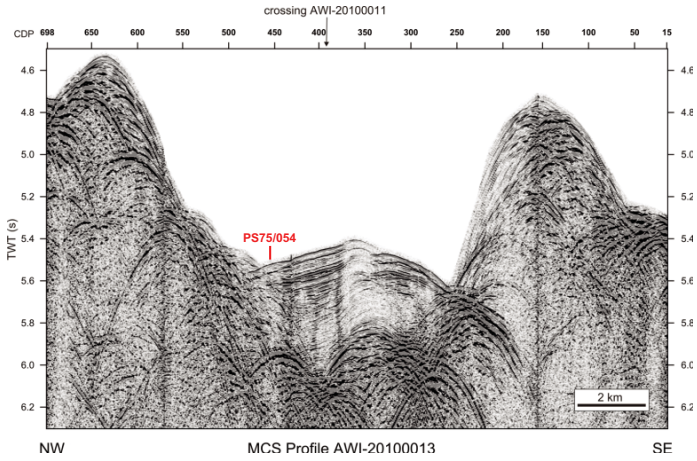

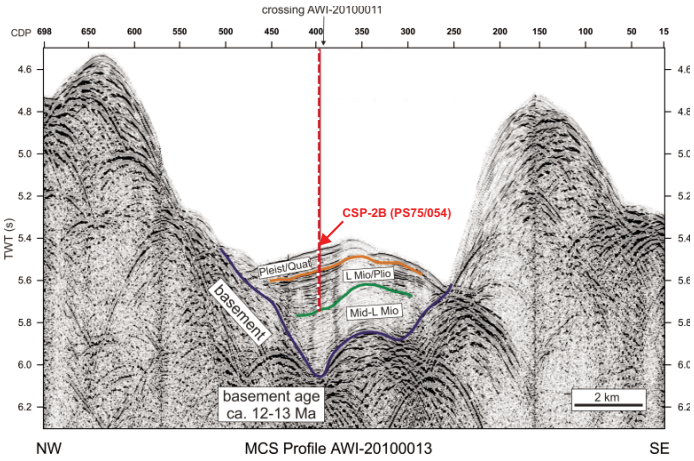

Site CSP-5A

Priority:	Alternate
Position:	60°46.716′S, 116°00.018′W
Jurisdiction	Antarctic Treaty
Water depth (m):	5130
Target drilling depth (mbsf):	300
Approved maximum penetration (mbsf):	Pending EPSP approval
Survey coverage (track map; seismic profile):	380 AWI-20100143
Objective(s):	• Moderate to high-resolution subantarctic late Miocene-Quaternary carbonate record from lower CDW depth • Subantarctic SST, water mass, pCO_2, productivity record • Southernmost site of cross-frontal transect
Coring program:	Triple APC to 300 m or refusal
Logging/downhole measurements program:	Temperature measurements (with APCT-3)
Nature of rock anticipated:	Calcareous-biosiliceous ooze

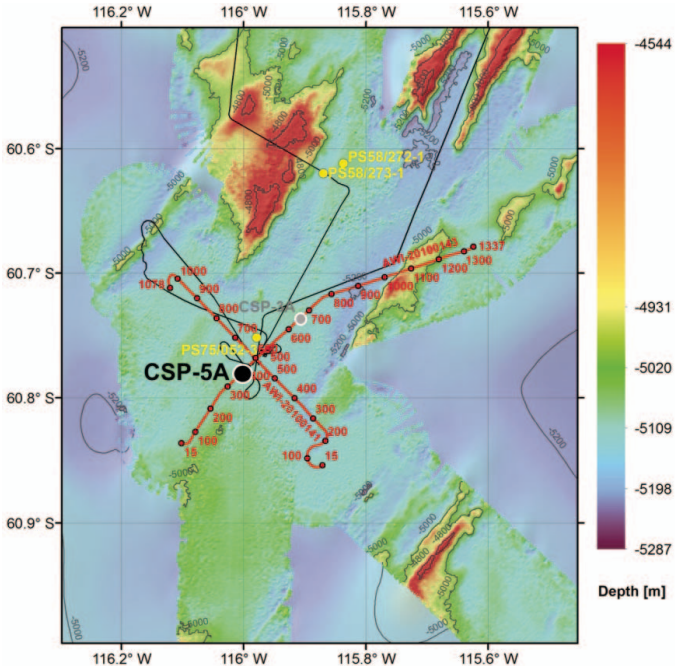

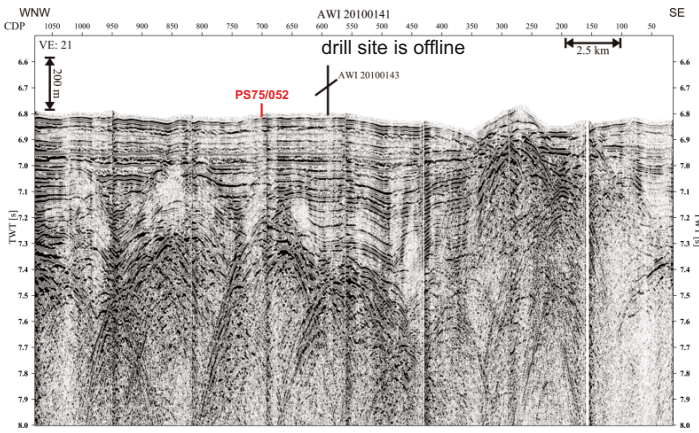

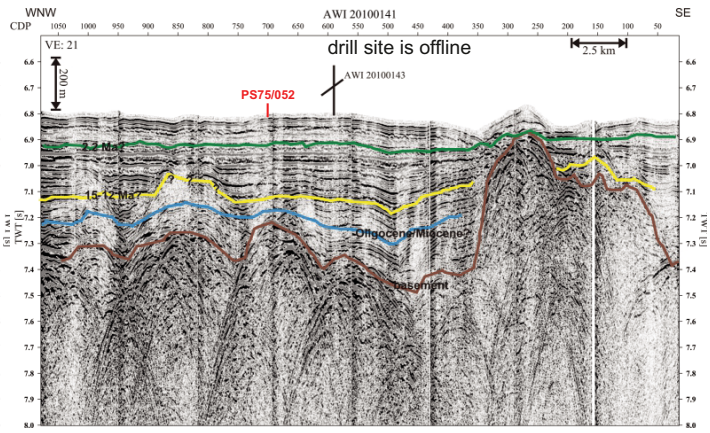

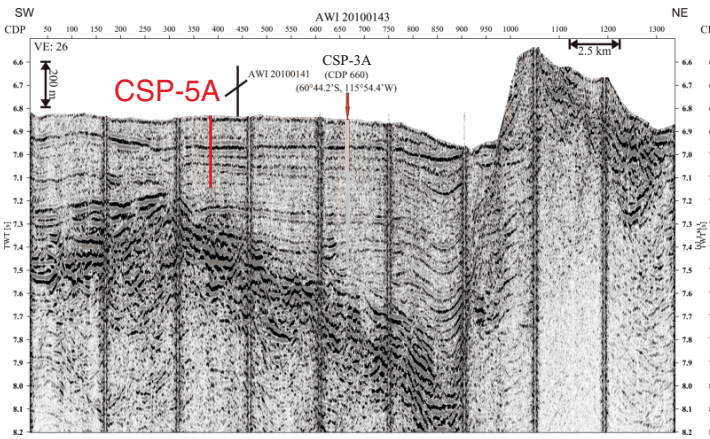

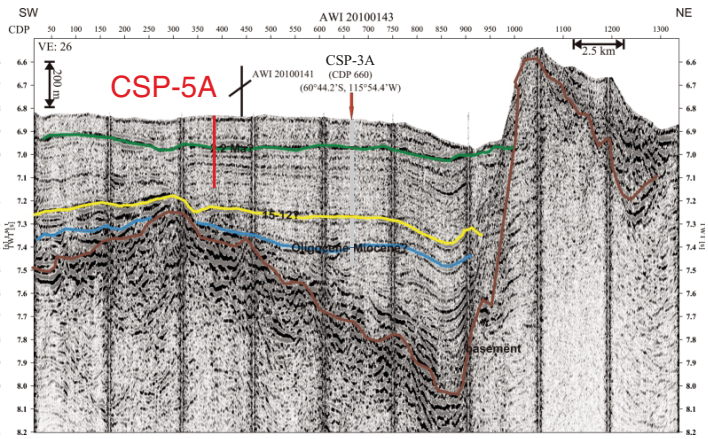

Site CSP-6A

Priority:	Alternate
Position:	55°9.4896′S, 114°47.322′W
Jurisdiction	International
Water depth (m):	3570
Target drilling depth (mbsf):	125
Approved maximum penetration (mbsf):	Pending EPSP approval
Survey coverage (track map; seismic profile):	Based on Parasound only (SP 3900)
Objective(s):	• Moderate to high-resolution subantarctic late Miocene-Quaternary carbonate record from lower CDW depth. • Subantarctic SST, water mass, pCO_2, productivity record • Central site of cross-frontal transect
Coring program:	Triple APC to 300 m or refusal
Logging/downhole measurements program:	Temperature measurements (with APCT-3)
Nature of rock anticipated:	Calcareous-biosiliceous ooze

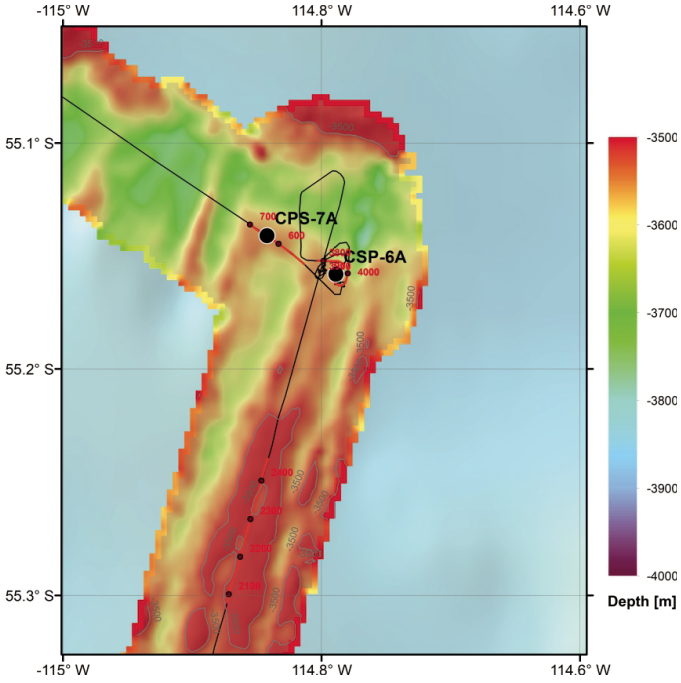

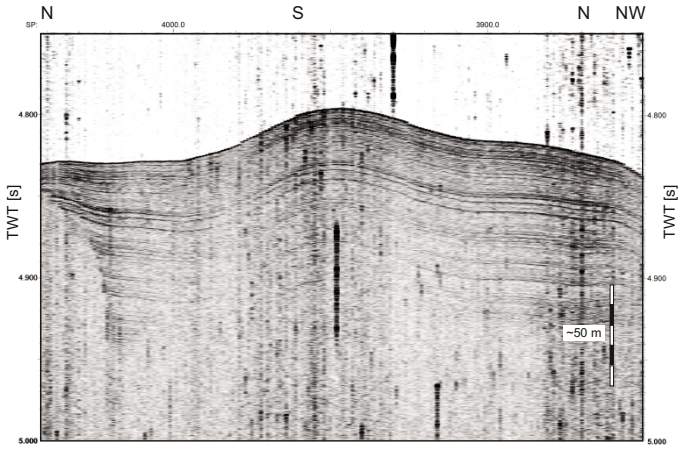

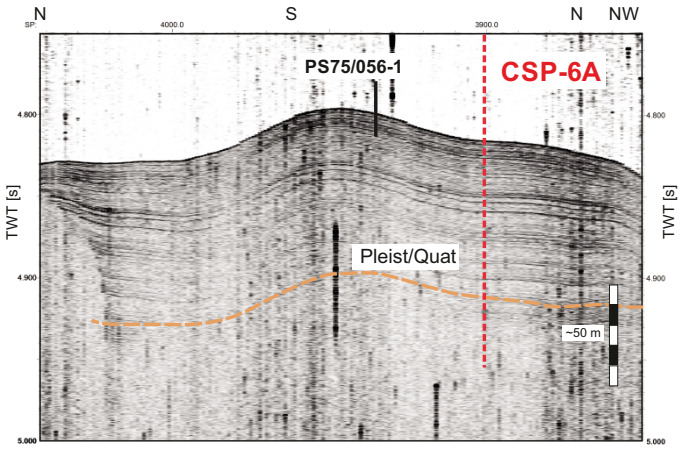

Site CSP-7A

Priority:	Alternate
Position:	55°8.4666′S, 114°50.520′W
Jurisdiction	International waters
Water depth (m):	3540
Target drilling depth (mbsf):	150
Approved maximum penetration (mbsf):	Pending EPSP approval
Survey coverage (track map; seismic profile):	Based on Parasound only (SP 640)
Objective(s):	• Moderate to high-resolution subantarctic late Miocene-Quaternary carbonate record from lower CDW depth. • Subantarctic SST, water mass, pCO_2, productivity record • Central site of cross-frontal transect
Coring program:	Triple APC to 300 m or refusal
Logging/downhole measurements program:	Temperature measurements (with APCT-3)
Nature of rock anticipated:	Calcareous-biosiliceous ooze